A SEARCH FOR NEW PHYSICS
Qweak

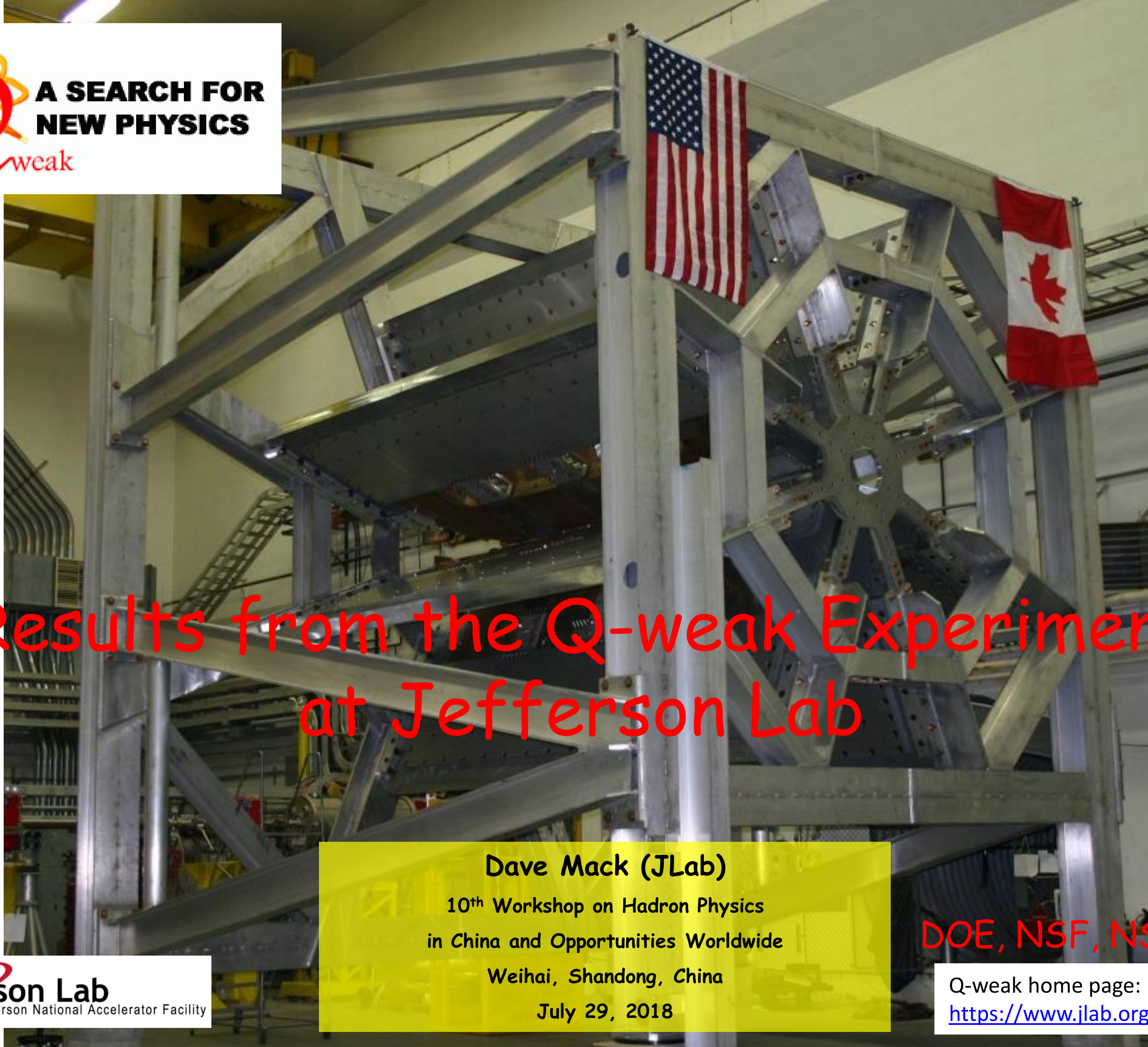

Results from the Q-weak Experiment at Jefferson Lab

Dave Mack (JLab)

10th Workshop on Hadron Physics
in China and Opportunities Worldwide
Weihai, Shandong, China
July 29, 2018

DOE, NSF, NSERC

Q-weak home page:
https://www.jlab.org/qweak/

Jefferson Lab
Thomas Jefferson National Accelerator Facility

The Quark Weak Vector Charges

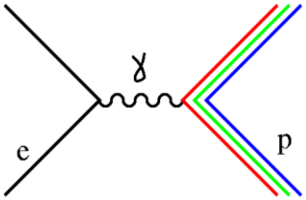

$\boxed{\text{EM Charge}}$

q^{up}	$+2/3$
q^{down}	$-1/3$
$Q^p = 2q^{up} + 1q^{down}$	$+1$
$Q^n = 1q^{up} + 2q^{down}$	0

The Quark Weak Vector Charges

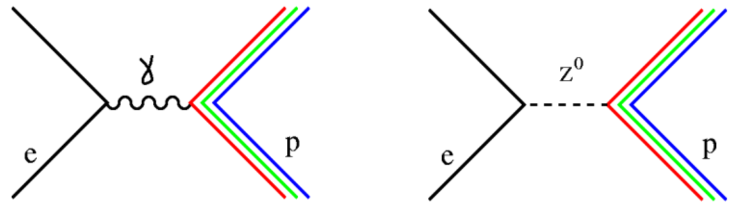

	EM Charge	Weak Charge
q^{up}	$+2/3$	$1 - \frac{8}{3}\sin^2\theta_W \approx 1/3$
q^{down}	$-1/3$	$-1 + \frac{4}{3}\sin^2\theta_W \approx -2/3$
$Q^p = 2q^{up} + 1q^{down}$	$+1$	$1 - 4\sin^2\theta_W = -.048$
$Q^n = 1q^{up} + 2q^{down}$	0	-1

Q_w^p is the neutral-weak analog of the proton's electric charge

Note the roles of the proton and neutron are almost reversed:

ie, neutron weak charge is dominant, while proton weak charge is almost zero.

The Quark Weak Vector Charges

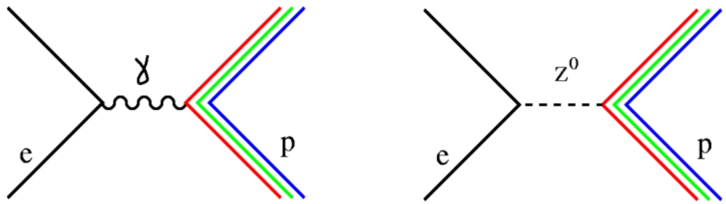

	EM Charge	Weak Charge
q^{up}	$+2/3$	$1 - \frac{8}{3}\sin^2\theta_W \approx 1/3$
q^{down}	$-1/3$	$-1 + \frac{4}{3}\sin^2\theta_W \approx -2/3$
$Q^p = 2q^{up} + 1q^{down}$	$+1$	$1 - 4\sin^2\theta_W = -.048$
$Q^n = 1q^{up} + 2q^{down}$	0	-1

Q_W^p is the neutral-weak analog of the proton's electric charge

Note the roles of the proton and neutron are almost reversed:

ie, neutron weak charge is dominant, while proton weak charge is almost zero.

This suppression of Q_W^p has two benefits:

1. A weak proton charge measurement of a given relative accuracy lets you measure $\sin^2\theta_W$ with almost an order of magnitude better relative accuracy.
2. Potential pulls from TeV-scale physics on Q_W^p are relatively large.

What is this θ_W?

In the Weinberg-Salam theory, it is the angle by which the W^0 and B^0 are rotated to produce the physical Z boson and photon.

$$\begin{pmatrix} \gamma \\ Z^0 \end{pmatrix} = \begin{pmatrix} \cos\theta_W & \sin\theta_W \\ -\sin\theta_W & \cos\theta_W \end{pmatrix} \begin{pmatrix} B^0 \\ W^0 \end{pmatrix}$$

While G_F controls the overall coupling strength in the weak interaction, the weak mixing angle θ_W determines the specific neutral current couplings to quarks, leptons, and neutrinos.

A SM Test at High Energy with $\sin^2\theta_W$

In the on-shell scheme,

$$\sin^2\theta_W = 1 - M_W^2/M_Z^2 \quad .$$

M_Z is extremely well known. This means that M_W can be determined *indirectly* at Born level using

$$M_W^2 = M_Z^2\,(1-\sin^2\theta_W)$$

(the real calculation has logarithmic dependences on the top quark and Higgs masses, α_{EM}, etc.)

This indirect result can then be compared to direct measurements of M_W. (yellow at right)

Combined Tevatron 2 results:
PRD **97**, 112007 (2018)

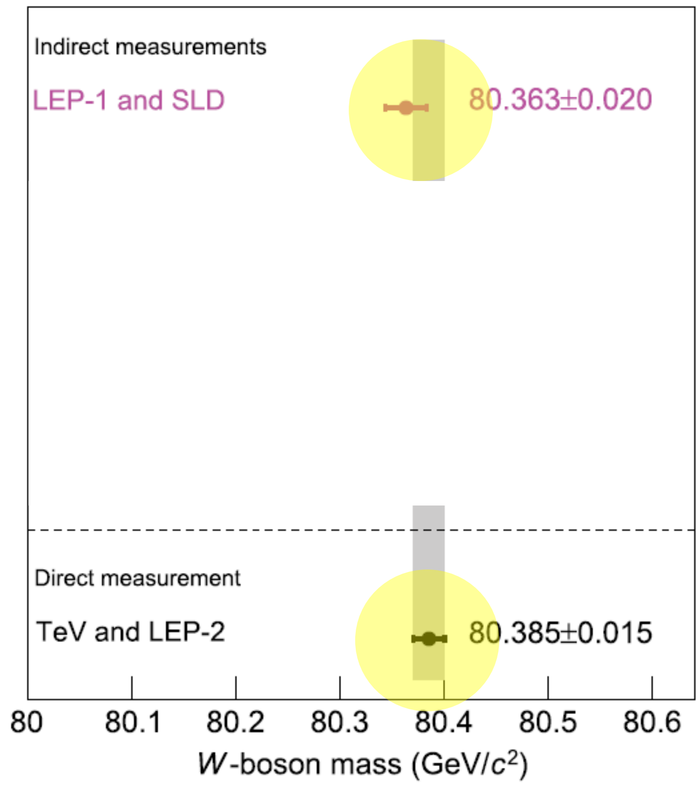

A SM Test at High Energy with $\sin^2\theta_W$

In the on-shell scheme,

$$\sin^2\theta_W = 1 - M_W^2/M_Z^2 \quad .$$

M_Z is extremely well known. This means that M_W can be determined *indirectly* at Born level using

$$M_W^2 = M_Z^2\,(1-\sin^2\theta_W)$$

(the real calculation has logarithmic dependences on the top quark and Higgs masses, α_{EM}, etc.)

This indirect result can then be compared to direct measurements of M_W. (yellow at right)

Recently, the combined CDF and D0 results from Tevatron 2 allow an improved comparison.

Combined Tevatron 2 results:
PRD **97**, 112007 (2018)

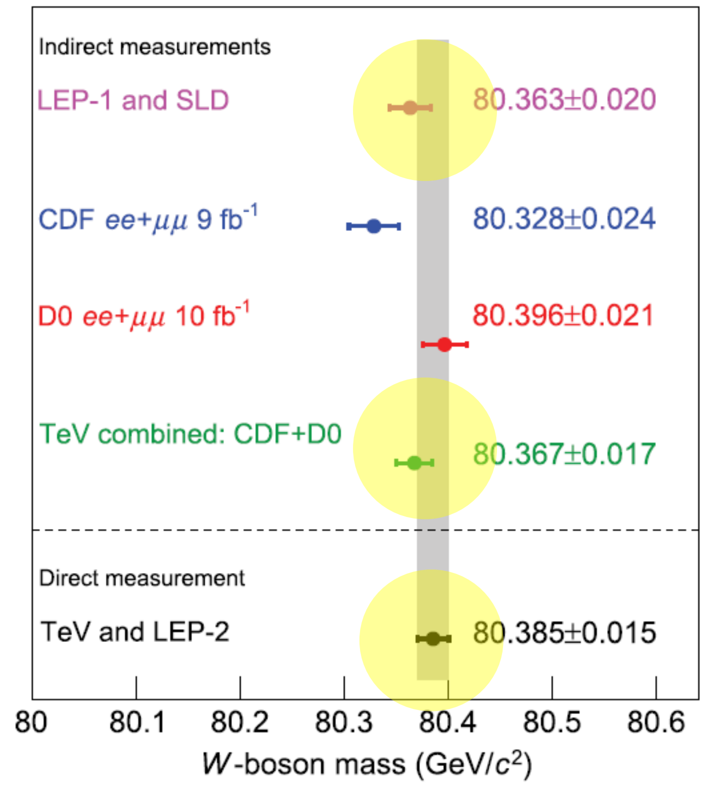

The direct and indirect measurements of M_W continue to agree.

The Running of $\sin^2\theta_W$

The magnitude of $\sin^2\theta_W$ is set by precision data near the Z pole.

The running due to γ-Z mixing is calculable at lower energy scales to high precision.

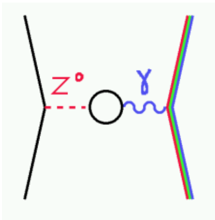

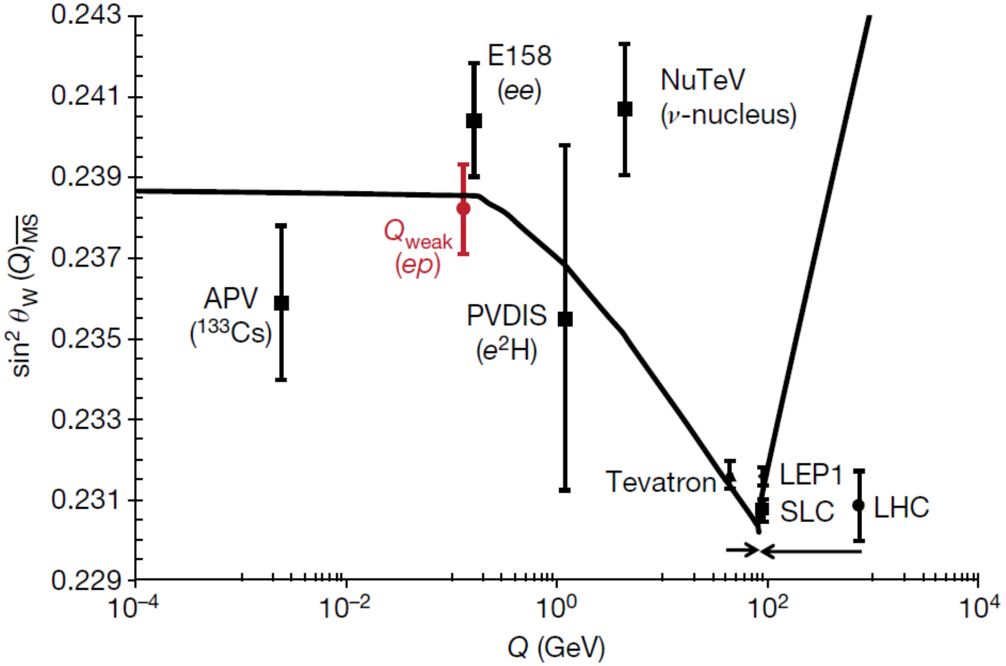

So what's the point of Q-weak?

Comparing $\sin^2\theta_W(0)$ with $\sin^2\theta_W(M_Z)$ constrains the presence of non-SM shifts in the EW radiative corrections.

The Running of $\sin^2\theta_W$

The magnitude of $\sin^2\theta_W$ is set by precision data near the Z pole.

The running due to γ-Z mixing is calculable at lower energy scales to high precision.

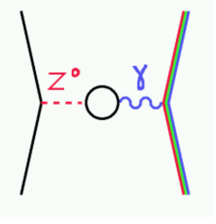

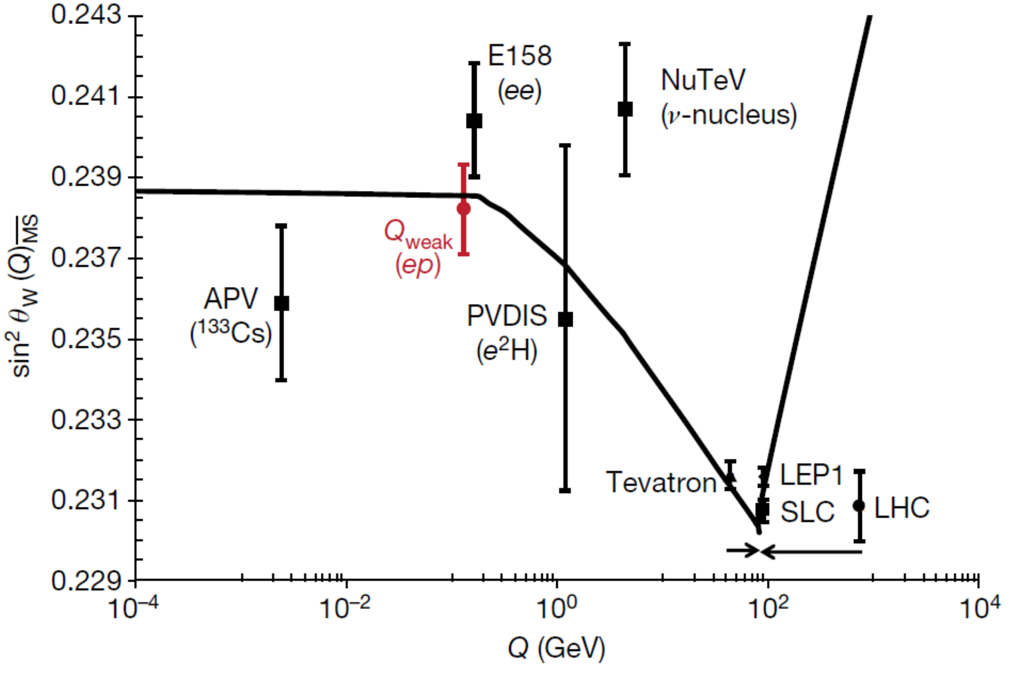

So what's the point of Q-weak?

Comparing $\sin^2\theta_W(0)$ with $\sin^2\theta_W(M_Z)$ constrains the presence of non-SM shifts in the EW radiative corrections.

- In the context of the SM, all data should be consistent with the same running curve.
- Experiments can be differentially sensitive to new physics (eg, e-e, e-q, ν-e, ν-q).
- The Q-weak experiment is sensitive to new electron-quark physics in a very different isospin combination than the Cesium APV experiment.

Interpretability of the Running of $\sin^2\theta_W$

Although $Q_w^p \sim 1-4\sin^2\theta_W$, there are substantial box diagram corrections.

$$Q_W^p = [\rho_{\rm NC} + \Delta_e][1 - 4\sin^2\hat{\theta}_{\rm W}(0) + \Delta_e'] + \Box_{WW} + \Box_{ZZ} + \Box_{\gamma Z}$$

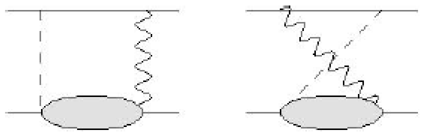

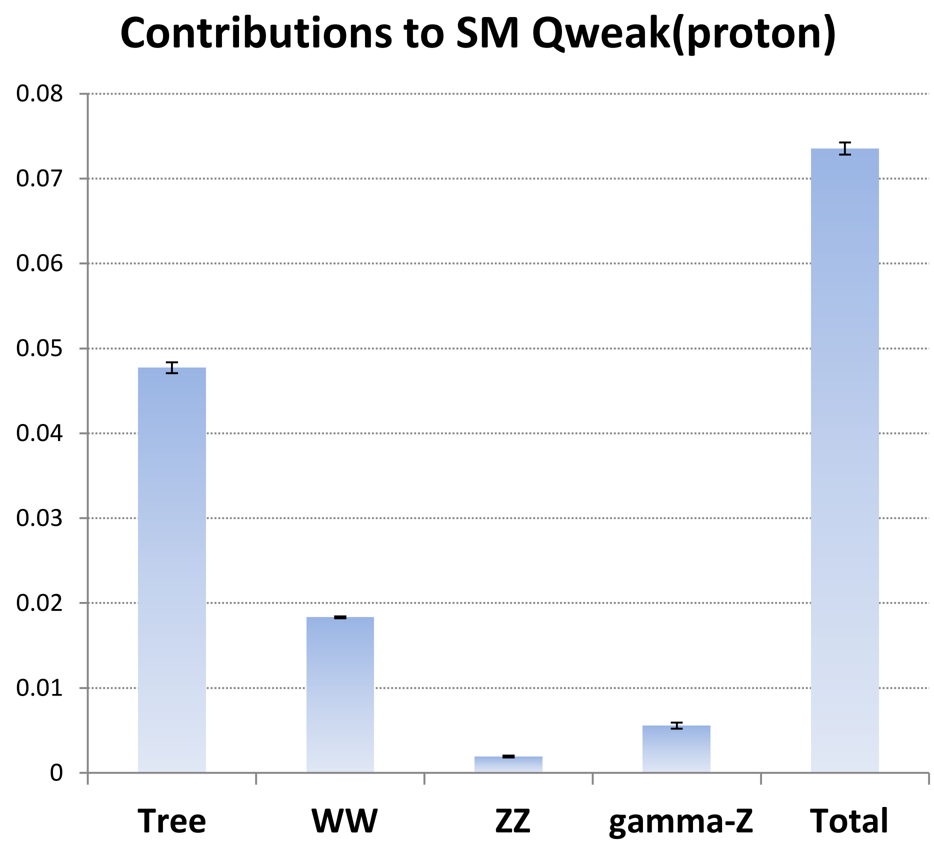

Interpretability of the Running of $\sin^2\theta_W$

Although $Q_w^p \sim 1\text{-}4\sin^2\theta_W$, there are substantial box diagram corrections.

$$Q_W^p = [\rho_{NC} + \Delta_e][1 - 4\sin^2\hat{\theta}_W(0) + \Delta_e'] + \Box_{WW} + \Box_{ZZ} + \Box_{\gamma Z}$$

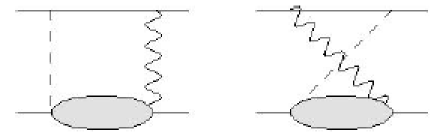

- WW box is relatively large, but precisely calculable due to point-like interactions of both bosons.

- γZ box contains significant long distance contributions, but the uncertainty makes a smaller contribution than Z pole data.

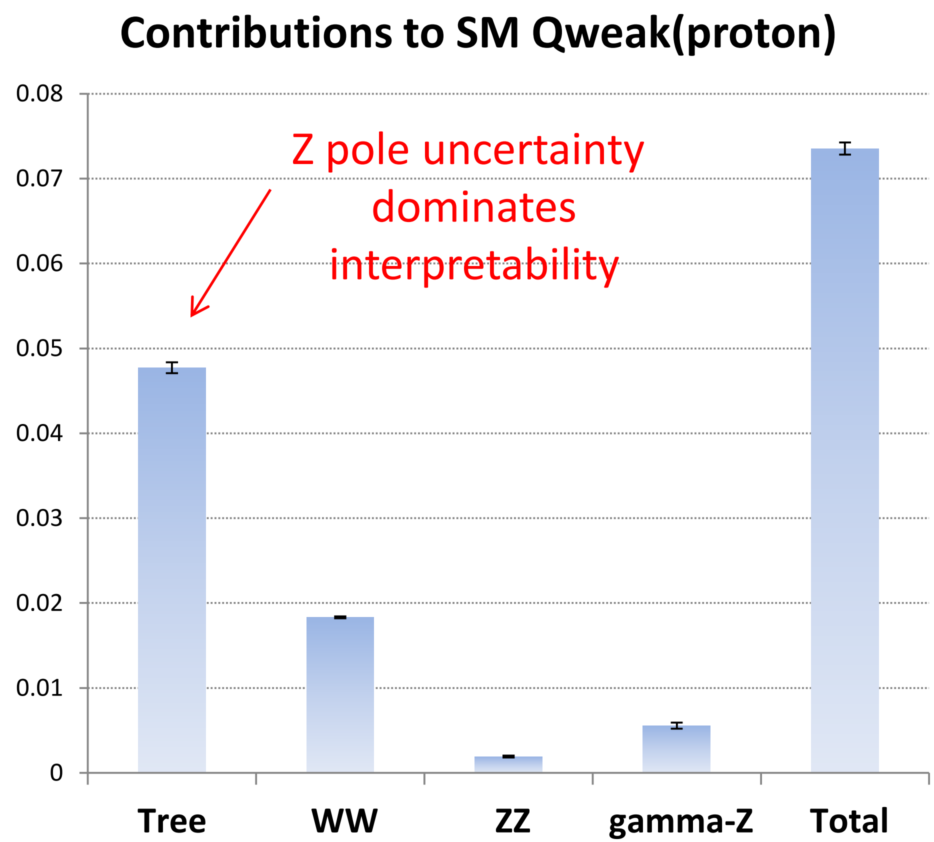

Qweak(proton) can be calculated to ~1%, well below our experimental sensitivity.

Determination of Qweak(proton) from PV Electron Scattering

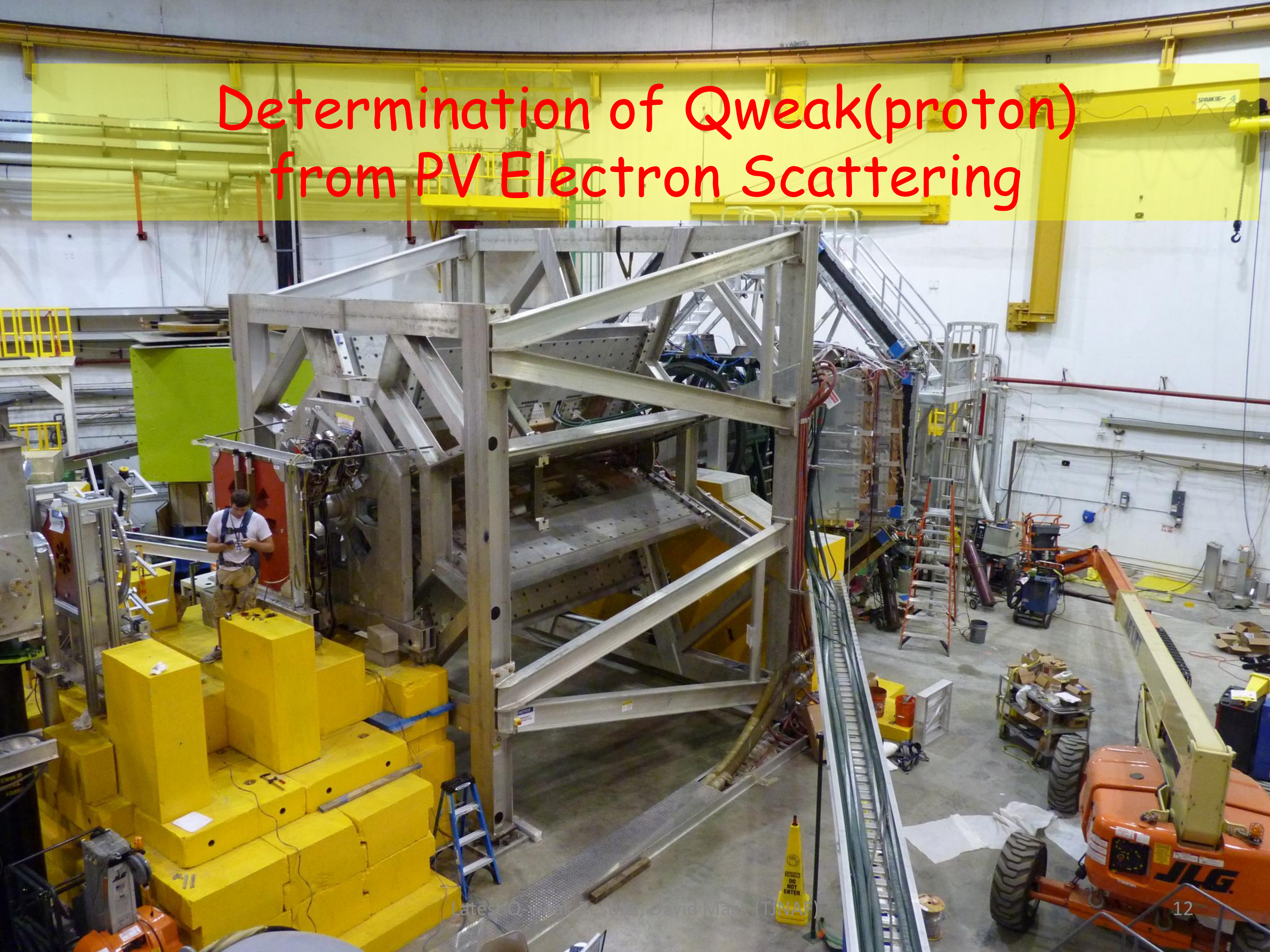

Accessing Q_w^p from PV Electron Scattering

Parity violation in electron scattering arises from V x A couplings of the Z.

We isolate the small EM x Weak interference term, normalized to $|EM|^2$, thru the PV asymmetry.

By varying the angle and momentum Xfer, one can extract Q_w^p and axial couplings, etc.

We wanted A(e) x V(q) to dominate.

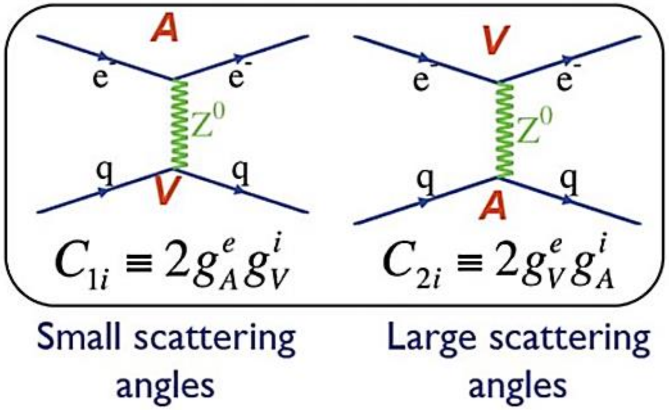

Accessing Q_w^p from PV Electron Scattering

Parity violation in electron scattering arises from V x A couplings of the Z.

We isolate the small EM x Weak interference term, normalized to $|EM|^2$, thru the PV asymmetry.

By varying the angle and momentum Xfer, one can extract Q_w^p and axial couplings, etc.

We wanted A(e) x V(q) to dominate.

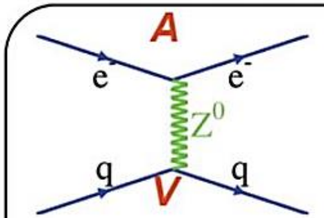

$$C_{1i} \equiv 2 g_A^e g_V^i$$

Small scattering angles

In the limit of low momentum transfer and forward kinematics, the leading order term for elastic scattering contains the weak charge:

$$A_{ep} = \frac{G_F Q^2}{4\pi\alpha\sqrt{2}}\left[Q_w^p + Q^2 B(Q^2,\theta)\right]$$

Roughly

-200 ppb

At our chosen kinematics, Q_w^p dominates at ~2/3 of the total asymmetry.

Fully Corrected Elastic e+p Asymmetry
(evolved to θ = 0° at fixed Q^2)

This is the world PV elastic electron scattering dataset as of 2013 when our first paper came out.

D. Androic et al., Phys. Rev. Lett. 111, 141803 (2013)
http://arxiv.org/abs/1307.5275v2

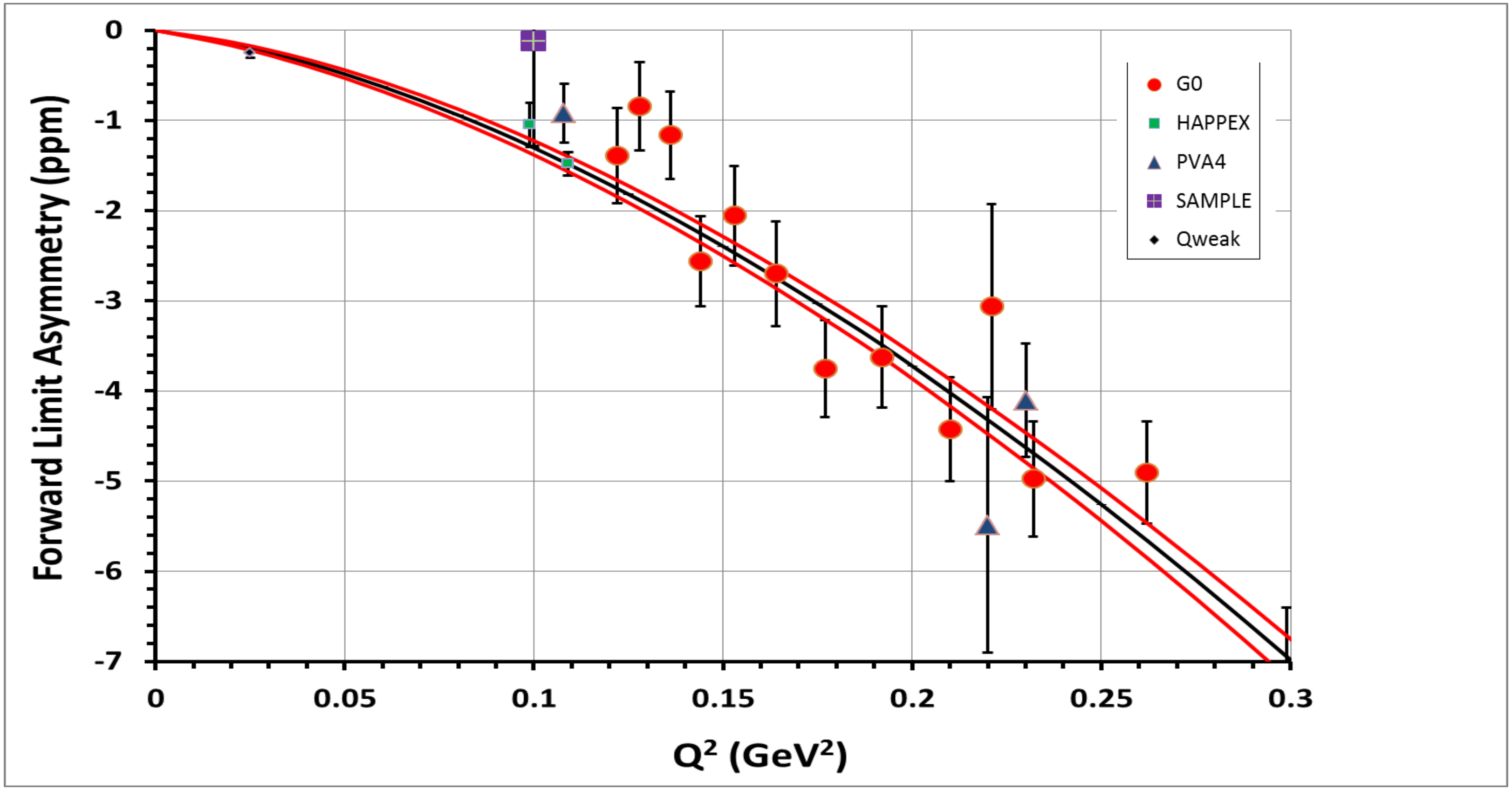

Fully Corrected Elastic e+p Asymmetry

(evolved to $\theta = 0°$ at fixed Q^2)

This is the world PV elastic electron scattering dataset as of 2013 when our first paper came out.

D. Androic et al., Phys. Rev. Lett. 111, 141803 (2013)
http://arxiv.org/abs/1307.5275v2

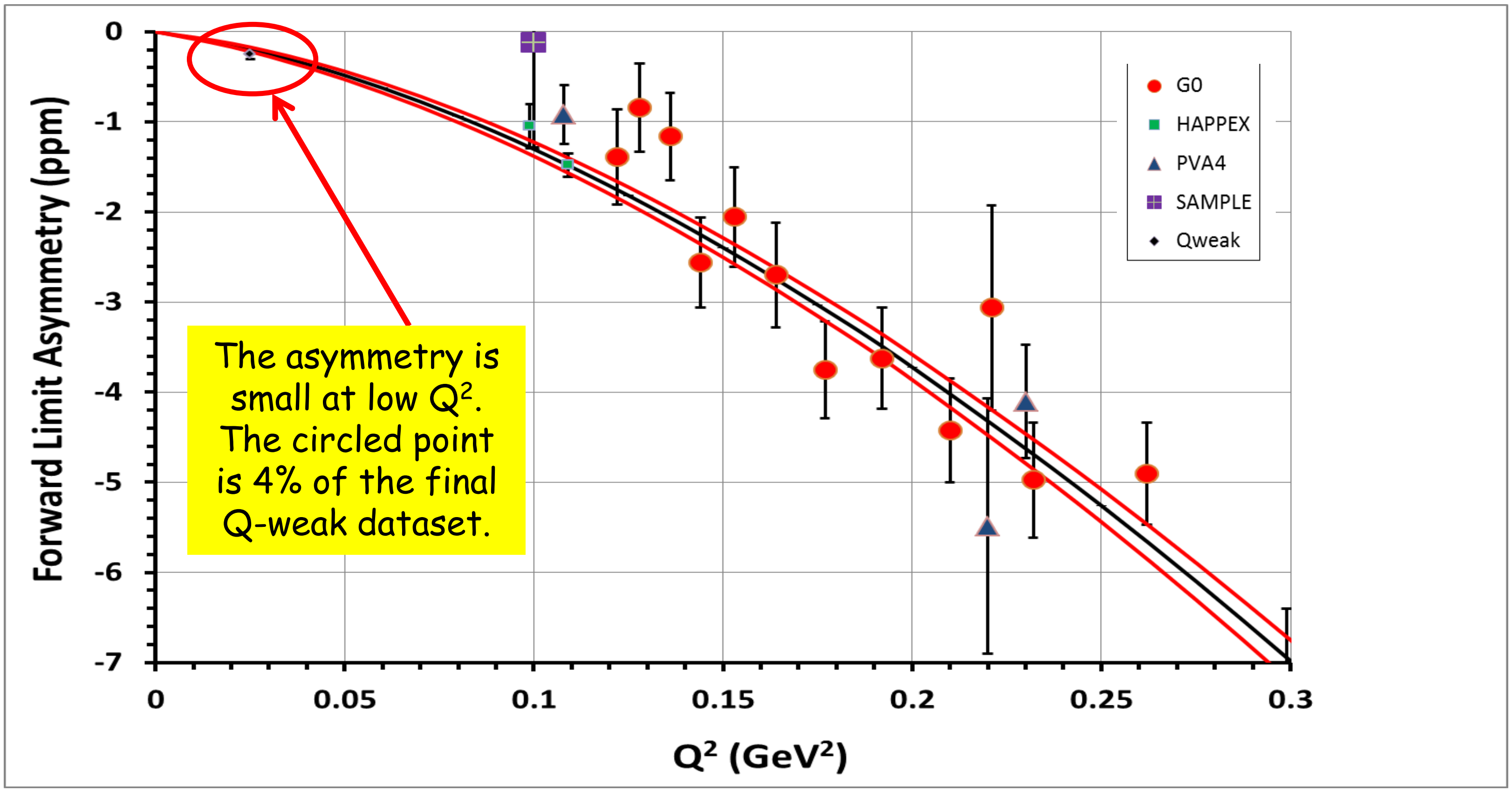

Methodology

We flip the longitudinal beam polarization about 1000 times per second, with a brief pause for the beam polarization and intensity to stabilize.

(Faster than that would lead to excessive dead-time.)

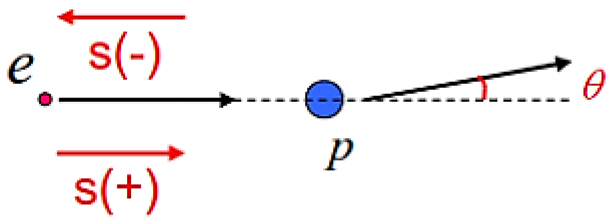

Methodology

We flip the longitudinal beam polarization about 1000 times per second, with a brief pause for the beam polarization and intensity to stabilize.

(Faster than that would lead to excessive dead-time.)

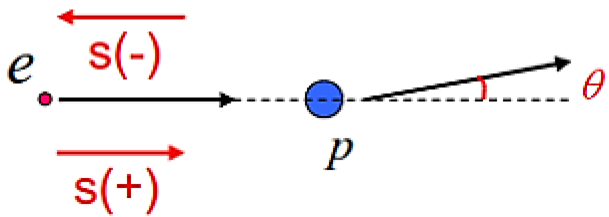

With an electron scattered into each detector every nsec, the signal must be integrated.

$$A_{PV} = \frac{1}{P}\frac{Y^{+} - Y^{-}}{Y^{+} + Y^{-}} = \frac{1}{P}\frac{\frac{N^{+}}{Q^{+}} - \frac{N^{-}}{Q^{-}}}{\frac{N^{+}}{Q^{+}} + \frac{N^{-}}{Q^{-}}}$$

Methodology

We flip the longitudinal beam polarization about 1000 times per second, with a brief pause for the beam polarization and intensity to stabilize.
(Faster than that would lead to excessive dead-time.)

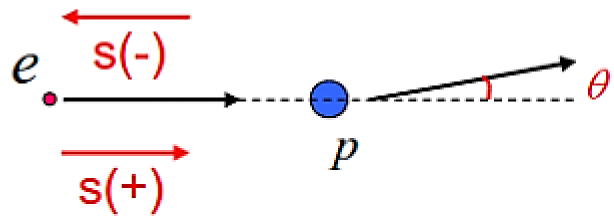

With an electron scattered into each detector every nsec, the signal must be integrated.

$$A_{PV} = \frac{1}{P}\frac{Y^{+} - Y^{-}}{Y^{+} + Y^{-}} = \frac{1}{P}\frac{\frac{N^{+}}{Q^{+}} - \frac{N^{-}}{Q^{-}}}{\frac{N^{+}}{Q^{+}} + \frac{N^{-}}{Q^{-}}}$$

- Effect of target density fluctuations and charge monitor are coherent in all 8 detectors, so their noise specs must be << $1/\sqrt{N_{\text{whole detector}}}$ ~ 200 ppm per quad.
- Minimal beam parameter changes on spin flip (averaged over the run)
  ie, << wavelength of visible light!
- Corrections for remaining small false asymmetries that *do* occur on spin flip
- Precise absolute measurements of Q^2, beam polarization, and backgrounds.

How Small is the ~200 ppb Q-weak PV Signal?

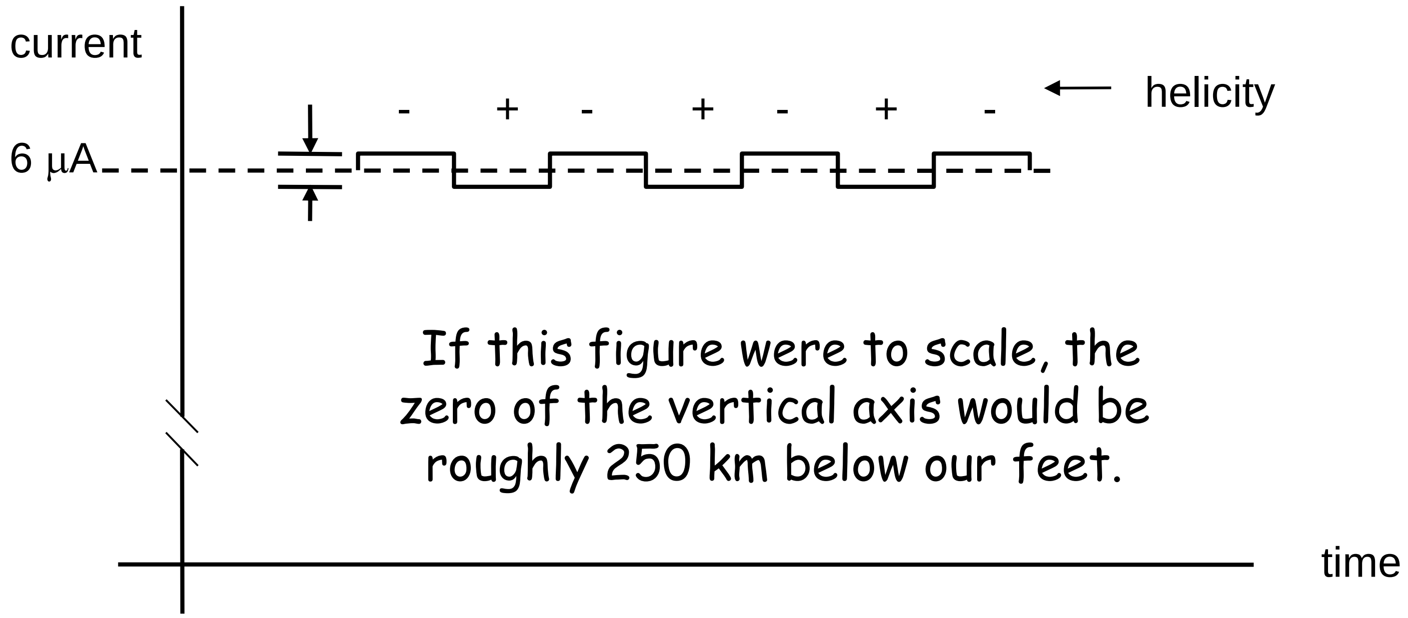

If this figure were to scale, the zero of the vertical axis would be roughly 250 km below our feet.

How Small is the ~200 ppb Q-weak PV Signal?

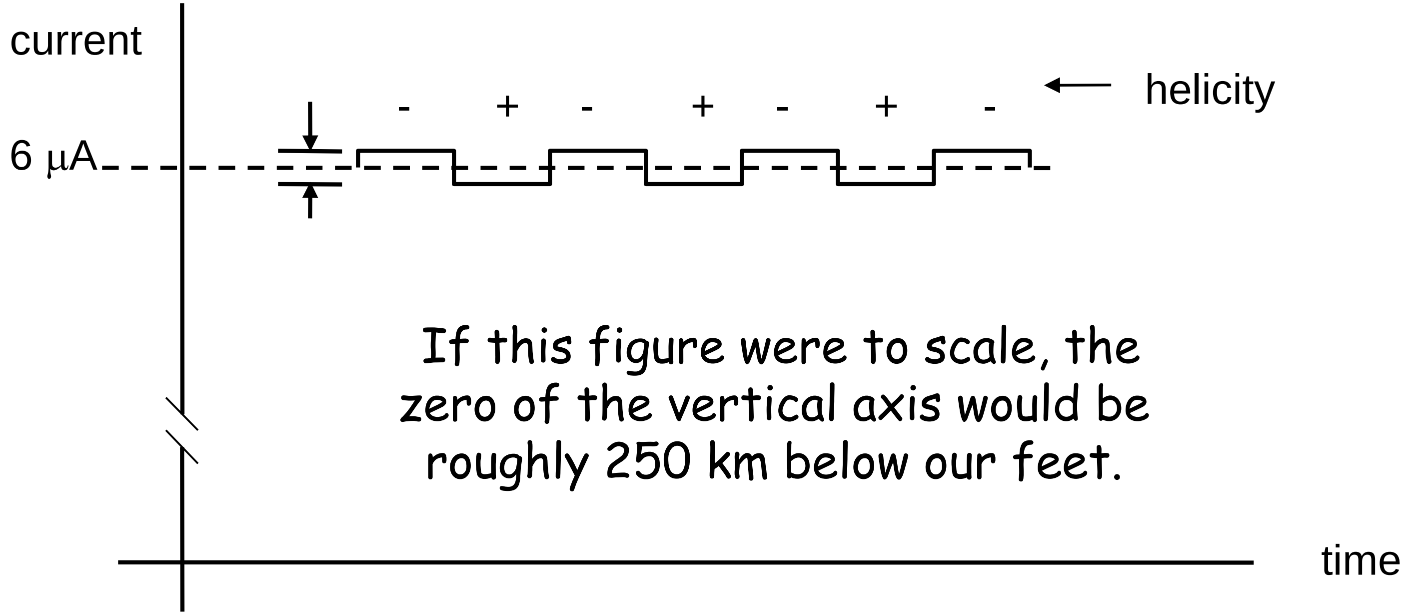

If this figure were to scale, the zero of the vertical axis would be roughly 250 km below our feet.

It is like the thickness of a coat of paint on top of the 325m Eiffel Tower.

And we have to measure it to few percent accuracy!

Statistical Facts of Life of Measuring Very Small Asymmetries

How long would it take to measure a 200 ppb asymmetry to 1% if one were tracking particles at Rate = 10 MHz (eg, 10 detectors each with 1 MHz rate)?

$\Delta A = 1/\sqrt{N}$

$N = 1/\Delta A^2 = 1/(0.01*200\times10^{-9})^2 = 2.5\times10^{17}$ events

That's 0.25 billion billion events.

Statistical Facts of Life of Measuring Very Small Asymmetries

How long would it take to measure a 200 ppb asymmetry to 1% if one were tracking particles at Rate = 10 MHz (eg, 10 detectors each with 1 MHz rate)?

$\Delta A = 1/\sqrt{N}$

$N = 1/\Delta A^2 = 1/(0.01*200\times10^{-9})^2 = 2.5\times10^{17}$ events

That's 0.25 billion billion events.

Time = N/Rate = 2.5×10^{10} sec

1 year = 3.2×10^{7} sec → 793 years

For ΔA < 10 ppb like Q-weak, experiments are not feasible in event- or tracking-mode.

The only choice is to design a low-background experiment and integrate.

The Apparatus

Bird's-eye View of Accelerator Site

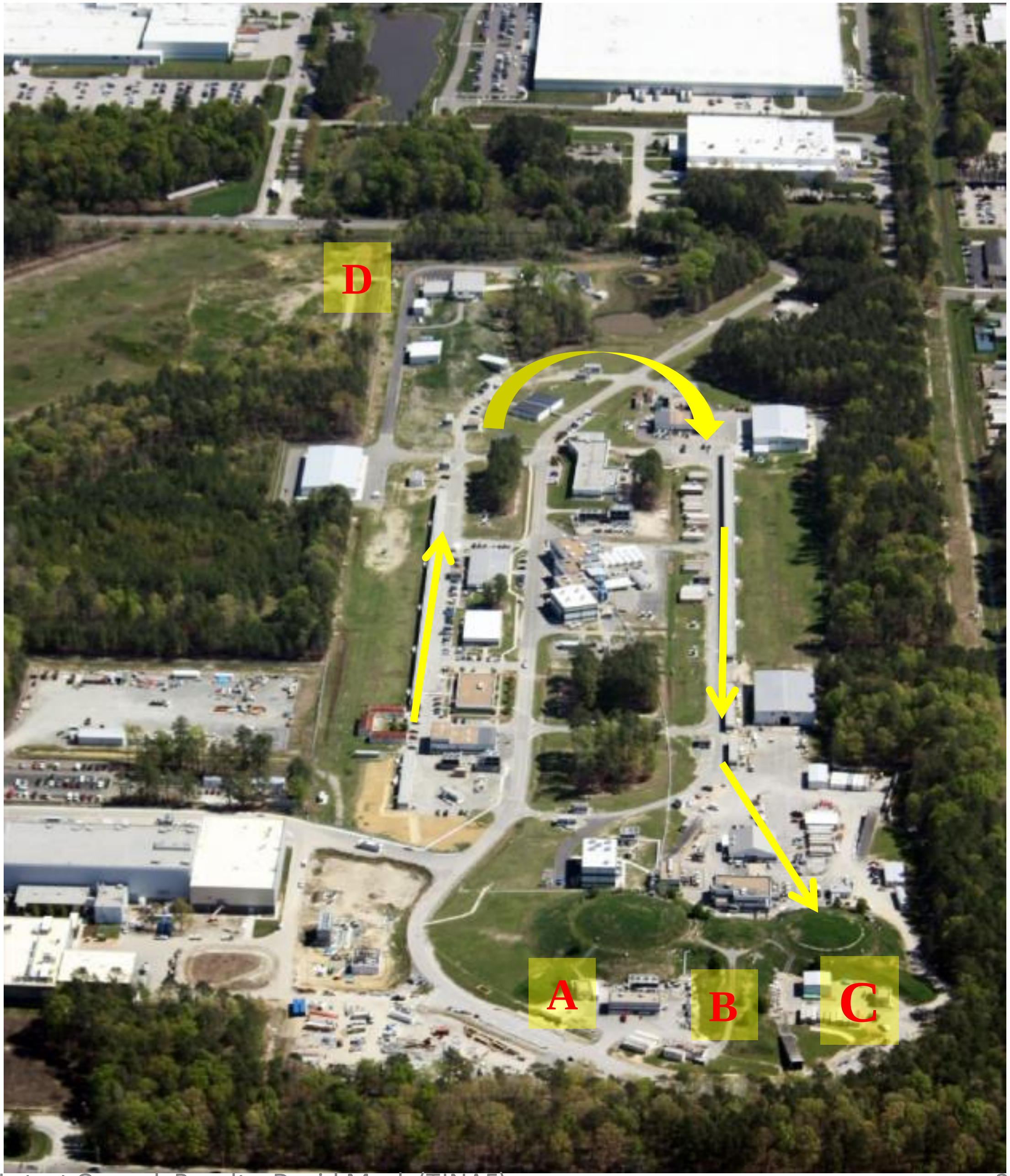

JLab Proposal

The Qweak Experiment:
"A Search for New Physics at the TeV Scale via a Measurement of the Proton's Weak Charge",
December 10, 2007

http://qweak.jlab.org/doc-public/ShowDocument?docid=703

From Polarized Injector to Detectors

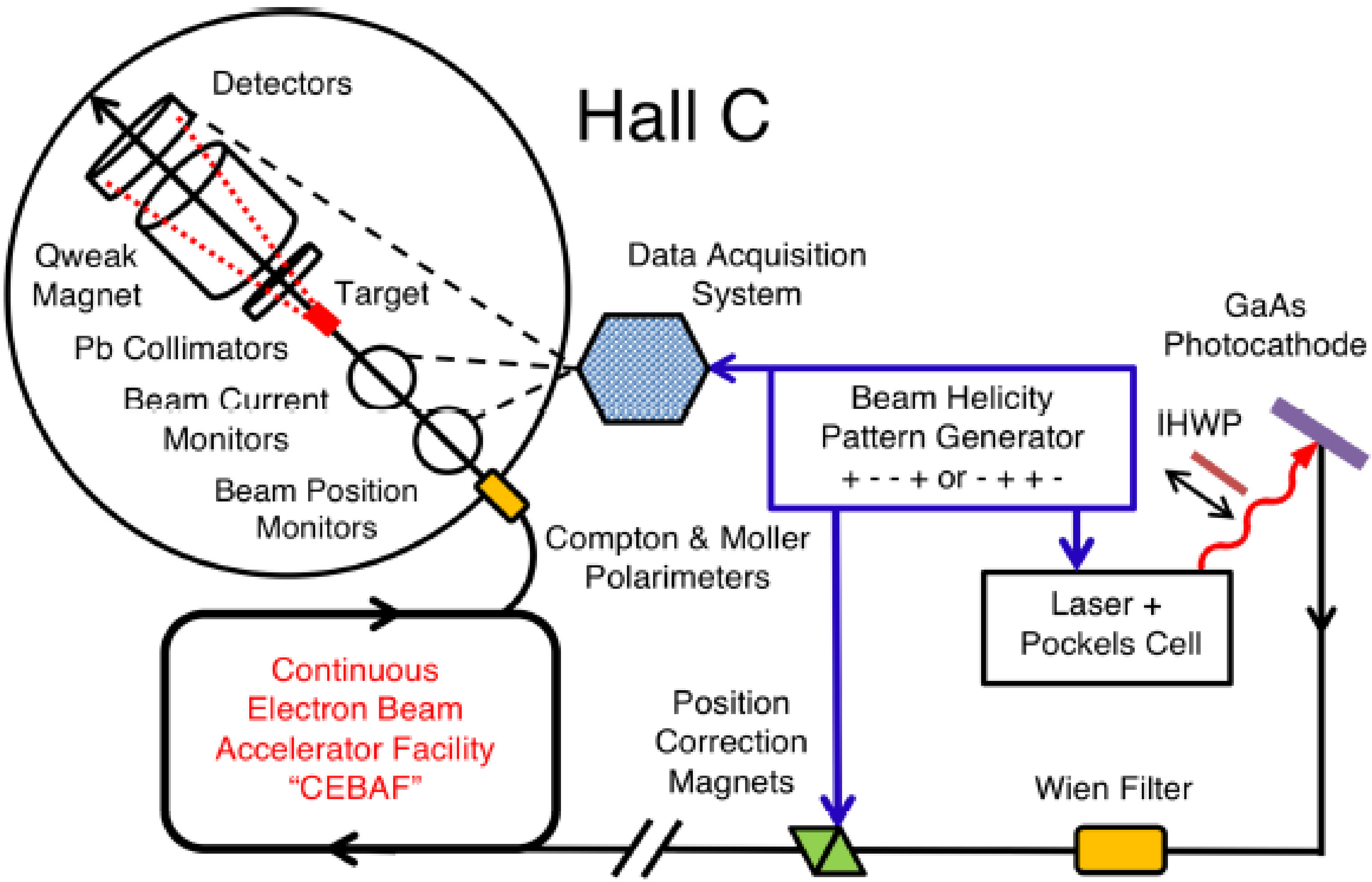

Q-weak Spectrometer (basics)

Must isolate elastic e+p events at small angles, with the largest acceptance possible, without tracking.

(A new particle traverses each detector every nsec.)

Electromagnet! No ferro-magnetic materials could be used.

E_{beam} = 1.16 GeV

Lum. = 1.7×10^{39} $cm^{-2}s^{-1}$

$\theta = 6^\circ - 12^\circ$

$Q^2 = 0.025\ (GeV/c)^2$

Total Rate = 6.4 GHz

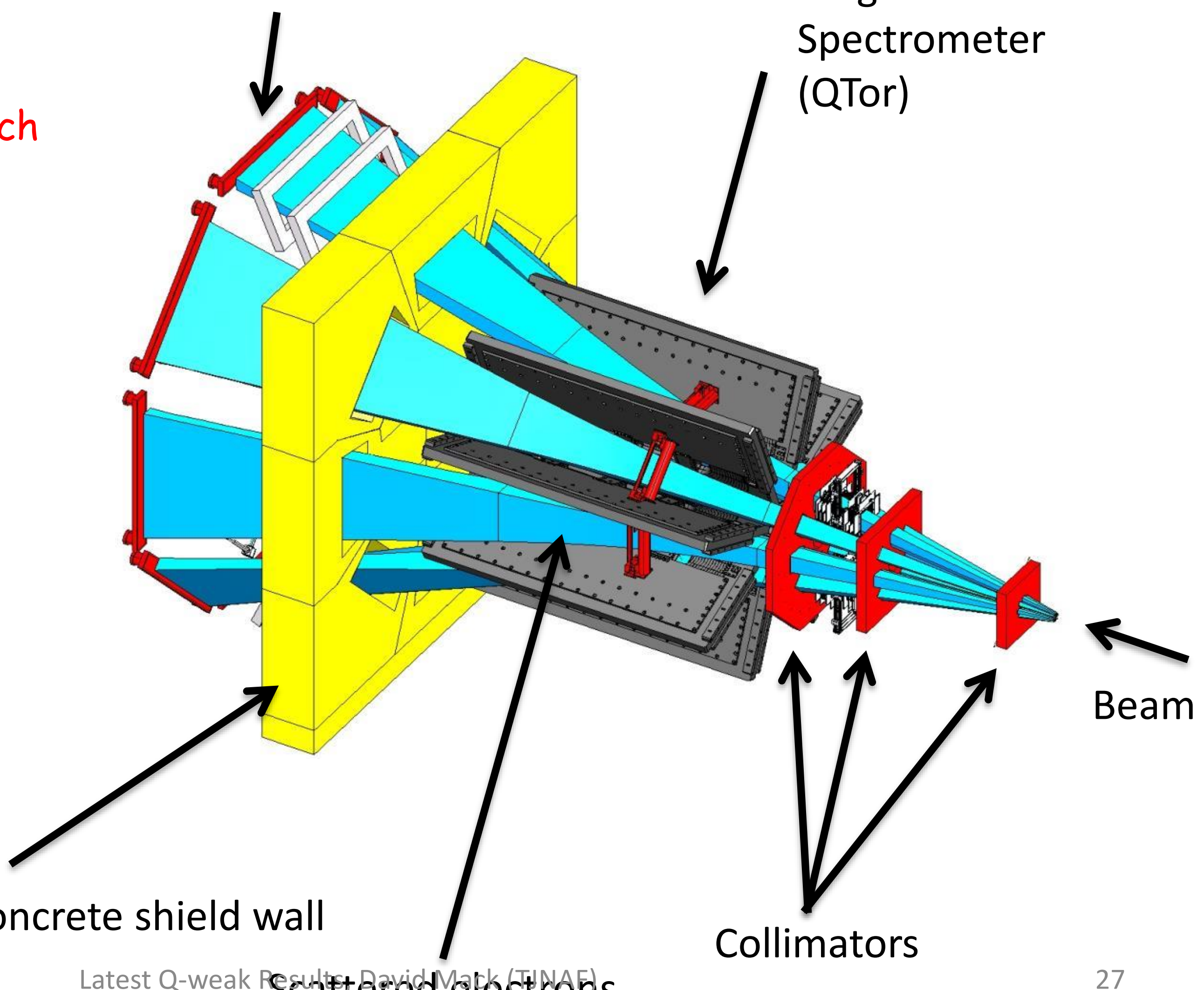

Q-weak Spectrometer (dressed)

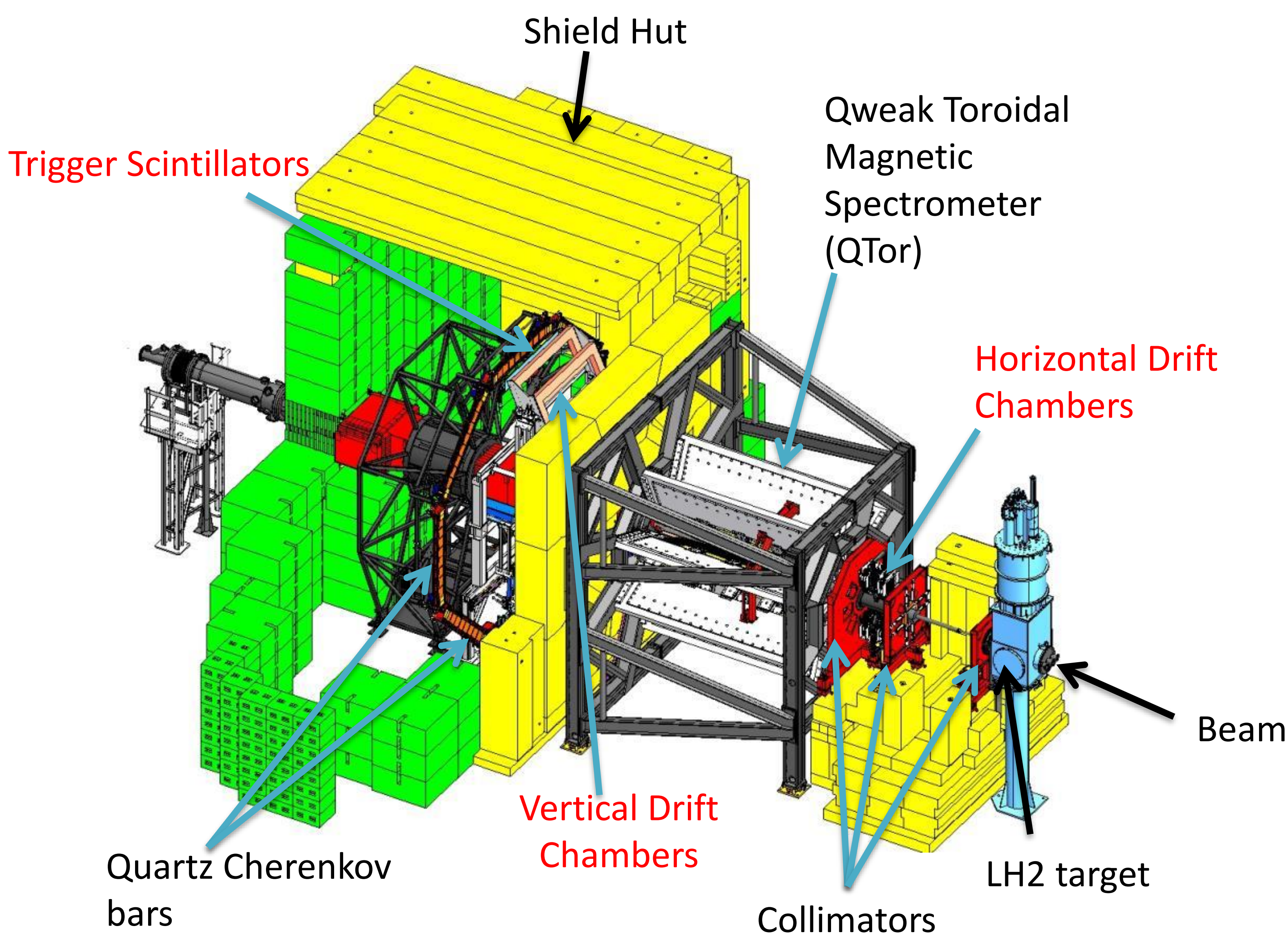

Q-weak Spectrometer (dressed)

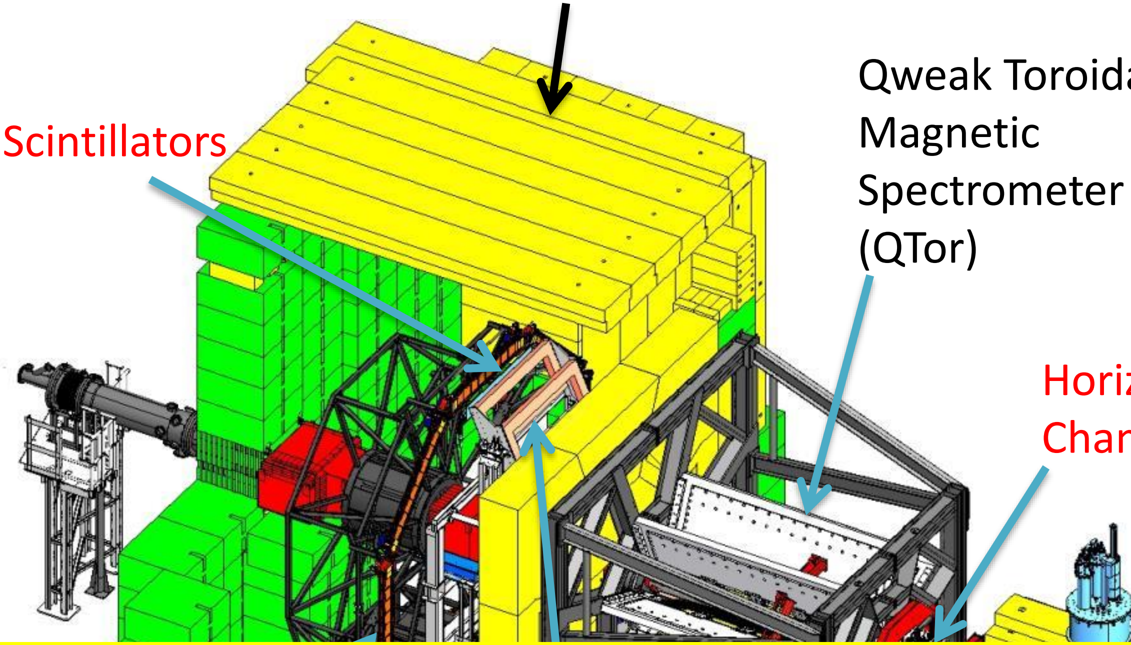

Too many custom subsystems to discuss. Essentially two experiments in one:

1. Parity production with integrating detectors at 180 muA (luminosity of 2E39)

2. Background and acceptance studies with standard event mode detectors down to 100 pA (6 orders of magnitude range in beam currents)

Target Cell

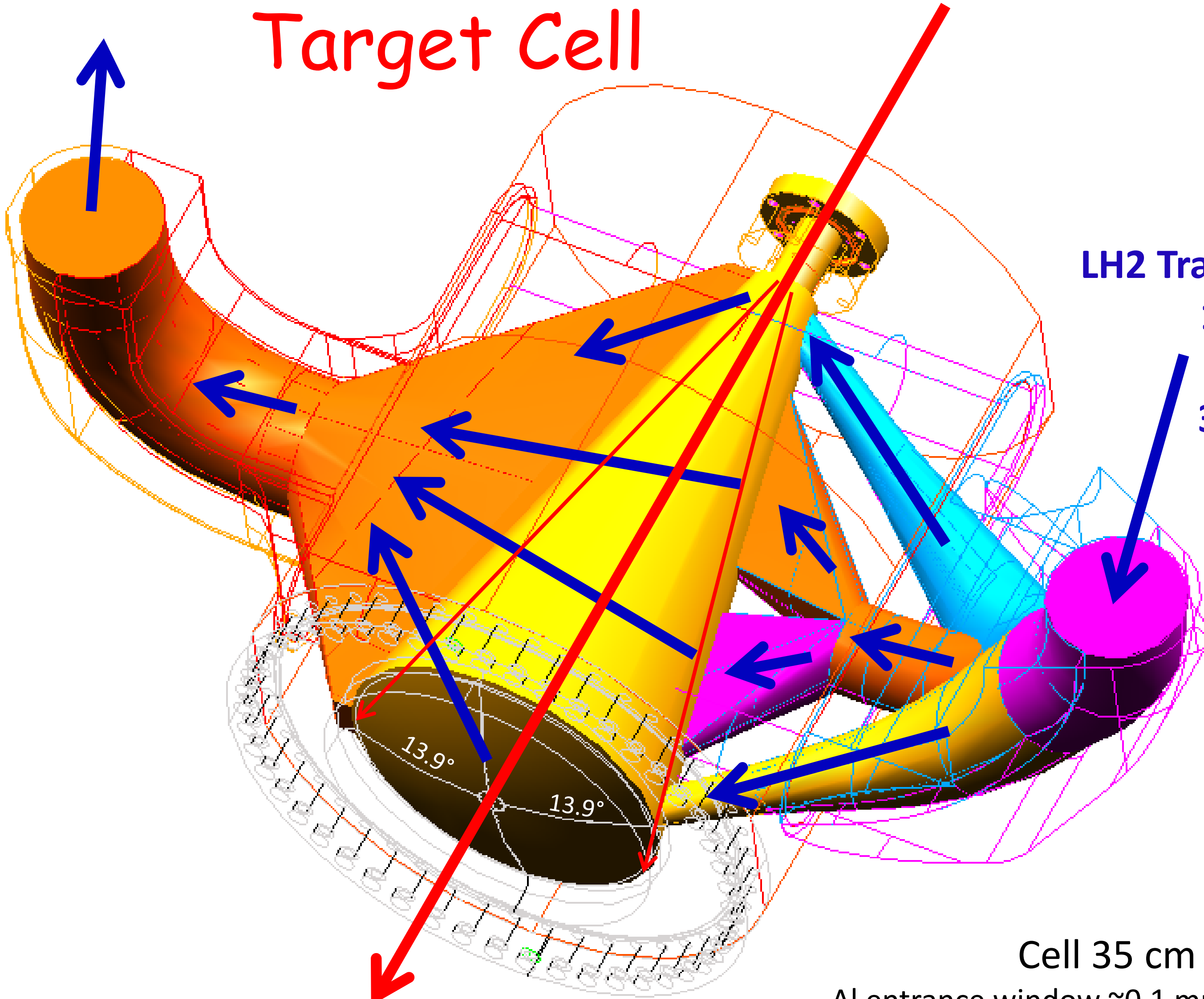

LH2 Transverse Flow:
1.1 kg/s
15 L/s
3-7 m/s

Electron Beam
180 μA, 4x4 mm²

Cell 35 cm long

Al entrance window ~0.1 mm thick, 22.2 mm Φ
Al exit window ~0.125 mm thick over 15 mm Φ,
0.635 mm thick over 173.5 mm
Scattered electron acceptance ±13.9°

Target Bubble-ology

Changes in column density between + helicity and – helicity samples are a source of noise. The main source is transient bubble formation on the Al windows. This is seen coherently by all 8 detectors so it doesn't average away. Need a great target!

Main Detector Yield (V/μA)

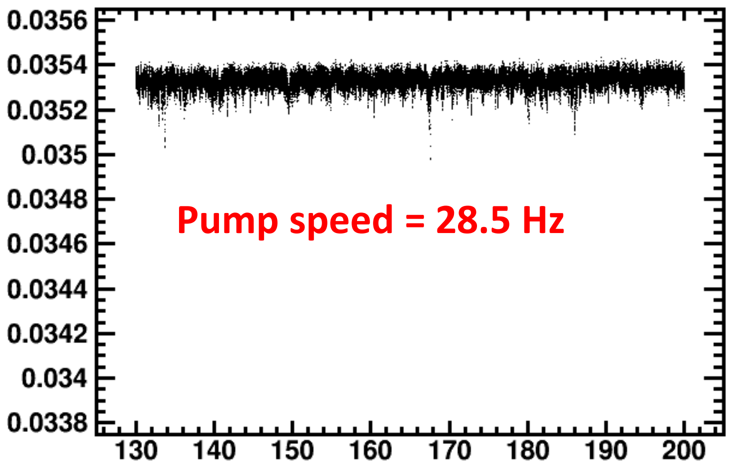

Time (sec)

The target under nominal running conditions.
(rare 1% drops in ρ*t)

Target Bubble-ology

Changes in column density between + helicity and – helicity samples are a source of noise. The main source is transient bubble formation on the Al windows. This is seen coherently by all 8 detectors so it doesn't average away. Need a great target!

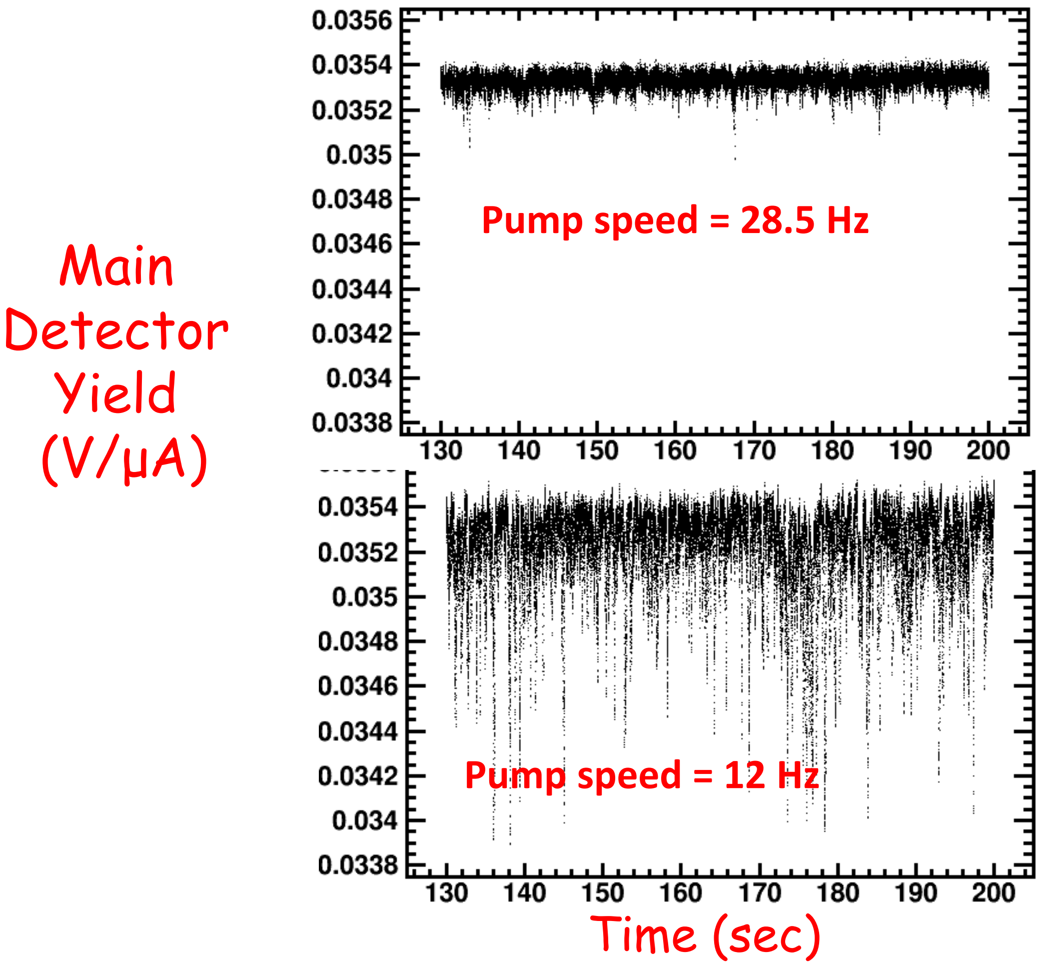

The target under nominal running conditions.
(rare 1% drops in ρ*t)

The target during a stress test.
(frequent 3% drops in ρ*t)

Precision Polarimetry

The proposal assumed $\Delta P/P \leq 1\%$, so two independent polarimeters were employed:

1. Legacy Hall C Møller polarimeter (e+e→e+e):
- Limited to few muA beam currents
- Known analyzing power provided by polarized Fe foil inserted into the beam in a 3.5 T field
- Invasive to production

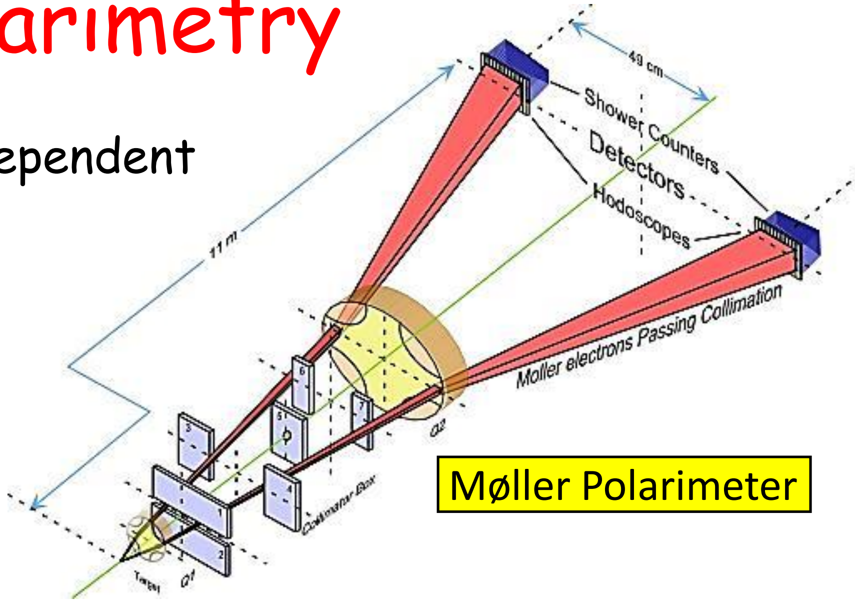

Møller Polarimeter

Precision Polarimetry

The proposal assumed $\Delta P/P \leq 1\%$, so two independent polarimeters were employed:

1. Legacy Hall C Møller polarimeter (e+e→e+e):
- Limited to few muA beam currents
- Known analyzing power provided by polarized Fe foil inserted into the beam in a 3.5 T field
- Invasive to production

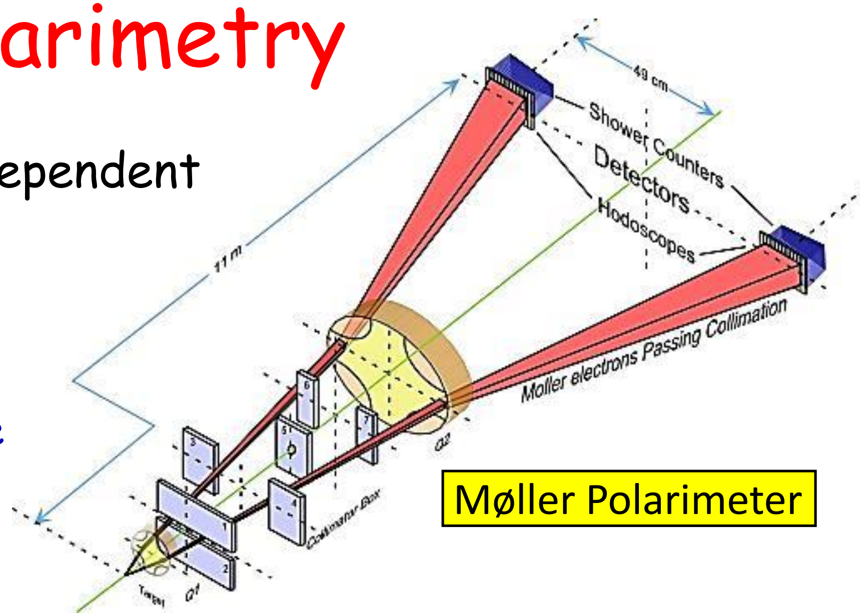

Møller Polarimeter

2. New Compton polarimeter (γ+e→γ+e):
- Full production beam current
- Known analyzing power provided by circularly-polarized laser
- Non-invasive to production

Compton Polarimeter

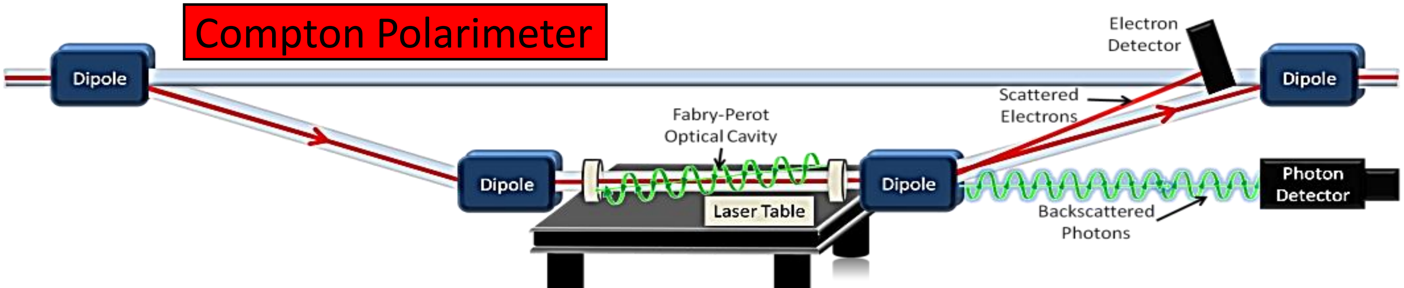

Precision Polarimetry

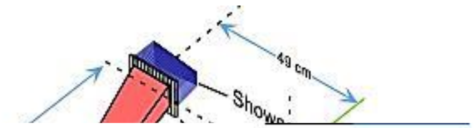

The proposal assumed ΔP/
polarimeters were employe

1. Legacy Hall C Møller polarim
- Limited to few muA beam c
- Known analyzing power prov foil inserted into the beam
- Invasive to production

2. New Compton polarimeter (
- Full production beam curre
- Known analyzing power prov circularly-polarized laser
- Non-invasive to production

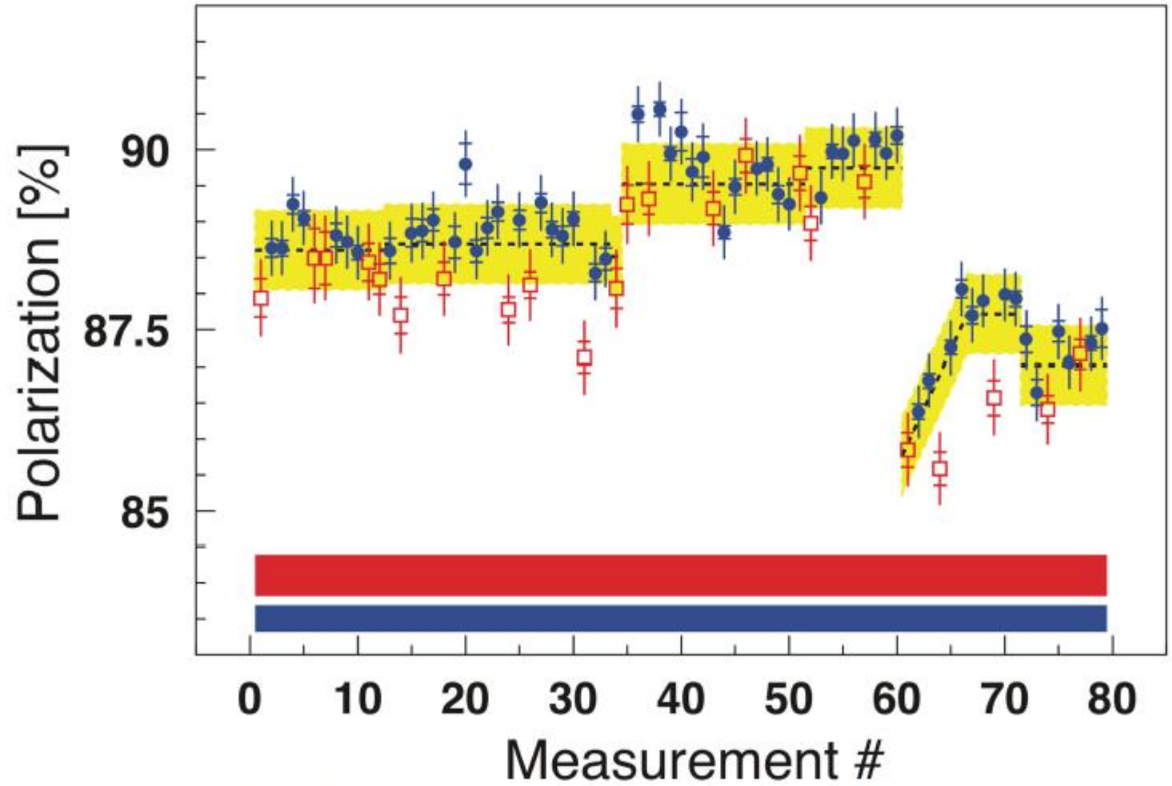

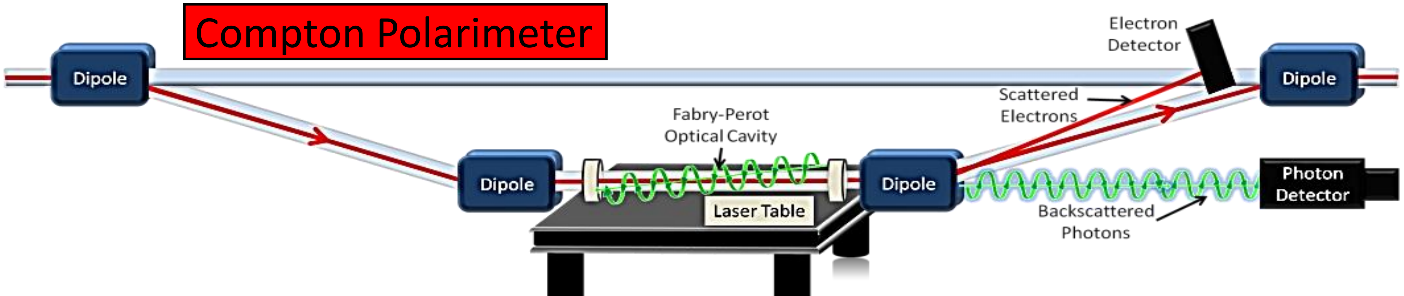

A Mini-Measurement in 1/250 Second

- Helicity flip every 1/960 sec
  ("freeze frames" the target)

- PMT anode current integrated for each helicity state, normalized to beam charge
(corrects for variations in beam current)

- Quartet asymmetries calculated
  (cancels linear drifts in signals!)

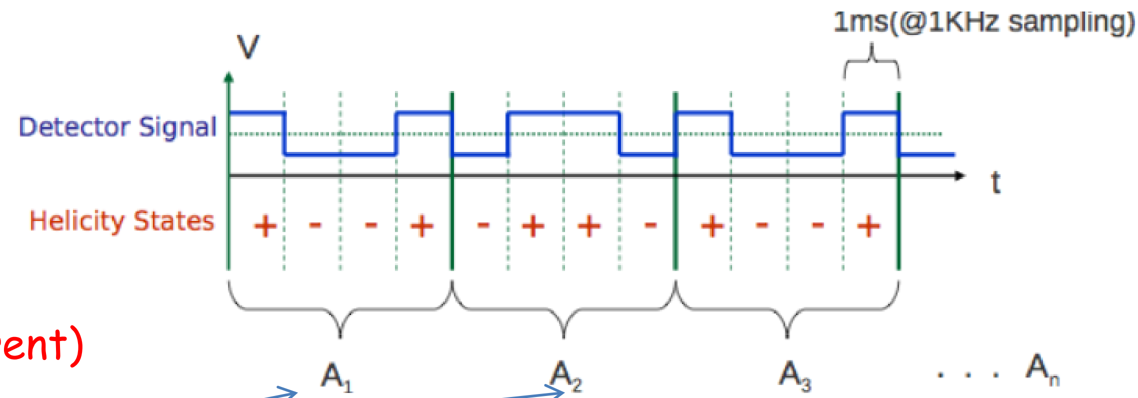

A Mini-Measurement in 1/250 Second

- Helicity flip every 1/960 sec
  ("freeze frames" the target)
- PMT anode current integrated for each helicity state, normalized to beam charge
  (corrects for variations in beam current)

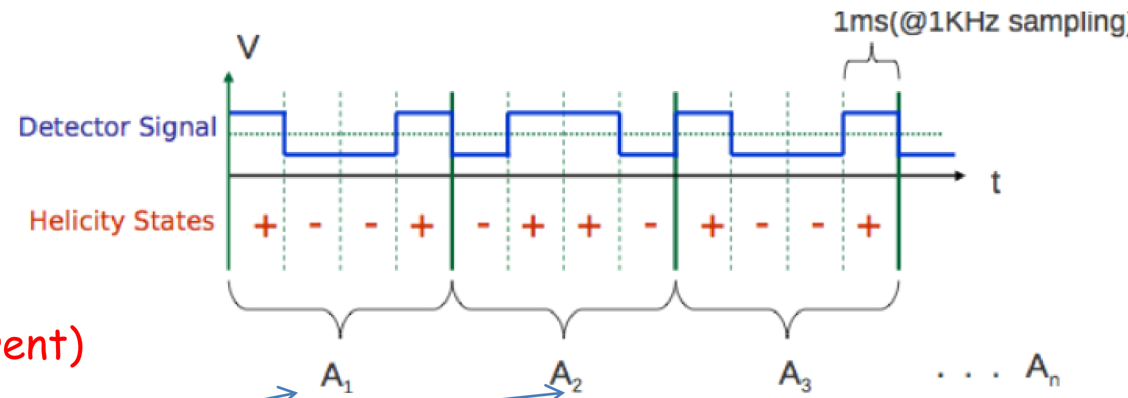

- Quartet asymmetries calculated
  (cancels linear drifts in signals!)

Plot of the ensemble of asymmetry mini-measurements at right.

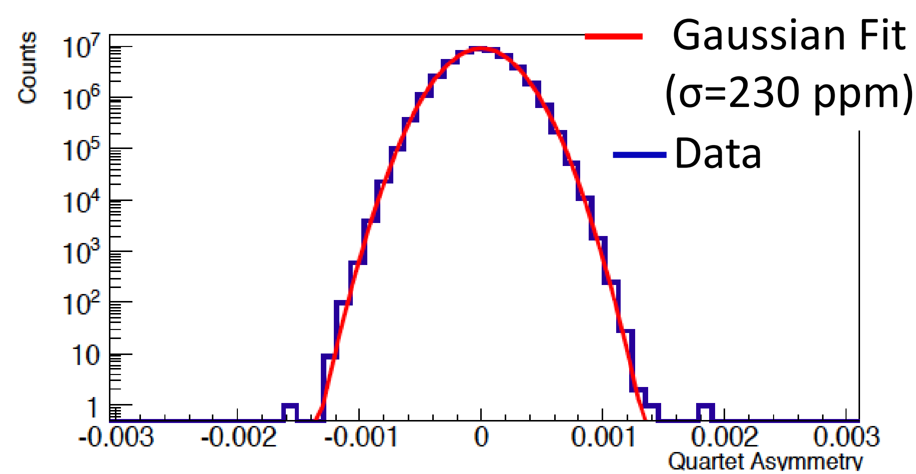

(Quartet Asymmetries over several days)

Asymmetry width ~230 ppm at 180 μA is dominated by √N .

Requires 8 hours of integration to achieve +-100pb sensitivity.

Requires days of integration for a blurry statistical picture to emerge.

The Analysis –
several years of strangling snakes

Beamline Background

Although the main detector had only 0.2% background dilution, the latter turned out to have an unexpectedly large and (slowly) time-dependent asymmetry. (Right)

•This background injected slug-scale excess noise at the O(10) ppb level, or O(5)% of our experimental asymmetry.

Asymmetry in
Blocked Main Detector
(diffuse background only)

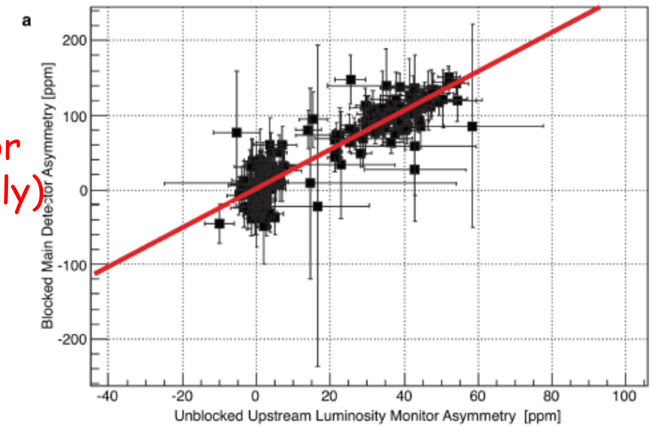

Asymmetry in
Luminosity Monitor
(diffuse background plus ee→ee)

Beamline Background

Although the main detector had only 0.2% background dilution, the latter turned out to have an unexpectedly large and (slowly) time-dependent asymmetry. (Right)

•This background injected slug-scale excess noise at the O(10) ppb level, or O(5)% of our experimental asymmetry.

• Cause? One hypothesis is that ps-scale, helicity dependent *time* differences in the injector are converted by bunching into *halo* differences.

• The HW plate didn't cancel all of it, possibly because the bunching drifted over 8 hours.

Asymmetry in
Blocked Main Detector
(diffuse background only)

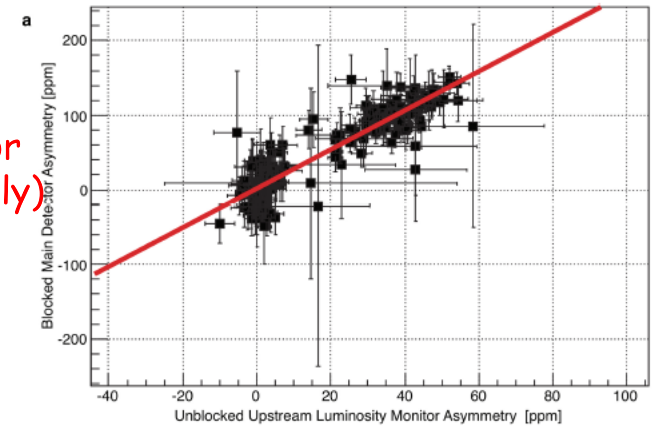

Asymmetry in
Luminosity Monitor
(diffuse background plus ee→ee)

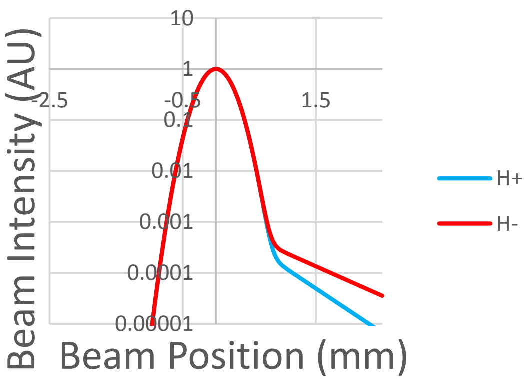

This background was strangled by removing residual correlations between the main detector and background detectors.

E. Kargiantoulakis, U. of Virginia,
https://qweak.jlab.org/do-public/ShowDocument?docid=2276

Checking the Quality of Integrating Mode Data

with no peaks, no tracks, no side-band subtractions etc.

Qweak Run 2 - Blinded Asymmetries

(statistics only - not corrected for beam polarization, Al target windows, ΔQ^2, etc.)

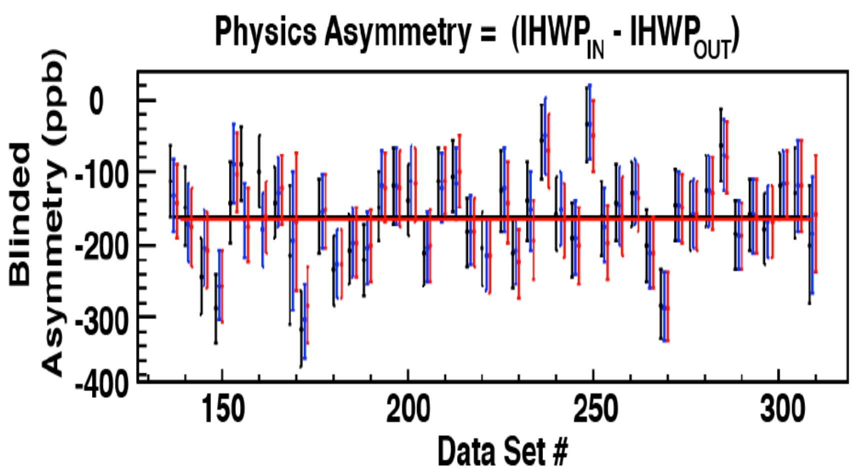

Experimental Asymmetry – Corrections make small changes in the average of fitted $P*A_{pv}$:

raw→ regressed → BB corrected
-161.8 → -160.9 → -164.5 ppb (+-7.6ppb)

In-Out already cancels some noise, but probability suggests that corrections are successful:

P = 4.3% → 18% → 33%

Checking the Quality of Integrating Mode Data

with no peaks, no tracks, no side-band subtractions etc.

Qweak Run 2 - Blinded Asymmetries

(statistics only - not corrected for beam polarization, Al target windows, ΔQ^2, etc.)

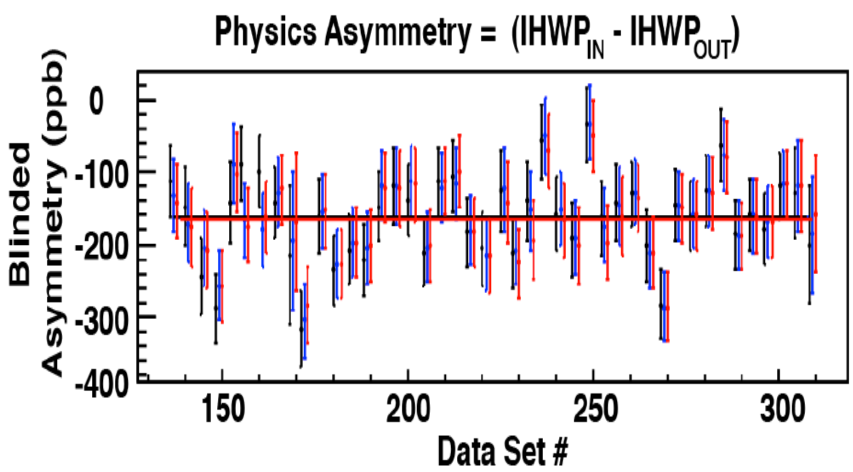

Experimental Asymmetry – Corrections make small changes in the average of fitted P^*A_{pv}:

raw → regressed → BB corrected

-161.8 → -160.9 → -164.5 ppb (+-7.6ppb)

In-Out already cancels some noise, but probability suggests that corrections are successful:

P = 4.3% → 18% → 33%

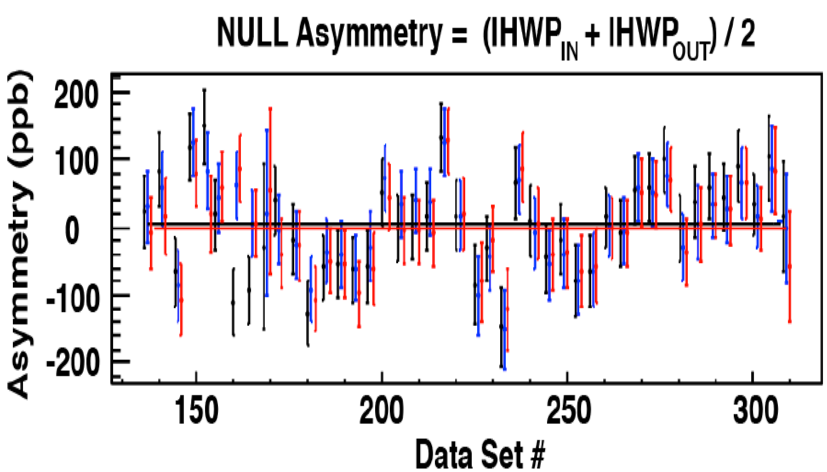

Null Asymmetry – P^*A_{pv} is consistent with zero as desired even before correction:

raw → regressed → BB corrected

4.7 → 7.9 → -1.4 ppb (+-7.7ppb)

But the probability suggests the noise was there (as expected) and the corrections are successful since it improves from unlikely to credible:

P = 0.1% → 4.8% → 9.7%

PC Transverse Asymmetry

Even small amounts of transverse beam polarization will cause the asymmetry to have a sinusoidal distribution.

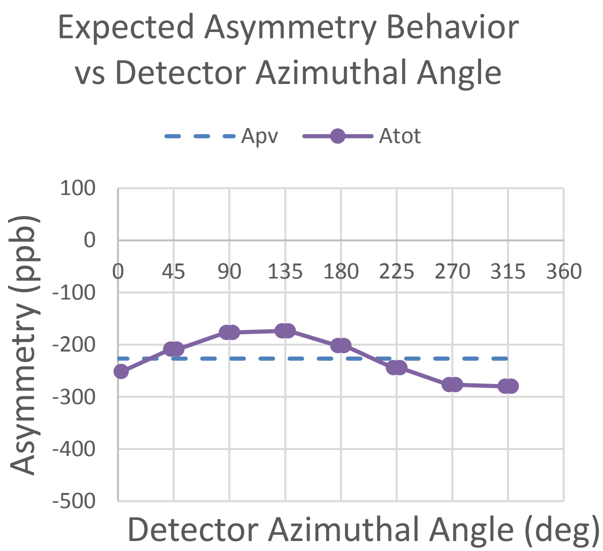

PC Transverse Asymmetry

Even small amounts of transverse beam polarization will cause the asymmetry to have a sinusoidal distribution.

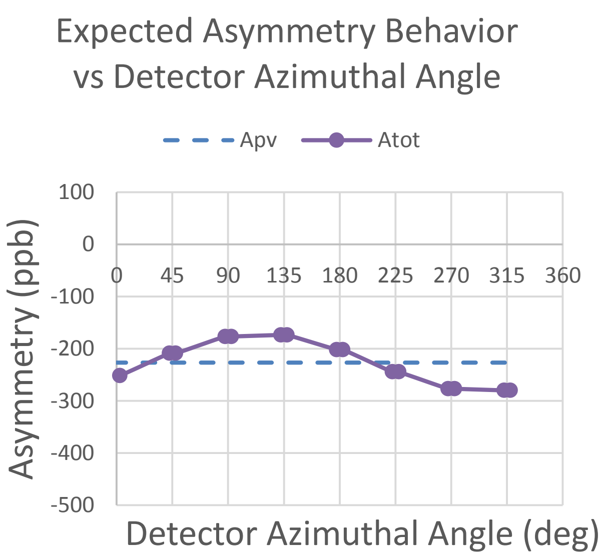

But it looked like this!

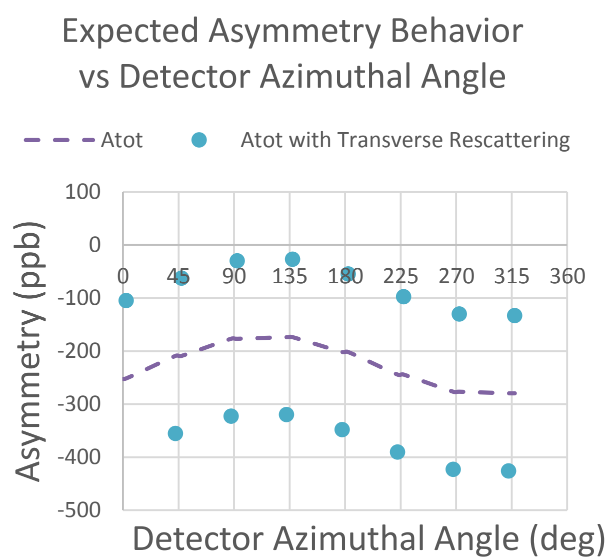

PC Transverse Asymmetry

Even small amounts of transverse beam polarization will cause the asymmetry to have a sinusoidal distribution.

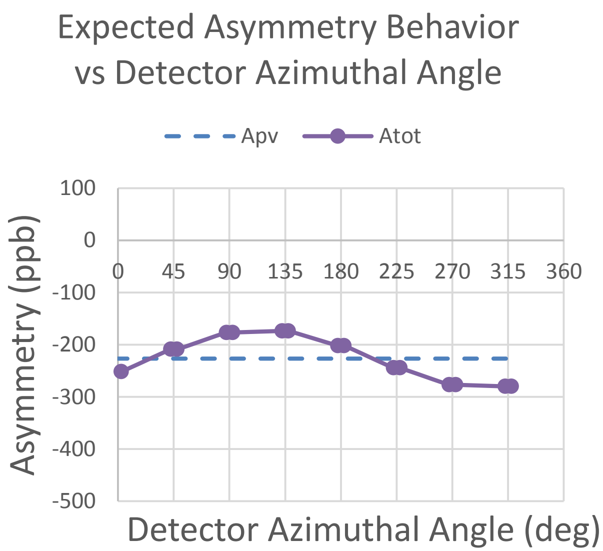

But it looked like this!

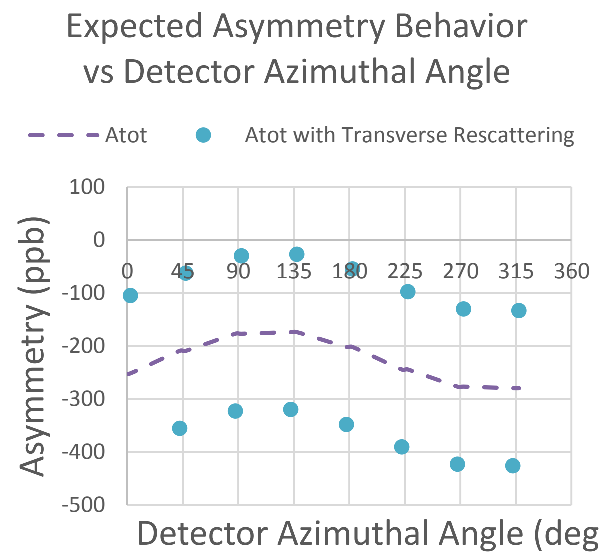

The cause: electrons hitting the detectors have precessed, giving them large transverse polarizations. A large PC asymmetry and light collection do the rest:

Less scattering toward the left pmt

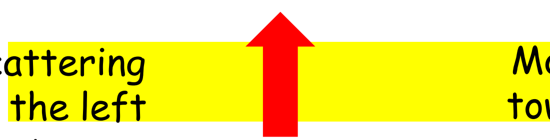

More scattering toward the right pmt

The effect nearly cancels in the average of the two pmts. But broken symmetries in light collection left us with a 0.5σ correction.

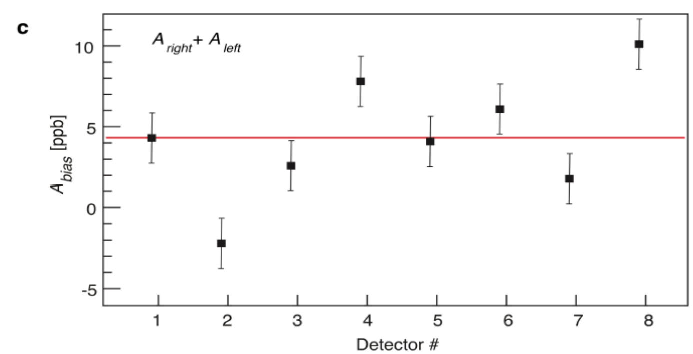

Results

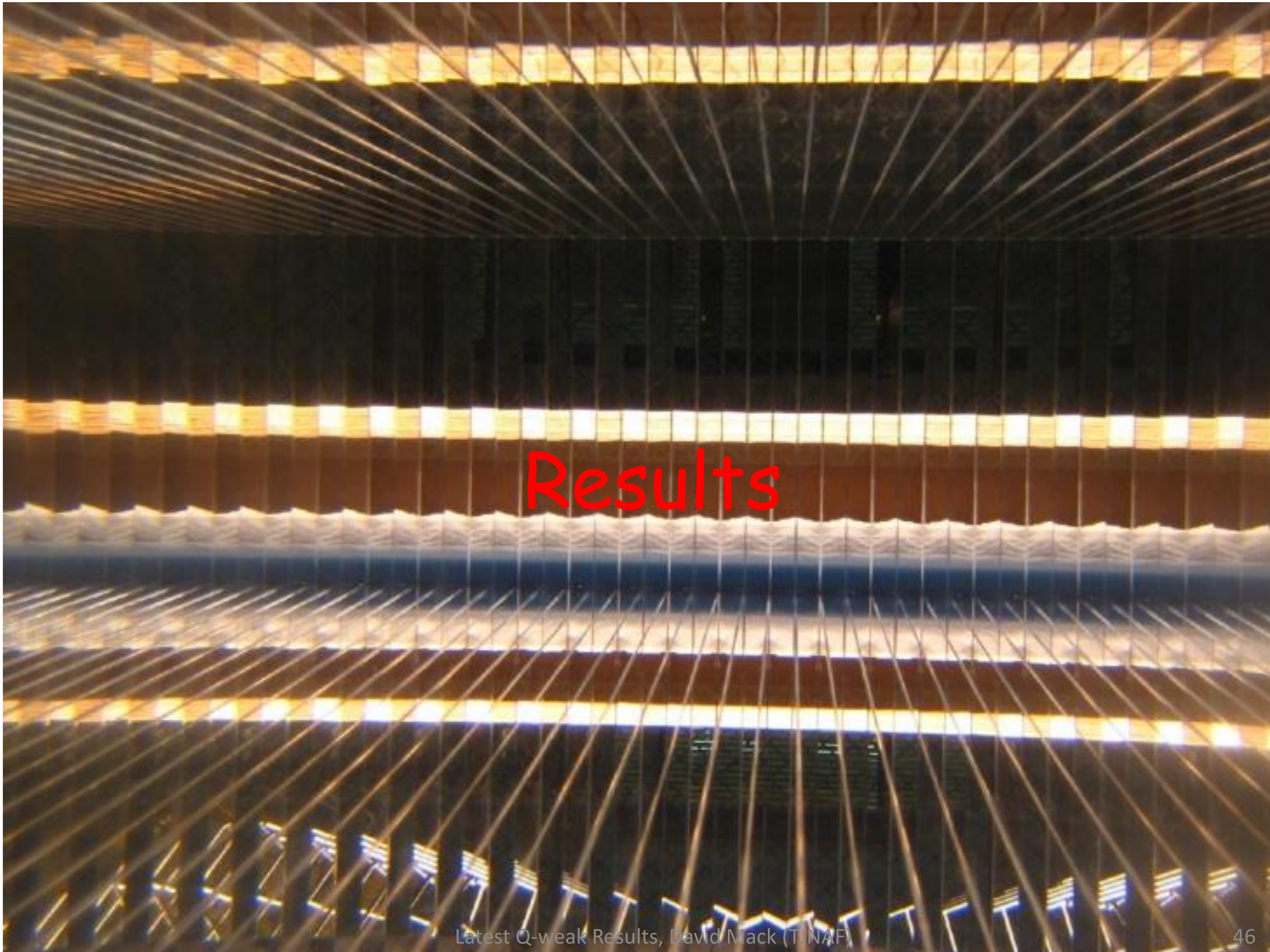

Global fit of PV Elastic Electron Scattering Data

Recall $$A_{ep} = \frac{G_F Q^2}{4\pi\alpha\sqrt{2}}\left[Q_w^p + Q^2 B(Q^2,\theta)\right]$$

Dividing out the leading Q^2 dependence and constants, and making some small angle-dependent corrections, make it easier to see the Q-weak point and world data on the same plot:

Nature **557**, 207–211 (2018)

$Q_W^p + Q^2\,B$

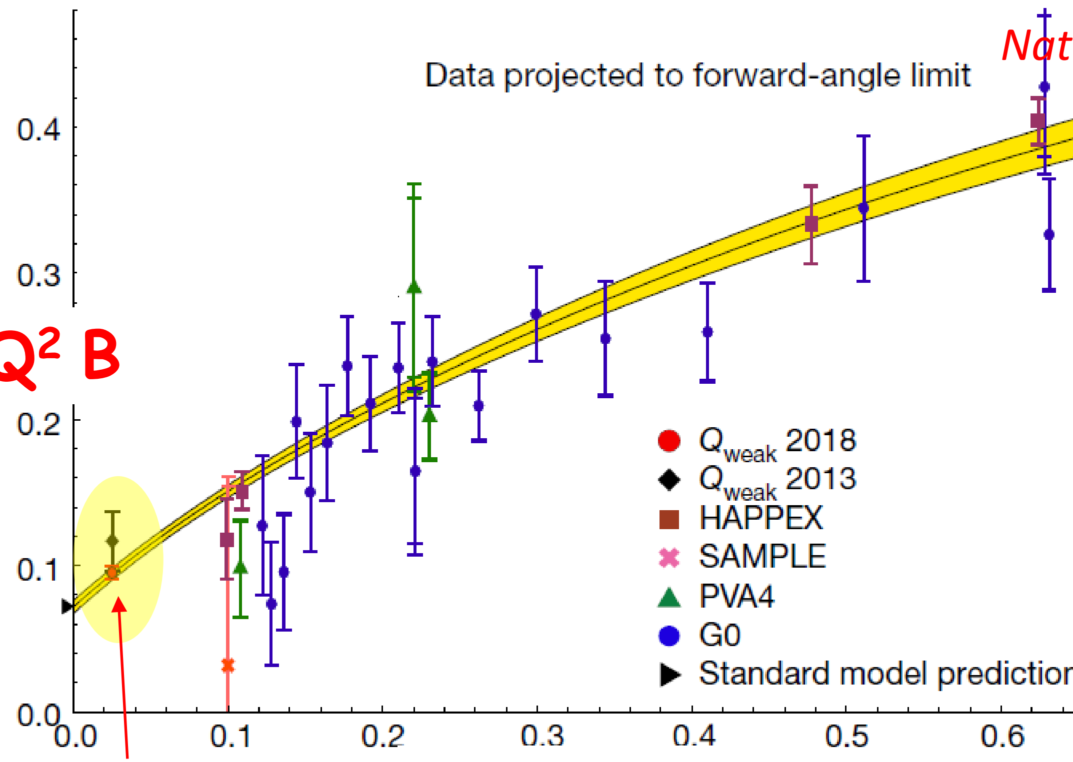

Q-weak Expt

Q^2 (GeV/c)^2

Global fit of PV Elastic Electron Scattering Data

Recall

$$A_{ep} = \frac{G_F Q^2}{4\pi\alpha\sqrt{2}}\left[Q_w^p + Q^2 B(Q^2,\theta)\right]$$

Dividing out the leading Q^2 dependence and constants, and making some small angle-dependent corrections, make it easier to see the Q-weak point and world data on the same plot:

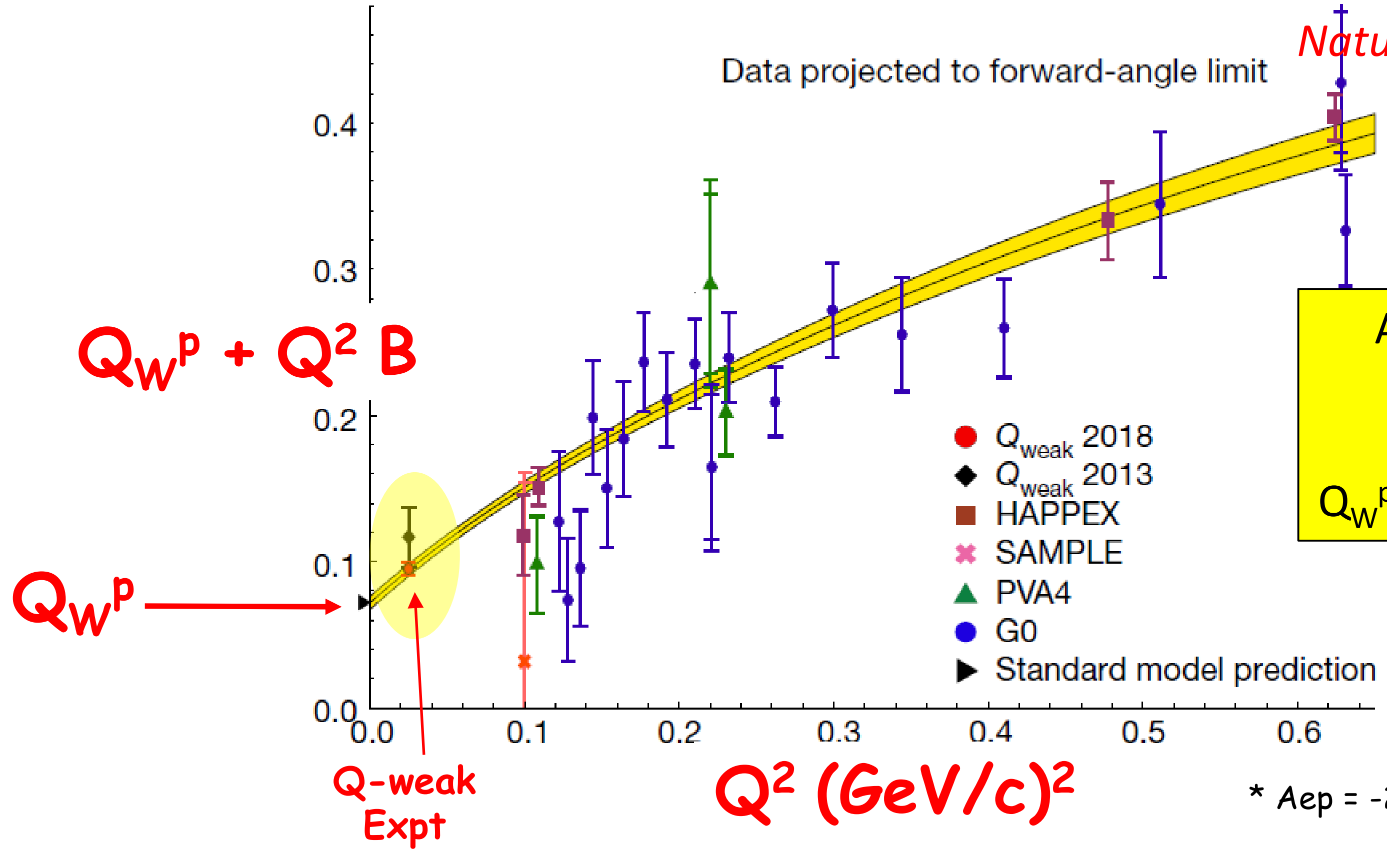

Nature **557**, 207–211 (2018)

A = -226.5 ± 9.3 ppb*

Q_W^p(SM) = 0.0708(3)

Q_W^p(Q-weak) = 0.0719(45)

* Aep = -226.5 +- 7.3 (statistical) +- 5.8 (systematic) ppb

Separating the Weak Charges of Up and Down Quarks

$C_{1d} = -Q_W^d/2$

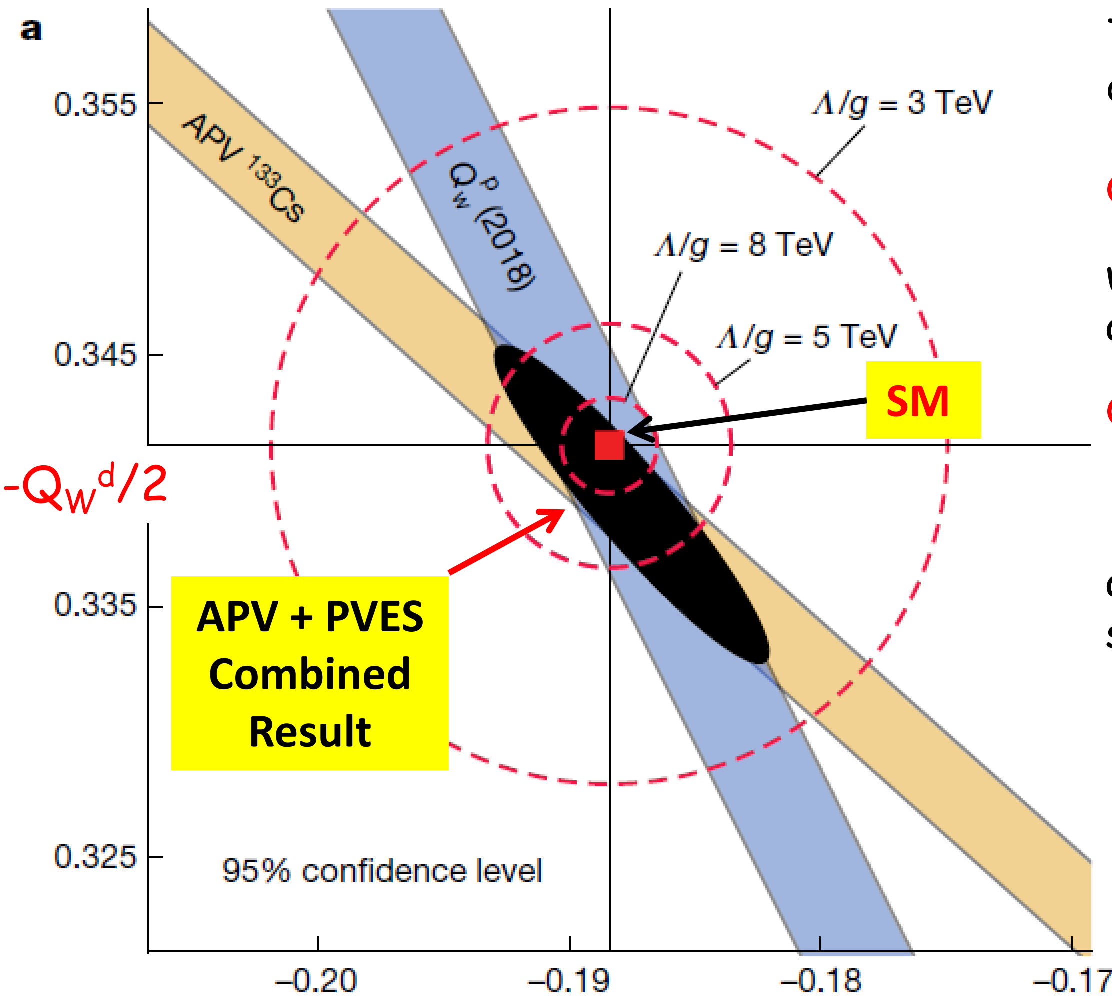

$C_{1u} = -Q_W^u/2$

The Q-weak measurement defines one band:

$Q_W^p = 2Q_W^u + Q_W^d$

while Cs Atomic PV defines another

$Q_W^{Cs} = 188Q_W^u + 211Q_W^d$

allowing the weak charges of up and down quarks to be separated.

$C_{1u} = -0.1874(22)$
$C_{1d} = 0.3389(25)$

Weak Mixing Angle Result

Nature **557**, 207–211 (2018)

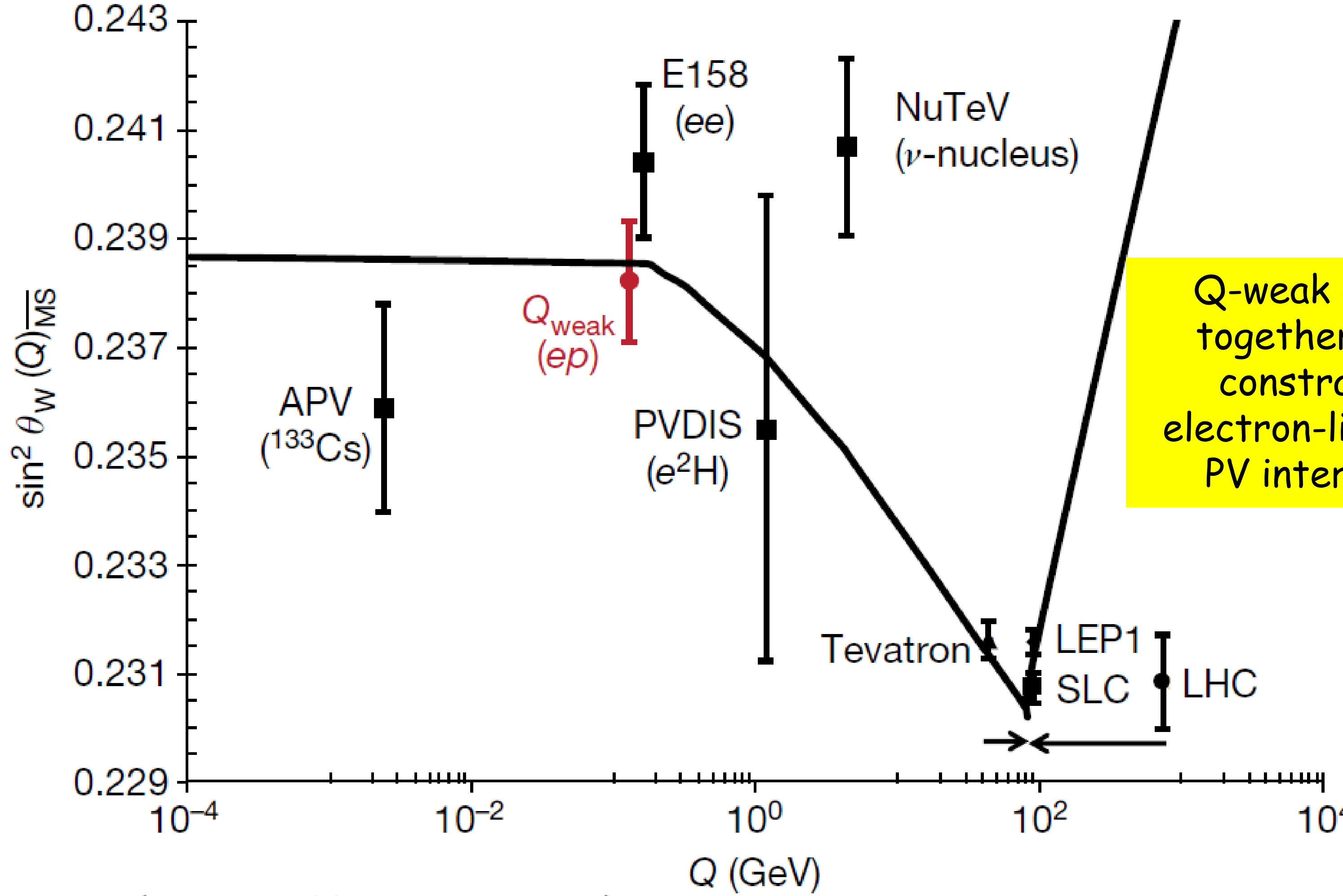

Q-weak and APV together tightly constrain new electron-light quark PV interactions

$$\sin^2\theta_w = \frac{1}{4}\left\{1 + \Delta'_e - \frac{Q_w(p) - \square_{WW} - \square_{ZZ} - \square_{\gamma Z}}{\rho_{NC} + \Delta_e}\right\}$$

Summary

- The weak vector charge of the proton, Q_w^p , is $1\text{-}4\sin^2\theta_W$ suppressed hence a good way
  i. to measure $\sin^2\theta_W$ at low energies,
  ii. to search for new PV interactions between electrons and light quarks.

- Elastic PV electron scattering at low momentum transfer allowed us to determine the weak vector charge of the proton.

- The Qweak Experiment finished successfully after 2 years in situ, ~1 year of beam on target. We have
  i. measured the smallest & most precise e+p PV asymmetry ever.
  ii. determined $Q_W(p)$ at low energies
  iii. Combined our result with Cs APV, sharpening C1u, C1d, and $Q_w(n)$.

Our results have the sensitivity to observe multi TeV-scale PV interactions, but are consistent with the SM.

- Along the way, we discovered two new backgrounds that future, higher precision PVES experiments will have to contend with:
  i. The source of the diffuse background asymmetry which changes with time is not well understood, but reversing the Half Wave Plate more frequently will help, and regression against a diffuse background detector will get the rest.
  ii. While microscopic modelling of PC transverse asymmetry effects in detectors is difficult, minimizing the relevant broken detector asymmetries will help.

The Q-weak Collaboration

W&M meeting

A. Almasalha, D. Androic, D.S. Armstrong, A. Asaturyan, T. Averett, J. Balewski, R. Beminiwattha, J. Benesch, F. Benmokhtar, J. Birchall, **R.D. Carlini**[1] **(Principal Investigator)**, G. Cates, J.C. Cornejo, S. Covrig, M. Dalton, C. A. Davis, W. Deconinck, J. Diefenbach, K. Dow, J. Dowd, J. Dunne, D. Dutta, R. Ent, J. Erler, W. Falk, **J.M. Finn**[1]*, T.A. Forest, M. Furic, D. Gaskell, M. Gericke, J. Grames, K. Grimm, D. Higinbotham, M. Holtrop, J.R. Hoskins, E. Ihloff, K. Johnston, D. Jones, M. Jones, R. Jones, K. Joo, E. Kargiantoulakis, J. Kelsey, C. Keppel, M. Kohl, P. King, E. Korkmaz, **S. Kowalski1**, J. Leacock, J.P. Leckey, A. Lee, J.H. Lee, L. Lee, N. Luwani, S. MacEwan, D. Mack, J. Magee, R. Mahurin, J. Mammei, J. Martin, M. McHugh, D. Meekins, J. Mei, R. Michaels, A. Micherdzinska, A. Mkrtchyan, H. Mkrtchyan, N. Morgan, K.E. Myers, A. Narayan, Nuruzzaman, A.K. Opper, **S.A. Page**[1], J. Pan, K. Paschke, S.K. Phillips, M. Pitt, B.M. Poelker, J.F. Rajotte, W.D. Ramsay, M. Ramsey-Musolf, J. Roche, B. Sawatzky, T. Seva, R. Silwal, N. Simicevic, **G. Smith**[2], T. Smith, P. Solvignon, P. Souder, D. Spayde, A. Subedi, R. Subedi, R. Suleiman, E. Tsentalovich, V. Tvaskis, W.T.H. van Oers, B. Waidyawansa, P. Wang, S. Wells, S.A. Wood, S. Yang, R.D. Young, S. Zhamkochyan, D. Zou

[1]Spokespersons *deceased [2]Project Manager

Misc. Q_w^p Related References

Description	Reference
Q-weak home page	https://www.jlab.org/qweak/
New Physics Sensitivities (most notably lepto-quarks)	"Weak Charge of the Proton and New Physics", Jens Erler et al. Phys. Rev. D 68, 016006 (2003). http://arxiv.org/abs/hep-ph/0302149
Proposal	The Qweak Experiment: "A Search for New Physics at the TeV Scale via a Measurement of the Proton's Weak Charge", December 10, 2007 http://qweak.jlab.org/doc-public/ShowDocument?docid=703
High accuracy calculation of the running of the weak mixing angle	"Weak Mixing Angle at Low Energies", J. Erler and M. J. Ramsey-Musolf, Phys. Rev. D 72 (2005) 073003 http://arxiv.org/abs/hep-ph/0409169
First Q-weak Result in PRL	"First Determination of the Weak Charge of the Proton", D. Androic et al., Phys. Rev. Lett. 111, 141803 (2013) http://arxiv.org/abs/1307.5275v2
Updated RPV SUSY Sensitivities	Fig 10 in "The Weak Neutral Current", Erler and Su, Prog. Part. Nucl. Phys. 71 (2013) 119-149, http://arxiv.org/abs/1303.5522
Dark Z'	"Muon Anomaly and Dark Parity Violation", H. Davoudiasl et al., PRL 109, 031802 (2012), http://arxiv.org/abs/1205.2709
Final $Q_w(p)$ results	"Precision Measurement of the Weak Charge of the Proton", D. Androic et al., Nature **557**, 207-211 (2018) . https://www.nature.com/articles/s41586-018-0096-0

Why Qwp and what is it?

1 Weak Vector Charges
2 What is Theta_W?
3 A SM test at high energy
4 Running of sin2thetaW
5 Interpretability of the Running

Determining Qwp from PVES

6 Accessing Qwp from PVES
7 Apv vs Q2
8 Methodology
9 How Small is the 200 ppb asymmetry?
10 Statistical facts of life of very small asymmetries

Apparatus

11 Accelerator site
12 Schematic of injector to detectors
13 Spectrometer basics
14 Spectrometer dressed
15 Target cell
16 Bubble-ology
17 Precision beam polarimetry
18 A mini-measurement every 1/250 second

Analysis

19 beamline bkg
20 checking data quality
21 PC transverse asymmetry

Results

22 Reduced Apv vs Q2 (and Qwp extraction)
23 Qw(up) vs Qw(down)
24 Weak mixing angle result

Summary

25 Summary

Extras

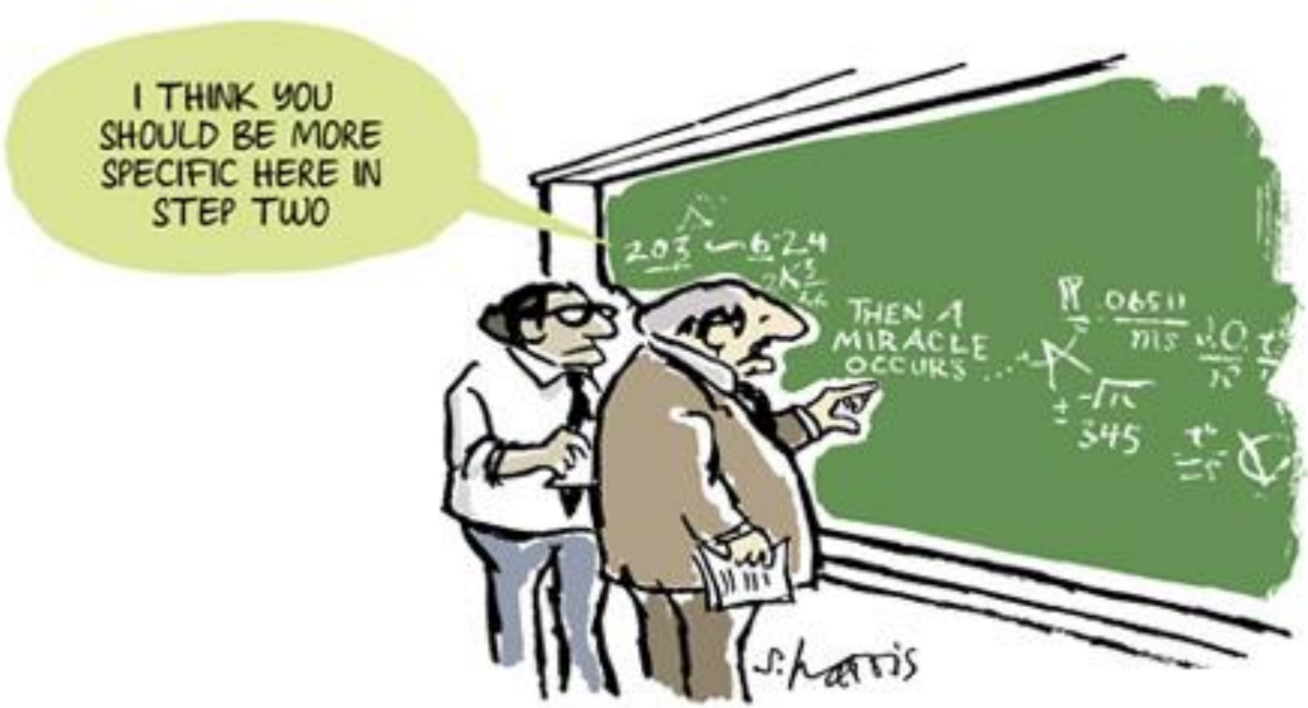
I THINK YOU SHOULD BE MORE SPECIFIC HERE IN STEP TWO
THEN A MIRACLE OCCURS
S. harris

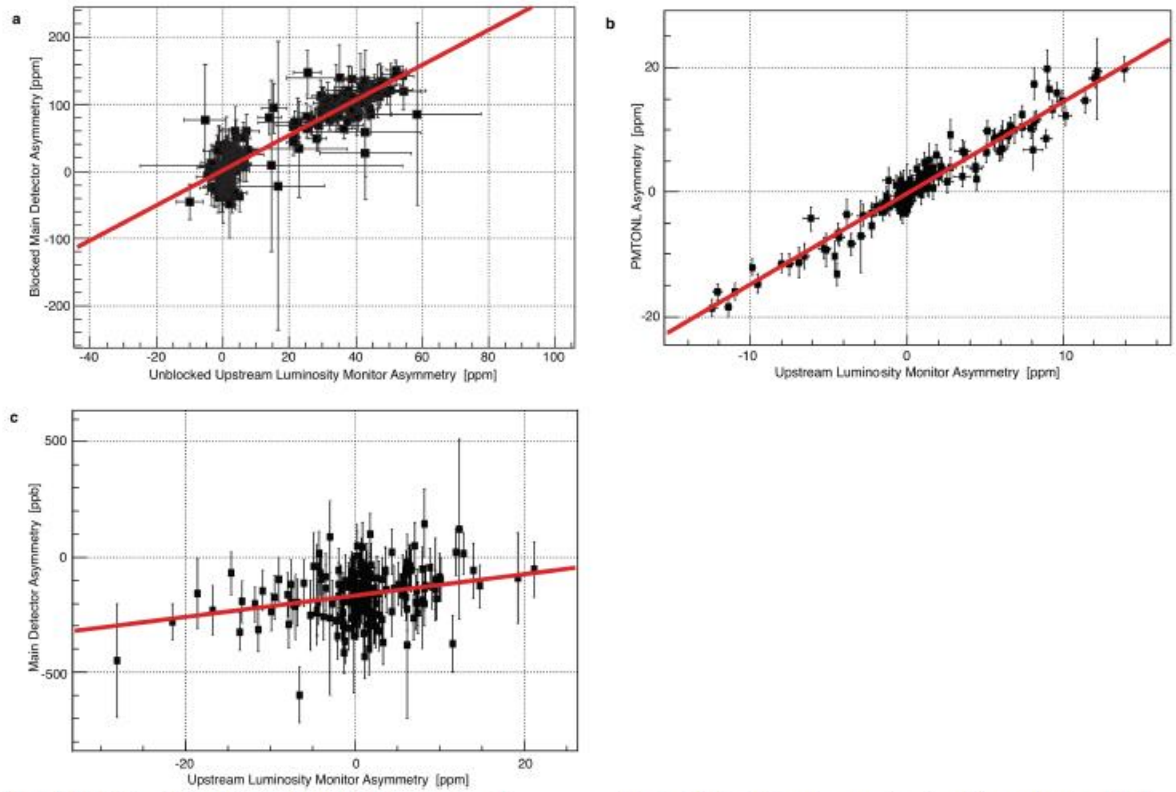

Extended Data Fig. 2 | Beamline background. Determination of A_{bb}, the false asymmetry arising from beamline background events. Uncertainties are 1 s.d. **a**, Correlation of the main detector asymmetry to that of the upstream luminosity monitors, measured when the signal from elastically scattered electrons in the main detectors was blocked at the first collimator. **b**, Correlation of asymmetries from the upstream luminosity monitors with one of the other background detectors (a bare PMT located in the detector shield house). **c**, Correlation of the unblocked main detector asymmetry to that of the upstream luminosity monitor for Run 2. Our A_{bb} determination was based on this slope.

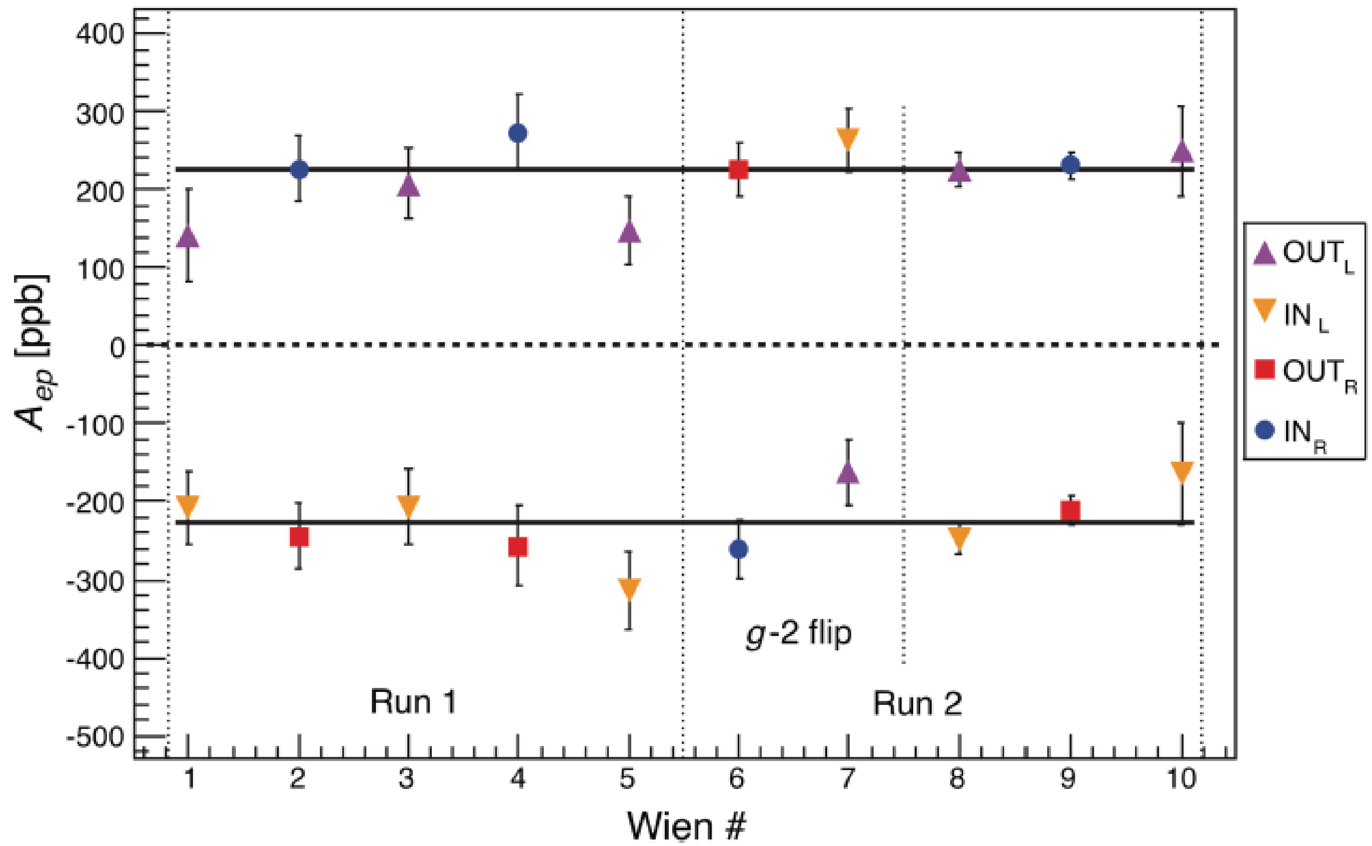

Extended Data Fig. 6 | Asymmetry from the proton. Observed parity-violating asymmetry A_{ep} after all corrections, versus the dataset number (acquired in the double-Wien-filter configuration). The Wien filter reversed the beam helicity at approximately monthly intervals. The subscripts denote the setting of the Wien filter as L or R, corresponding to the presence or absence, respectively, of a 180° rotation of the spin direction of the electron beam. IN and OUT refer to the state of the insertable half-wave plate at the electron source, generating an additional 180° flip of the spin when IN. A period in which a further 180° flip was generated through $(g_e - 2)$ precession via a modified accelerator configuration is indicated. The combinations OUT–R and IN–L with no $(g_e - 2)$ flip reveal the physical sign of the asymmetry. Solid lines represent the time-averaged values and the dashed line indicates zero asymmetry. The uncertainties (1 s.d.) shown are those of the corresponding A_{msr} values (see text) only—that is, they do not include time-independent uncertainties—so as to illustrate the time stability of the results. The weighted mean and P-value of the upper OUT–L and IN–R data are 226.9 ± 10.2, $P = 0.59$ (upper solid line), respectively. For the opposite combination, OUT–R and IN–L, we find a weighted mean of -226.1 ± 10.5 and $P = 0.36$ (lower solid line).

Uncertainties

Goals:

Source of error	Contribution to $\Delta A_{phys}/A_{phys}$	Contribution to $\Delta Q_w^p \,/\, Q_W^p$
Counting Statistics	2.1%	3.2%
Hadronic structure	—	1.5%
Beam polarimetry	1.0%	1.5%
Absolute Q^2	0.5%	1.0%
Backgrounds	0.7%	1.0%
Helicity-correlated beam properties	0.5%	0.8%
TOTAL:	2.5%	4.2%

Hadronic contributions to A_{PV} magnify the error in going from A_{PV} to Q_W^p

2% on A_z
$\approx$ 4% on Q_w
$\approx$ 0.3% on $sin^2\theta_W$

What	Goal on Apv	Achieved on Apv
Statistics	2.1%	3.2%
Systematics	1.36%	2.6%
Total Uncertainty	2.5%	4.1%

Achieved:

Extended Data Table 2 | Asymmetries and their corrections

Period	Asymmetry (ppb)	Stat. Unc. (ppb)	Syst. Unc. (ppb)	Tot. Uncertainty (ppb)
Run 1	-223.5	15.0	10.1	18.0
Run 2	-227.2	8.3	5.6	10.0
Run 1 and 2 combined with correlations	-226.5	7.3	5.8	9.3

Extended Data Table 2 | Asymmetries and their corrections

Period	Asymmetry (ppb)	Stat. Unc. (ppb)	Syst. Unc. (ppb)	Tot. Uncertainty (ppb)
Run 1	-223.5	15.0	10.1	18.0
Run 2	-227.2	8.3	5.6	10.0
Run 1 and 2 combined with correlations	-226.5	7.3	5.8	9.3

Quantity	Run 1 error (ppb)	Run 1 fractional	Run 2 error (ppb)	Run 2 fractional
BCM Normalization: A_{BCM}	5.1	25%	2.3	17%
Beamline Background: A_{BB}	5.1	25%	1.2	5%
Beam Asymmetries: A_{beam}	4.7	22%	1.2	5%
Rescattering bias: A_{bias}	3.4	11%	3.4	37%
Beam Polarization: P	2.2	5%	1.2	4%
Target windows: A_1	1.9	4%	1.9	12%
Kinematics: R_{Q^2}	1.2	2%	1.3	5%
Total of others	2.5	6%	2.2	15%
Combined in quadrature	10.1		5.6	

Top, corrected asymmetries A_{ep} for the Run 1 and Run 2 datasets, and the combined value, with their statistical (Stat. Unc.), systematic (Syst. Unc.) and total (Tot.) uncertainties (1 s.d.), in parts per billion (ppb). Bottom, fractional quadrature contributions $(\sigma_i/\sigma_{\mathrm{tot}})^2$ to the systematic uncertainty (1 s.d.) on A_{ep} for Run 1 and Run 2. Only error sources with fractional contribution $\geq 5\%$ in one of the runs are shown.

Extended Data Table 1 | Helicity-correlated beam parameter differences and sensitivities

Beam Parameter	Run 1 $\Delta\chi_i$	Run 2 $\Delta\chi_i$	Typical $\partial A/\partial\chi_i$
X	-3.5 ± 0.1 nm	-2.3 ± 0.1 nm	-2 ppb/nm
X'	-0.30 ± 0.01 nrad	-0.07 ± 0.01 nrad	50 ppb/nrad
Y	-7.5 ± 0.1 nm	0.8 ± 0.1 nm	< 0.2 ppb/nm
Y'	-0.07 ± 0.01 nrad	-0.04 ± 0.01 nrad	< 3 ppb/nrad
Energy	-1.69 ± 0.01 ppb	-0.12 ± 0.01 ppb	-6 ppb/ppb

The beam parameter differences and typical detector sensitivities for the five measured beam parameters for Run 1 and Run 2. Uncertainties are 1 s.d.

Table 1 | Results extracted from the asymmetry measured in the Q_{weak} experiment

Method	Quantity	Value	Error
PVES fit	Q_W^p	0.0719	0.0045
	ρ_s	0.20	0.11
	μ_s	−0.19	0.14
	$G_A^{Z\,(T=1)}$	−0.64	0.30
PVES fit + APV	Q_W^p	0.0718	0.0044
	Q_W^n	−0.9808	0.0063
	C_{1u}	−0.1874	0.0022
	C_{1d}	0.3389	0.0025
	C_1 correlation	−0.9318	
PVES fit + LQCD	Q_W^p	0.0685	0.0038
Q_{weak} datum only	Q_W^p	0.0706	0.0047
Standard model	Q_W^p	0.0708	0.0003

'PVES fit' refers to a global fit incorporating the Q_{weak} result and the PVES database, as described in Methods. When combined with APV[14,15] (to improve the C_{1d} precision), this method is denoted as 'PVES fit + APV'. If the strange form factors in the global fit (without APV) are constrained to match LQCD calculations[16], we label the result as 'PVES fit + LQCD'. The method labelled 'Q_{weak} datum only' uses the Q_{weak} datum, together with electromagnetic[9], strange[16] and axial[18] form factors from the literature in lieu of the global fit. Uncertainties are 1 s.d.

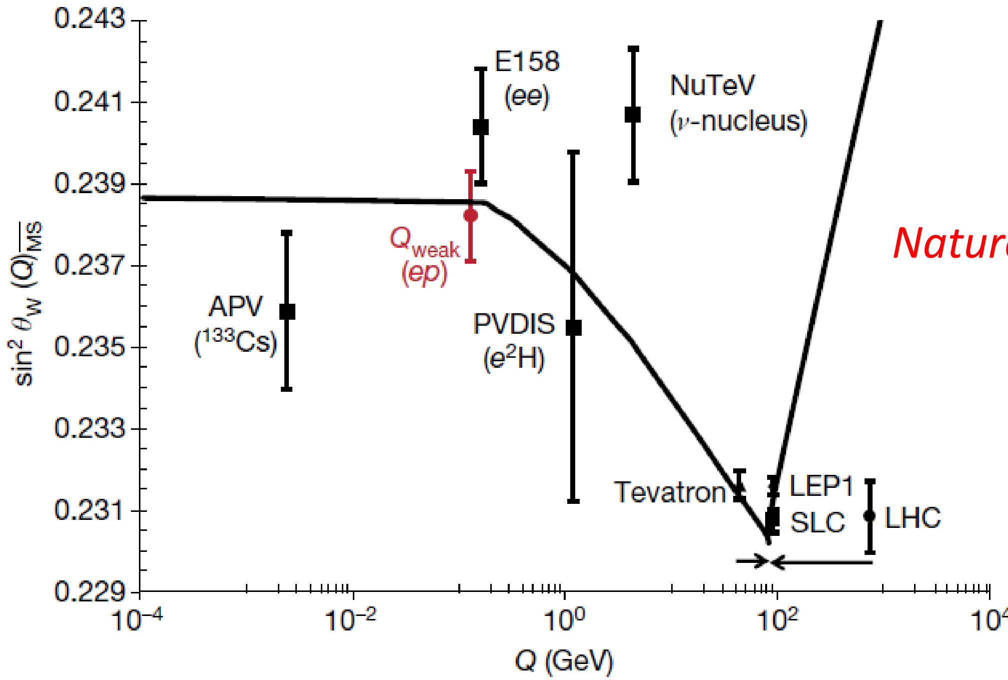

Nature **557**, 207–211 (2018)

Fig. 3 | Variation of $\sin^2\theta_W$ with energy scale Q. The modified-minimal-subtraction ($\overline{MS}$) scheme is shown as the solid curve[2,19], together with experimental determinations at the Z^0 pole[2] (Tevatron, LEP1, SLC, LHC), from APV on caesium[14,15], Møller scattering (E158)[22], deep inelastic scattering of polarized electrons on deuterons (e^2H; PVDIS)[23] and from neutrino–nucleus scattering (NuTeV)[24]. It has been argued[25], however, that the latter result contains substantial unaccounted-for nuclear physics effects, such as neutron-excess corrections to the quark momenta, charge-symmetry breaking and strange-quark momentum asymmetries. Our new result is plotted in red at the energy scale of the Q_{weak} experiment, $Q = 0.158$ GeV (slightly offset horizontally for clarity). Error bars (1 s.d.) include statistical and systematic uncertainties.

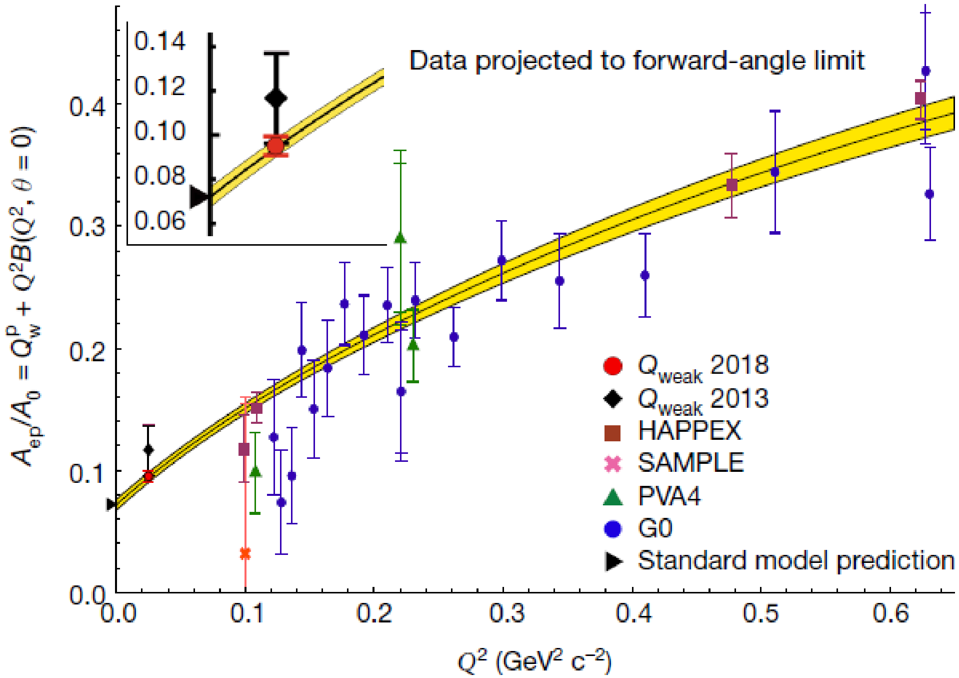

Fig. 2 | The reduced asymmetry $A_{ep}/A_0 = Q_w^p + Q^2B(Q^2, \theta = 0)$ versus Q^2. The global fit is illustrated using *ep* asymmetries from this experiment (Q_{weak} 2018), from the commissioning phase of this experiment[3] (Q_{weak} 2013), as well as from the earlier experiments HAPPEX, SAMPLE, PVA4 and G0 (see Methods), projected to $\theta = 0°$ and reduced by a factor $A_0(Q^2)$ appropriate for each datum. The data shown here include the γZ-box radiative correction and uncertainty. Inner error bars correspond to one standard deviation (s.d.) and include statistical and systematic uncertainties. Outer error bars on the data indicate the additional uncertainty estimated from the forward-angle projection (for some data points, inner and outer error bars coincide). The solid line represents the global fit to the complete PVES database (see Methods), and the yellow band indicates the fit uncertainty (1 s.d.). The arrowhead at $Q^2 = 0$ indicates the standard-model prediction[2], $Q_w^p = 0.0708(3)$, which agrees well with the intercept of the fit ($Q_w^p = 0.0719 \pm 0.0045$). The inset shows a magnification of the region around this experiment's result, at $\langle Q^2 \rangle = 0.0248$ GeV^2 c^{-2}.

Inelastic e+p Transverse Asymmetry Results

Parity conserving (2-boson exchange) azimuthal asymmetries

- Hydrogen elastic → constrains contribution to PV asymmetry, but also provides information on 2-photon exchange effects in form factor extraction
- **Hydrogen resonance (Delta)**
- Aluminum, carbon

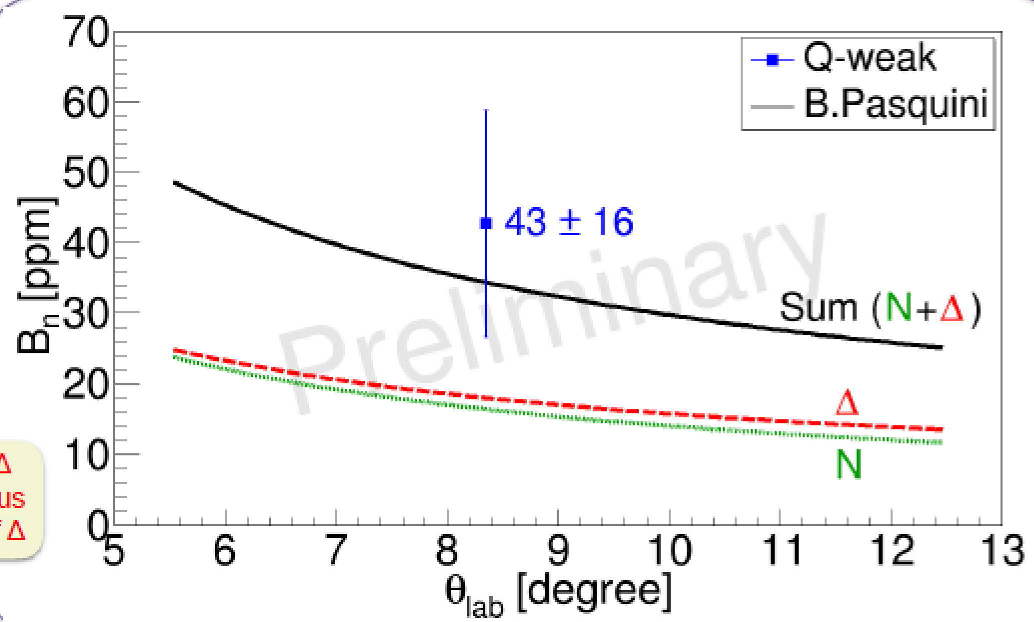

Unique tool to study g*ΔΔ form factors, charge radius and magnetic moment of Δ

The prediction of a very large asymmetry at forward angles is confirmed.

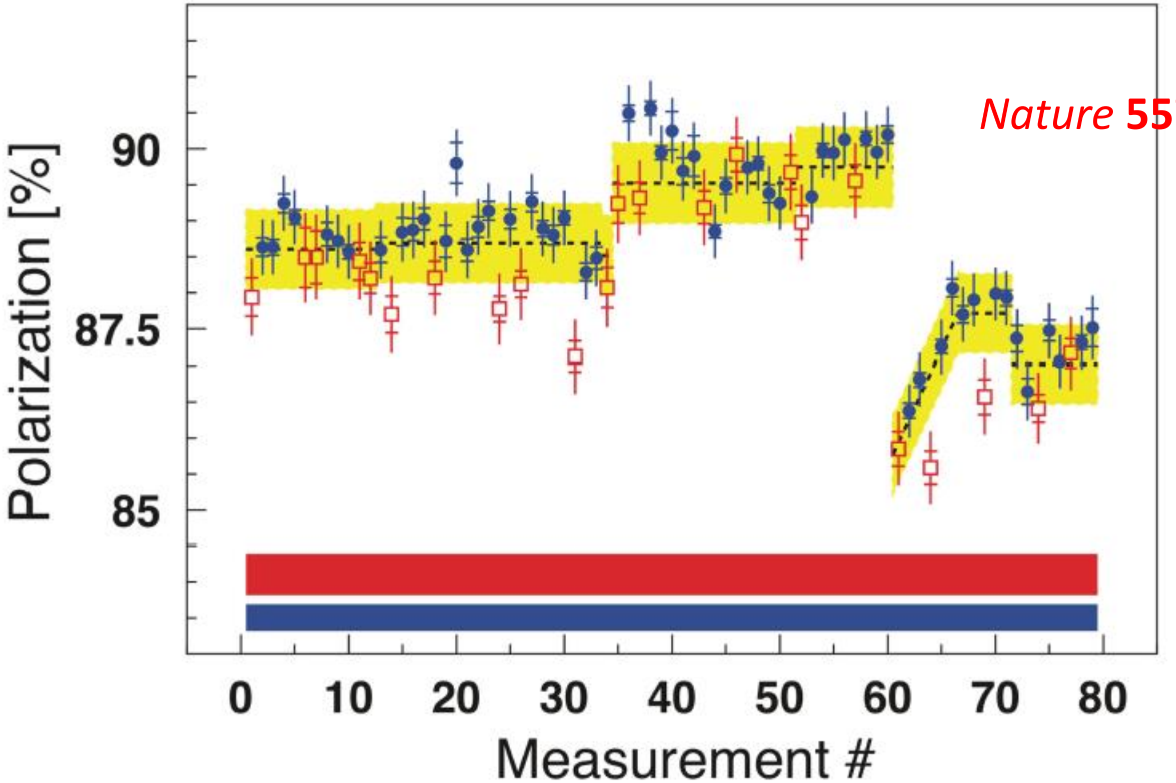

Nature **557**, 207–211 (2018)

Extended Data Fig. 4 | Electron beam polarization. Measurements from the Compton (closed blue circles) and Møller (open red squares) polarimeters during Run 2. Inner error bars denote statistical uncertainties and outer error bars show the statistical and point-to-point systematic uncertainties added in quadrature. Normalization, or scale-type, uncertainties are shown by the solid blue (Compton) and red (Møller) bands. All uncertainties are 1 s.d. The yellow band shows the derived polarization values used in the evaluation of the parity-violating asymmetry A_{ep}. The time dependence of the reported polarization is driven primarily by the continuous Compton measurements, with a small-scale correction (0.21%, not included in this figure) determined from an uncertainty-weighted global comparison of the Compton and Møller polarimeters.

Hadronic Physics Spinoff: Transverse Asymmetry B_n in e+p Elastic Scattering

B_n is a parity <u>conserving</u>, transverse, single-spin asymmetry due to the interference between 1γ and 2γ exchange.

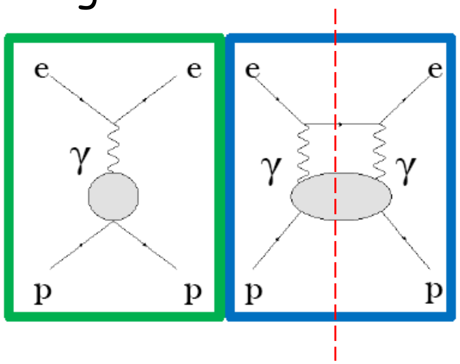

$$B_N = \frac{2T_{1\gamma} \times \mathrm{Im}\, T_{2\gamma}}{|T_{1\gamma}|}$$

As a background - B_n is O(100) times larger than Apv, so a few % P_T can give sinusoidal variations in the detector signal which are as large as the Q-weak signal. Small broken asymmetries in our detector could lead to O(1)ppb corrections.

In terms of physics - Since B_n depends on the imaginary part of the 2γ exchange amplitude, our 1.16 GeV beam energy data provide an integral measurement of all proton excitations up to E_{cm} = 1.7 GeV.

Uncorrected asymmetry

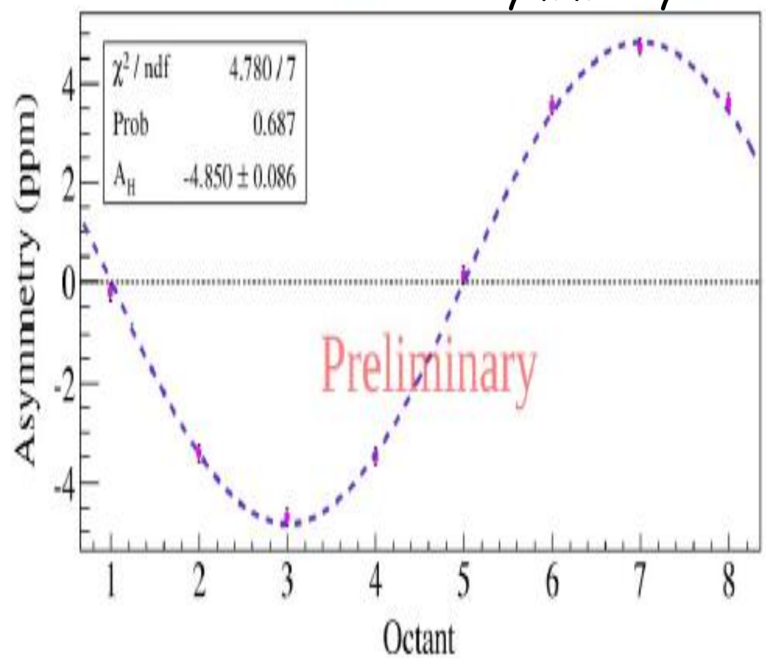

B Waidyawansa talk at PAVI14, http://pavi14.syr.edu/Slides.html

Elastic e+p Transverse Asymmetry Results

Good news – this is probably the most accurately measured e+p asymmetry at the GeV scale, < 3%.

Bad news – publication has been delayed for years while we studied the PC rescattering background (~1%).

Green curve - A pioneering model which used only MAID single π amplitudes significantly under-predicted the data.

Orange and **Purple** curves - Models which use photo-production data to constrain the forward Compton amplitude do reasonably well.

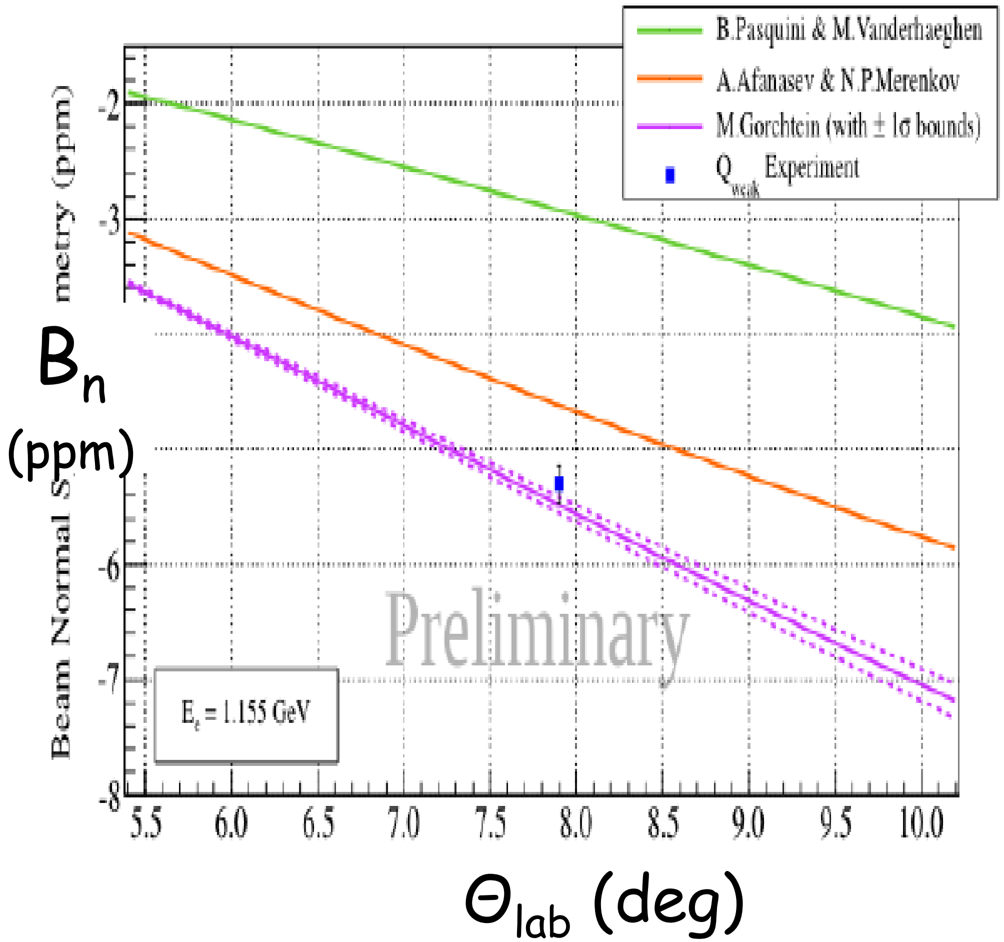

Intermediate states in the 2γ box diagram like N + multi-π are important.

Energy Scale of a Q_w^p Measurement

The sensitivity to new physics Mass/Coupling ratio can be estimated by adding a new PV contact term to the electron-quark Lagrangian (Erler et al. PRD 68, 016006 (2003)):

$$\begin{aligned} \mathcal{L}_{e-q}^{PV} &= \mathcal{L}_{SM}^{PV} + \mathcal{L}_{New}^{PV} \\ &= -\frac{G_F}{\sqrt{2}} \bar{e}\gamma_\mu\gamma_5 e \sum_q C_{1q} \bar{q}\gamma^\mu q + \frac{g^2}{4\Lambda^2} \bar{e}\gamma_\mu\gamma_5 e \sum_q h_V^q \bar{q}\gamma^\mu q \end{aligned}$$

where Λ is the mass and g is the coupling.

A new physics "pull" on the proton weak charge, ΔQ_w^p, can then be related to the mass to coupling ratio:

$$\frac{\Lambda}{g} = \frac{1}{\sqrt{\sqrt{2} G_F}} \cdot \frac{1}{\sqrt{\Delta Q_W(p)}}$$

- Assuming $\Delta Q_w^p = 4\% \times Q_w^p$, and $g \sim 1$, then Λ is TeV scale.
- But sensitivity is "broad band" in mass: a 200 MeV/c^2 new particle with small couplings could have the same pull as a 20 TeV/c^2 particle with large couplings.
- Note that accessing the TeV scale via precision electroweak measurements is tough due to the square root factor of the experimental error:

going from 1 TeV to 2 TeV requires a FOM which is $2^4 = 16$ times greater.

SUSY Sensitivities

updated with plot from Erler and Su (2013)

R-parity Violating (tree-level) SUSY:

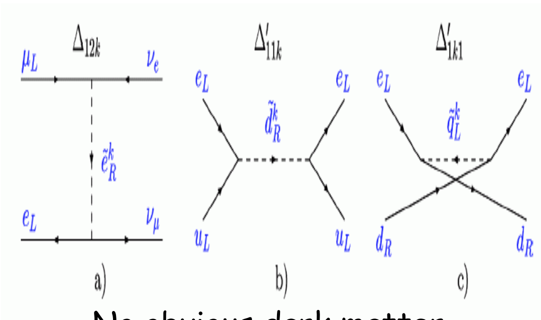

No obvious dark matter.
("New" particles would decay to normal matter.)

R-parity Conserving (loop-level) SUSY:

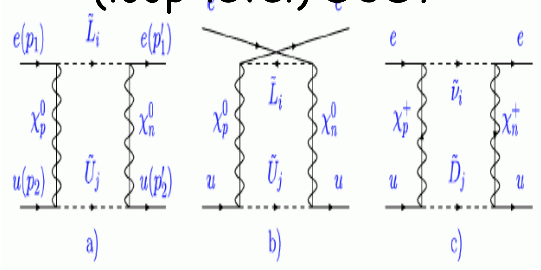

Dark matter may be the lightest SUSY particle.
(It got "stuck" carrying the R quantum number.)

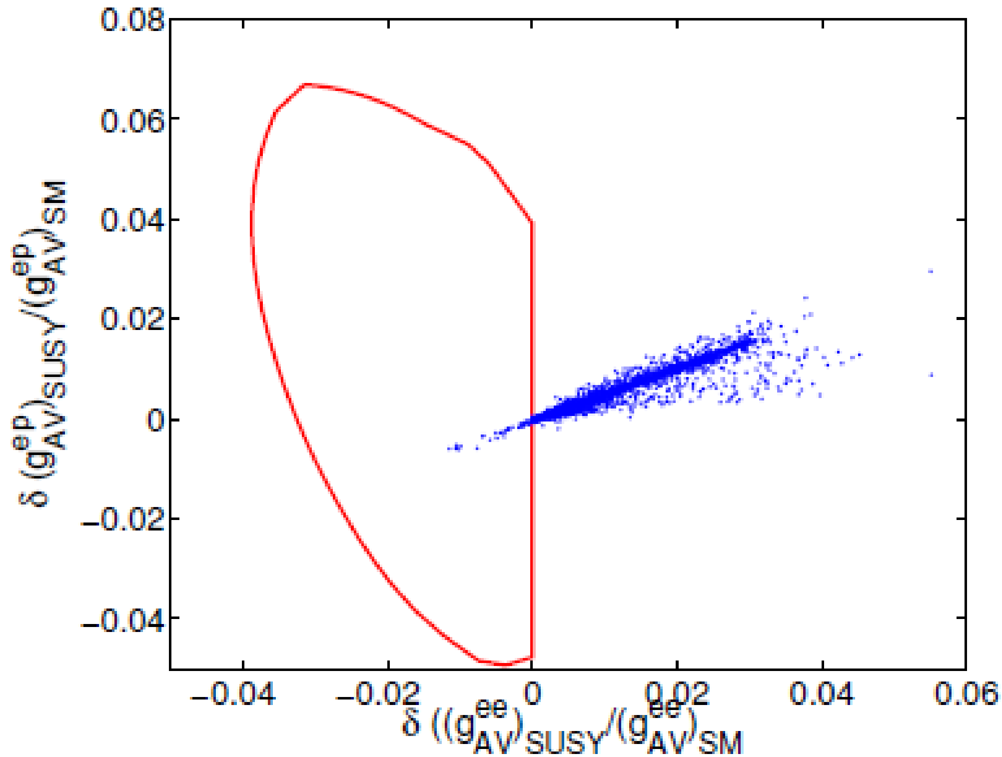

Figure 10: Relative shifts in g_{AV}^{ee} and g_{AV}^{ep} (normalized to the respective SM values) due to SUSY effects. The dots indicate the RPC corrections for ~ 3000 randomly generated SUSY-breaking parameters. The interior of the truncated elliptical region gives the possible shifts due to the RPV SUSY interactions at the 95% CL. (Figure updated from Ref. [169].)

"The Weak Neutral Current", Erler and Su, Prog. Part. Nucl. Phys. 71 (2013) 119-149, http://arxiv.org/abs/1303.5522

PRL 109, 031802 (2012)

New Physics Example - Dark Z

"Dark parity violation" (Davoudiasl, Lee, Marciano, arXiv 1402.3620)

- Introduces a new source of low energy parity violation through mass mixing between Z and Z_d with observable consequences.
- Complementary to direct searches for heavy dark photons.

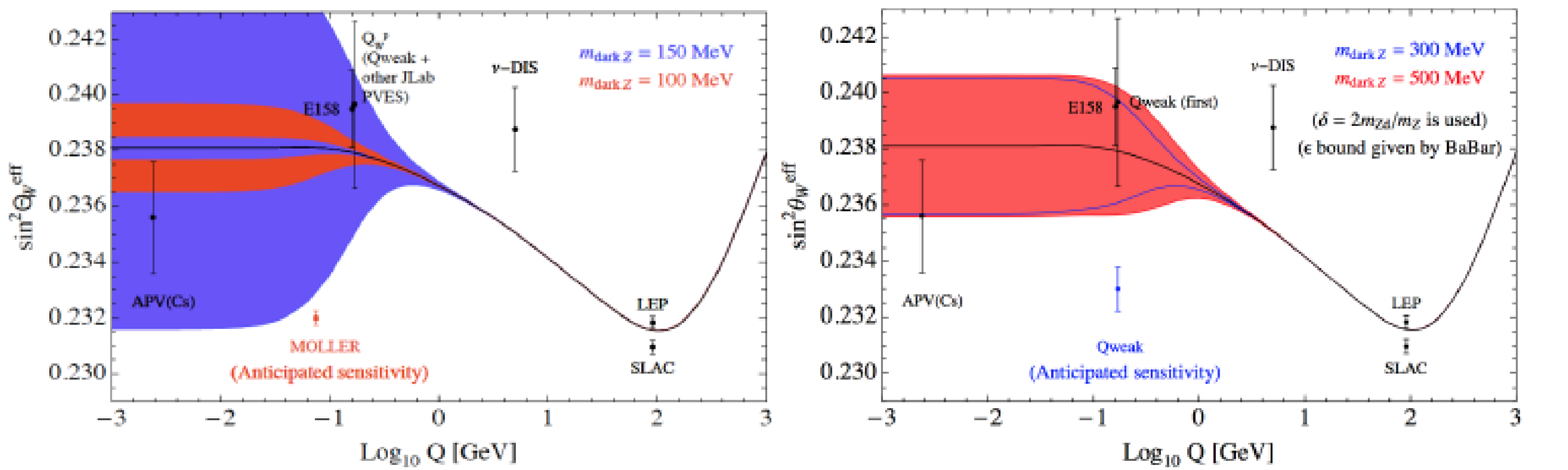

Low-E experiments most sensitive to deviations from SM due to Dark Z

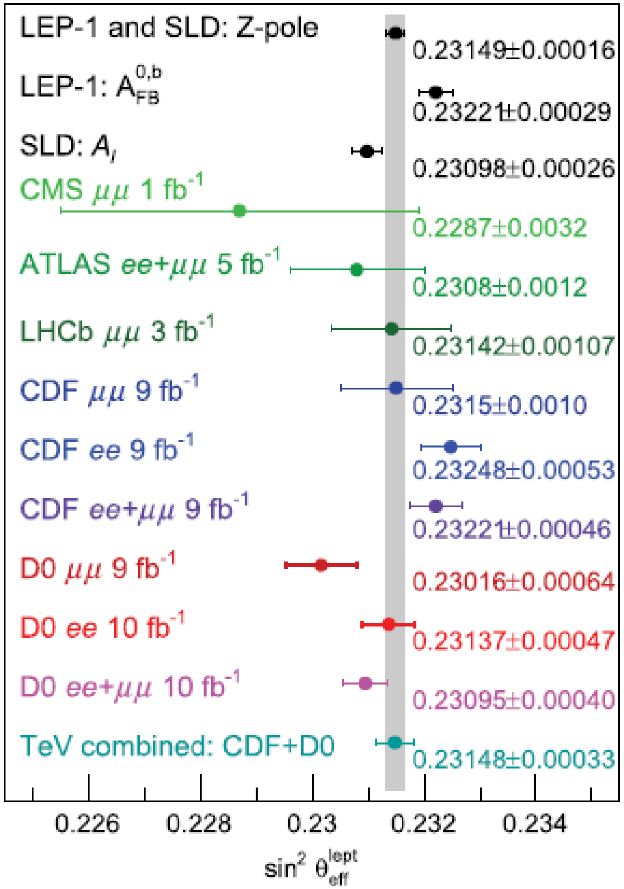

PRD **97**, 112007 (2018)

FIG. 3. Comparison of experimental measurements of $\sin^2\theta_{\rm eff}^{\rm lept}$ in the region of the Z-boson pole mass. The horizontal bars represent total uncertainties. The Tevatron combination (this paper) of CDF and D0 results is denoted as "TeV combined: CDF+D0". The other measurements are from LEP-1 combination [4], SLD [4], CMS [15], ATLAS [14], LHCb [16], CDF [8,9], and D0 [12,13]. The LEP-1 and SLD Z pole result is the combination of their six measurements, and the shaded vertical band shows its uncertainty.

Q-weak's Keyhole on New Physics

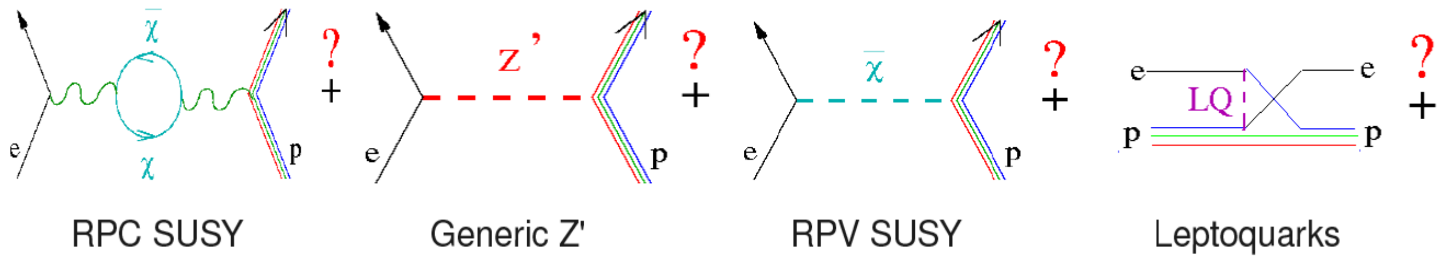

Our experiment is sensitive to new physics with PV couplings of electrons to light quarks.

In this 2003 study, our biggest sensitivity was to lepto-quarks.

The RPV SUSY limits got much tighter in 2013.

Erler and Su,
Prog. Part. Nucl. Phys. 71 (2013) 119-149.

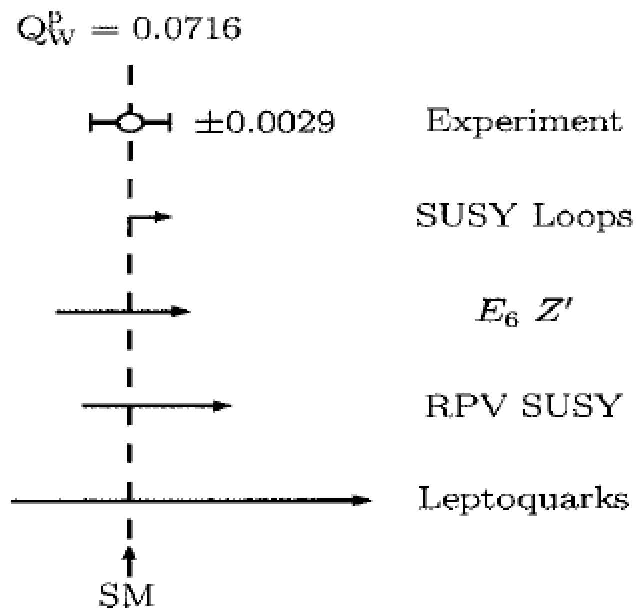

Erler et al., Phys. Rev. D 68, 016006 (2003).

Q-weak's Keyhole on New Physics

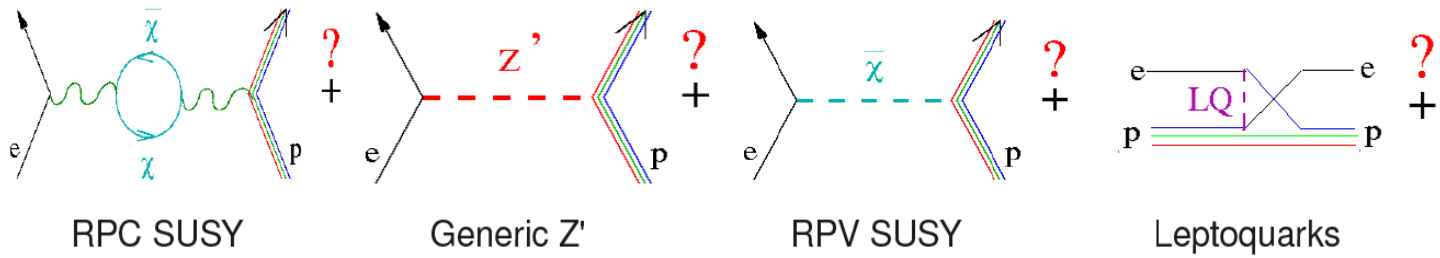

Our experiment is sensitive to new physics with PV couplings of electrons to light quarks.

In this 2003 study, our biggest sensitivity was to lepto-quarks.

The RPV SUSY limits got much tighter in 2013.

Erler and Su,
Prog. Part. Nucl. Phys. 71 (2013) 119-149.

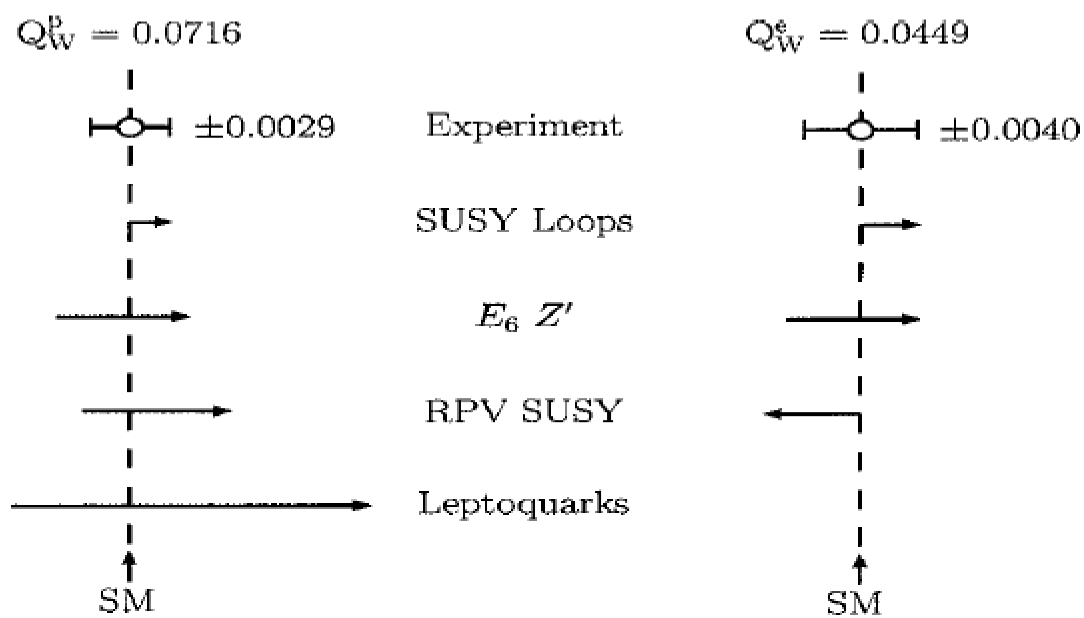

Erler et al., Phys. Rev. D 68, 016006 (2003).

Low Energy PV and the Tevatron Top A_{FB} Anomaly

M. Gresham et al., arXiv:1203.1320v1 [hep-ph] 6 Mar 2012

Tevatron CF and D0 collaborations saw an excess in the t-tbar forward-backward asymmetry, A_{FB}.
(Precision measurements can also be made at the energy frontier!)

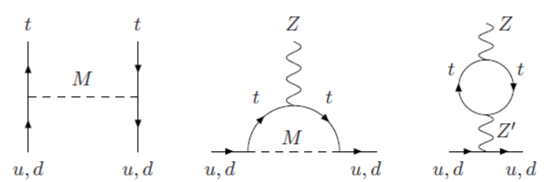

FIG. 1: A_{FB} from t-channel exchange of M (left). Anomalous coupling of Z to u, d at one-loop is generated by M (center) and by flavor-conserving Z′ associated with certain vector M models.

A possible explanation which avoided known constraints was a new, not-too-massive, scalar or vector particle.

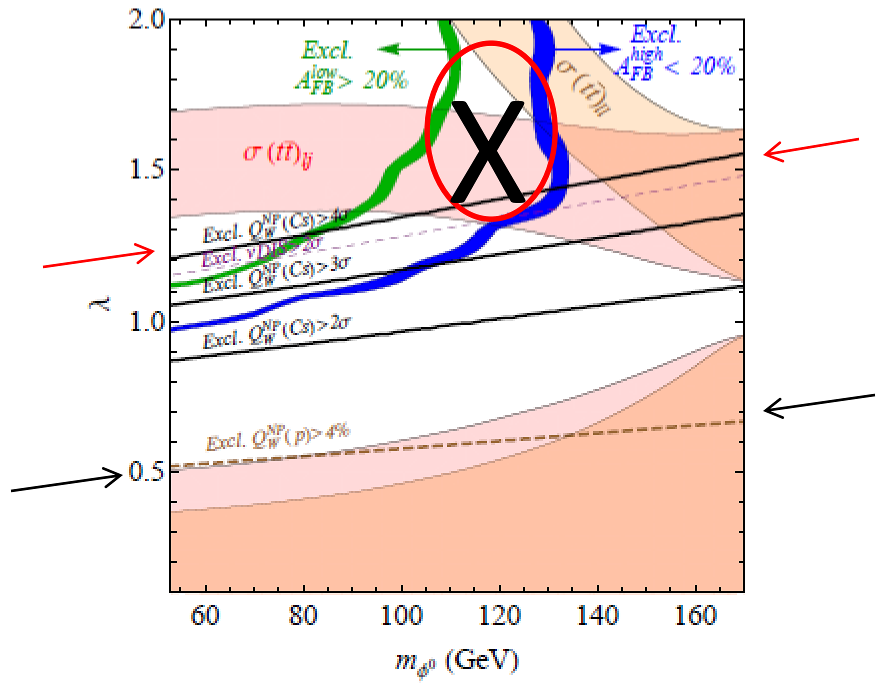

FIG. 2: Exclusion plot for weak doublet (ϕ) model. Pink and tan shaded regions are consistent with $\sigma(t\bar{t})_{\ell j}$ and $\sigma(t\bar{t})_{\ell\ell}$, respectively. Mass-dependent-A_{FB}-favored region is within the blue and green curves, marking $A_{FB}^{\rm high} > 20\%$ and $A_{FB}^{\rm low} < 20\%$, respectively. Constraints from $Q_W(\rm Cs)$, νDIS, and future $Q_W(p)$ measurements shown by black solid, purple dashed, and brown dashed lines, respectively.

Sufficiently precise low energy PV experiments can constrain new physics models.

Polarized Source

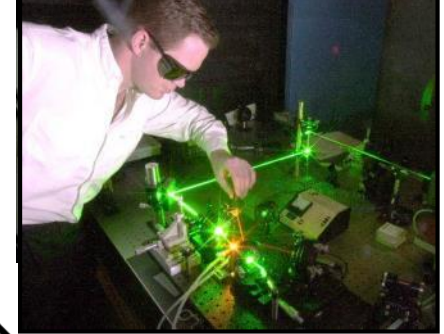

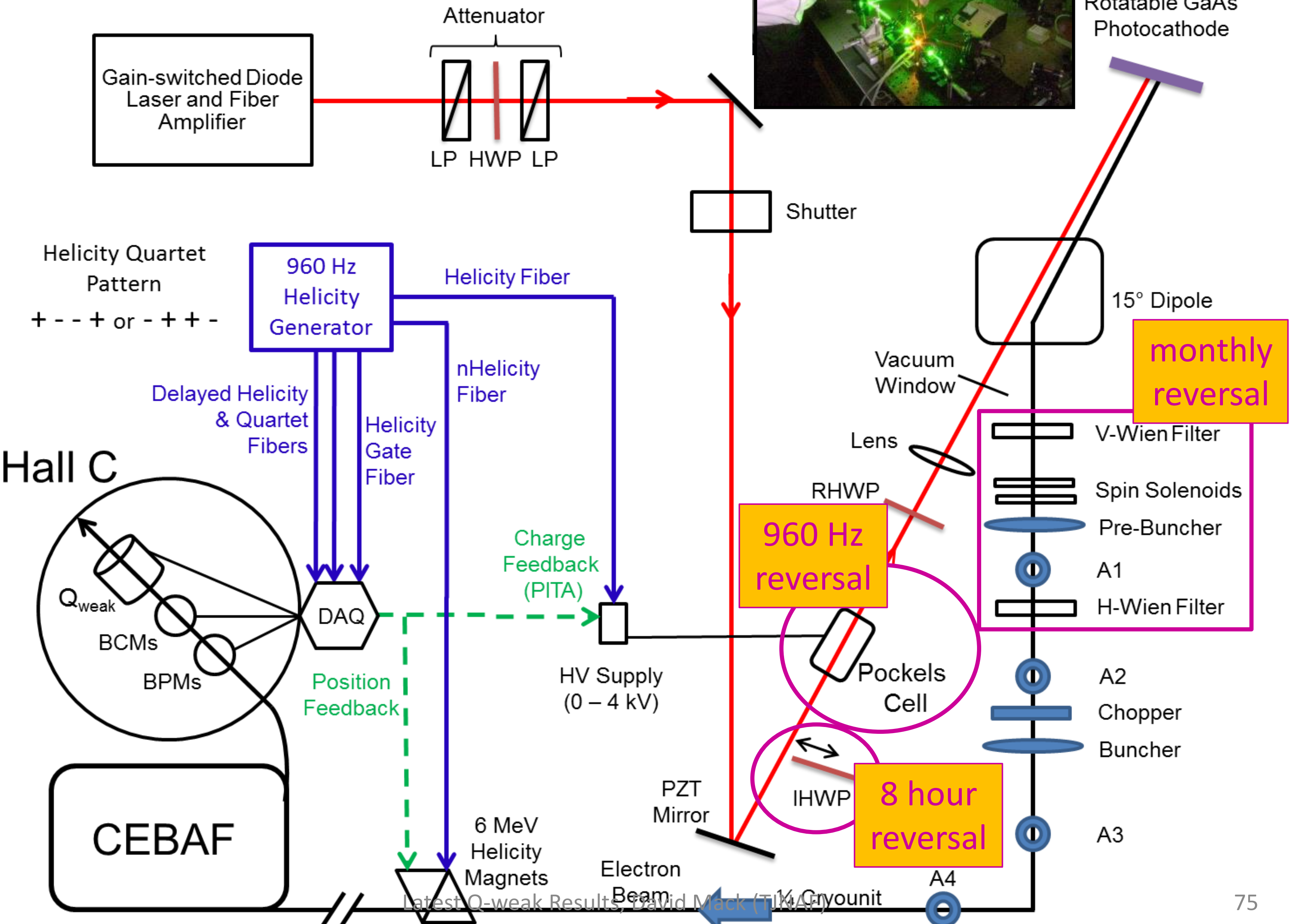

Gamma-Z Box Correction

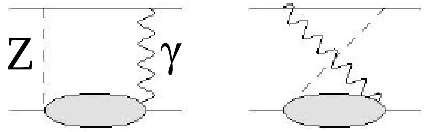

$$Q_W^p = [\rho_{\rm NC} + \Delta_e][1 - 4\sin^2\hat{\theta}_W(0) + \Delta_e'] + \Box_{WW} + \Box_{ZZ} + \Box_{\gamma Z}$$

~7% correction

Table 1: $\Box^V_{\gamma Z}$ contribution to Q^p_W (Qweak kinetmatics)

Gorchtein & Horowitz Phys. Rev. Lett. **102**, 091806 (2009)	0.0026 ± 0.0026
Sibirtsev, Blunden, Melnitchouk, & Thomas Phys. Rev. D **82**, 013011 (2010)	$0.0047^{+0.0011}_{-0.0004}$
Rislow & Carlson Phys. Rev. D **83**, 113007 (2007)	0.0057 ± 0.0009
Gorchtein, Horowitz, & Ramsey-Musolf Phys. Rev. C **84**, 015502 (2011)	0.0054 ± 0.0020
Hall, Blunden, Melnitchouk, Thomas, & Young Phys. Rev. D **88**, 013011 (2013)	0.00557 ± 0.00036

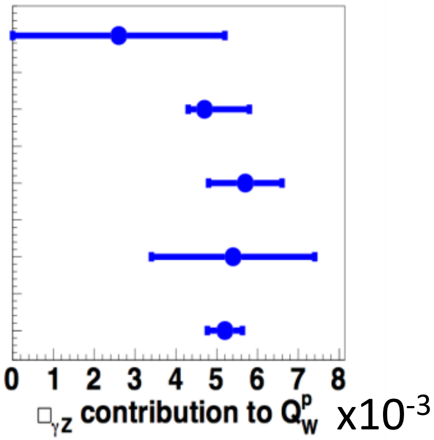

The $\Box_{\gamma Z}$ is the only E & Q^2 dependent EW correction.
→ Correct the PVES data for this E & Q^2 dependence.

- Calculations are primarily dispersion theory type
  - error estimates can be firmed up with data!

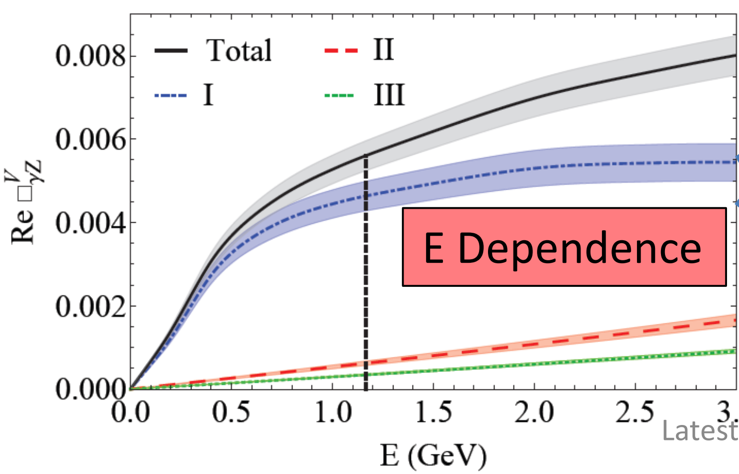

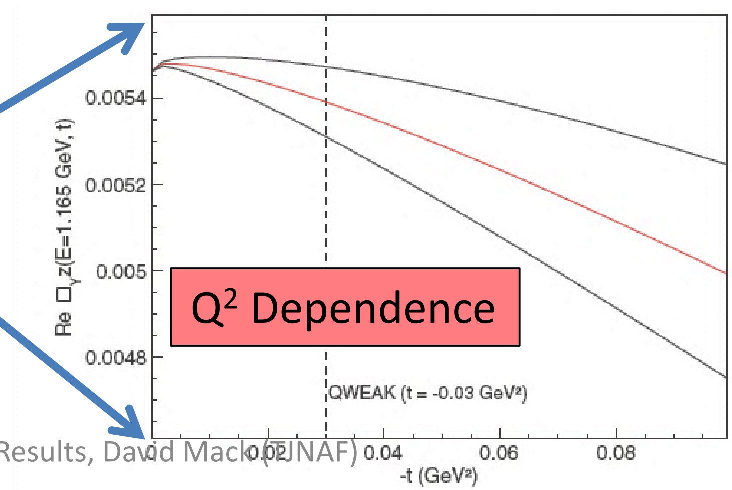

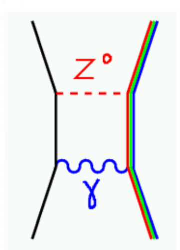

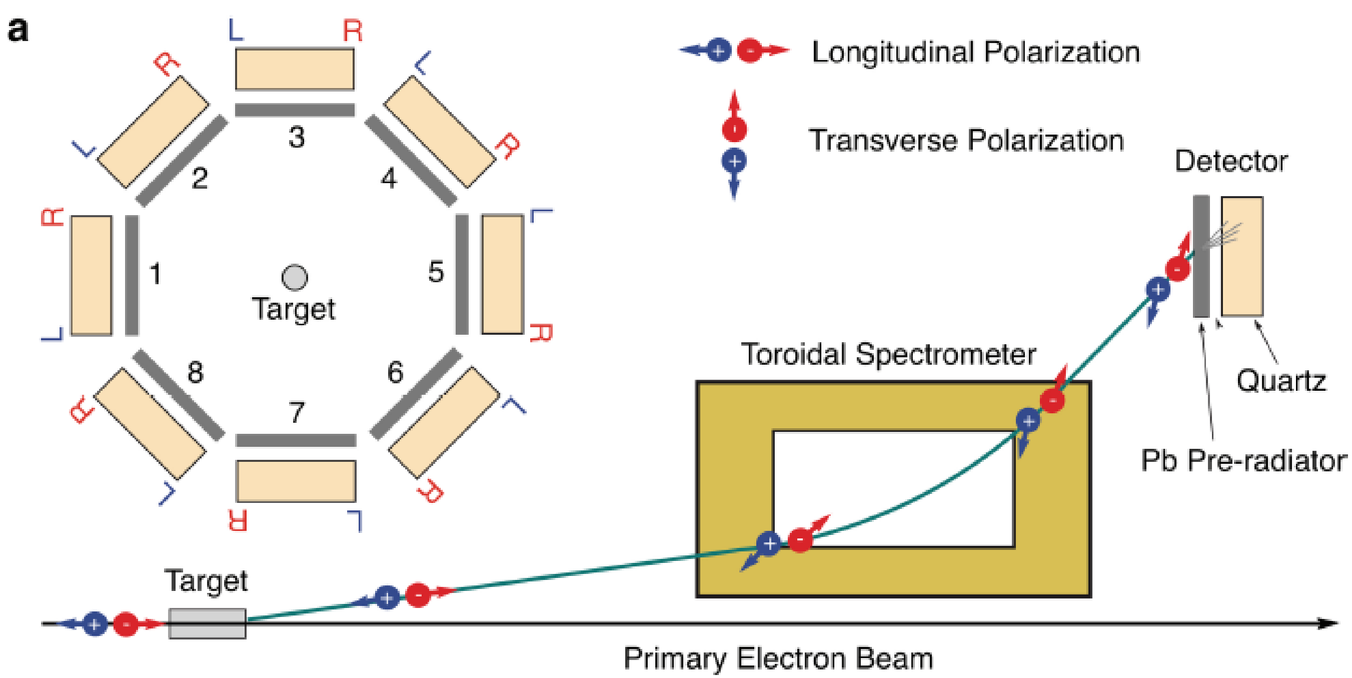
a
L
R
R
L
L
R
R
L
L
R
R
L
L
R
R
L
3
2
4
1
5
Target
8
6
7
Longitudinal Polarization
Transverse Polarization
Detector
Toroidal Spectrometer
Quartz
Pb Pre-radiator
Target
Primary Electron Beam

LH_2 Cryotarget Design

I_{Beam} = 180 uA
L = 35 cm (4% X_0)
P_{beam} = 2.2 kW
A_{spot} = 4x4 mm^2
V = 57 liters
T = 20.00 K
P ~ 220 kPa

World's highest power *and lowest noise* cryogenic target ~3 kW

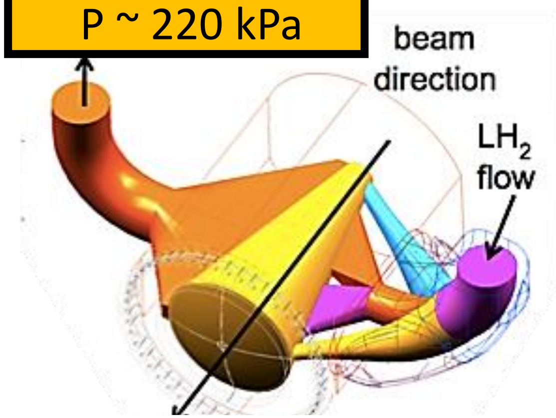

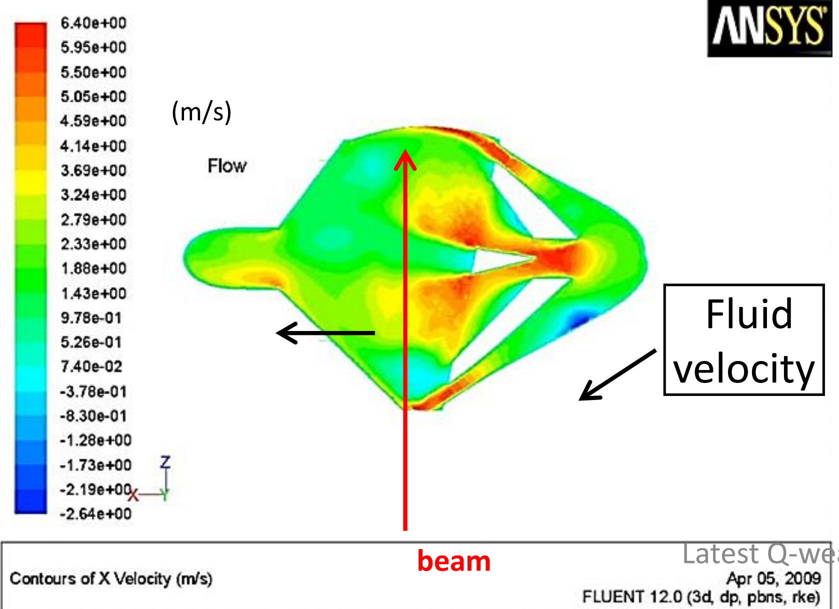

Fluid velocity

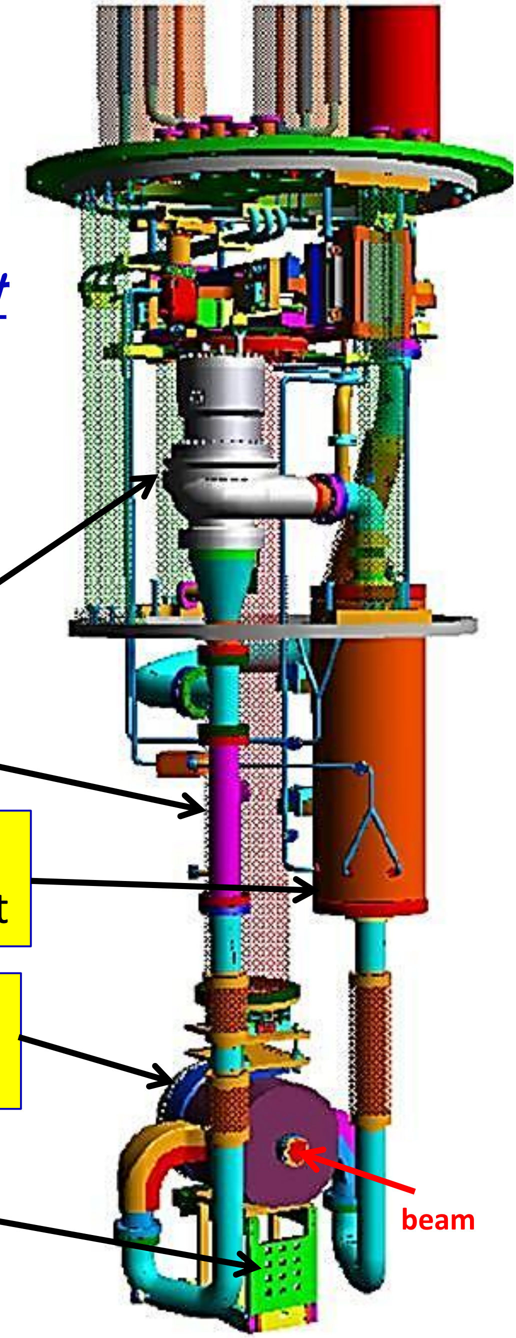

Centrifugal pump (17 l/s, 7.6 kPa)

3 kW Heater

3 kW HX utilizing 4K & 14K He coolant

35 cm cell (beam interaction volume)

Solid Tgts

Jlab Exo-Skeletons

Manitoba radiator modules (physicist responsibility) were installed in a strong, stiff Jlab exo-skeleton suitable for carrying Pb shielding and pre-radiators (engineering and safety responsibility).

Each module carries 200 lbs (90 kg) of Pb bricks to provide limited shielding for PMTs. (Pre-radiators would double that.)

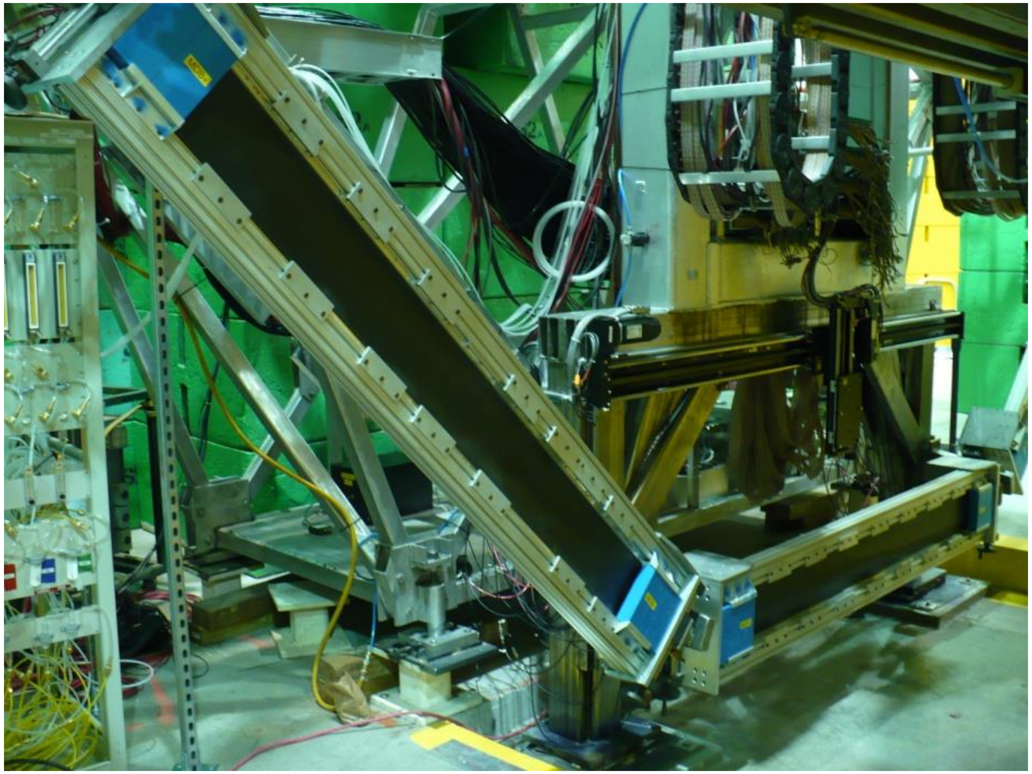

Collimation

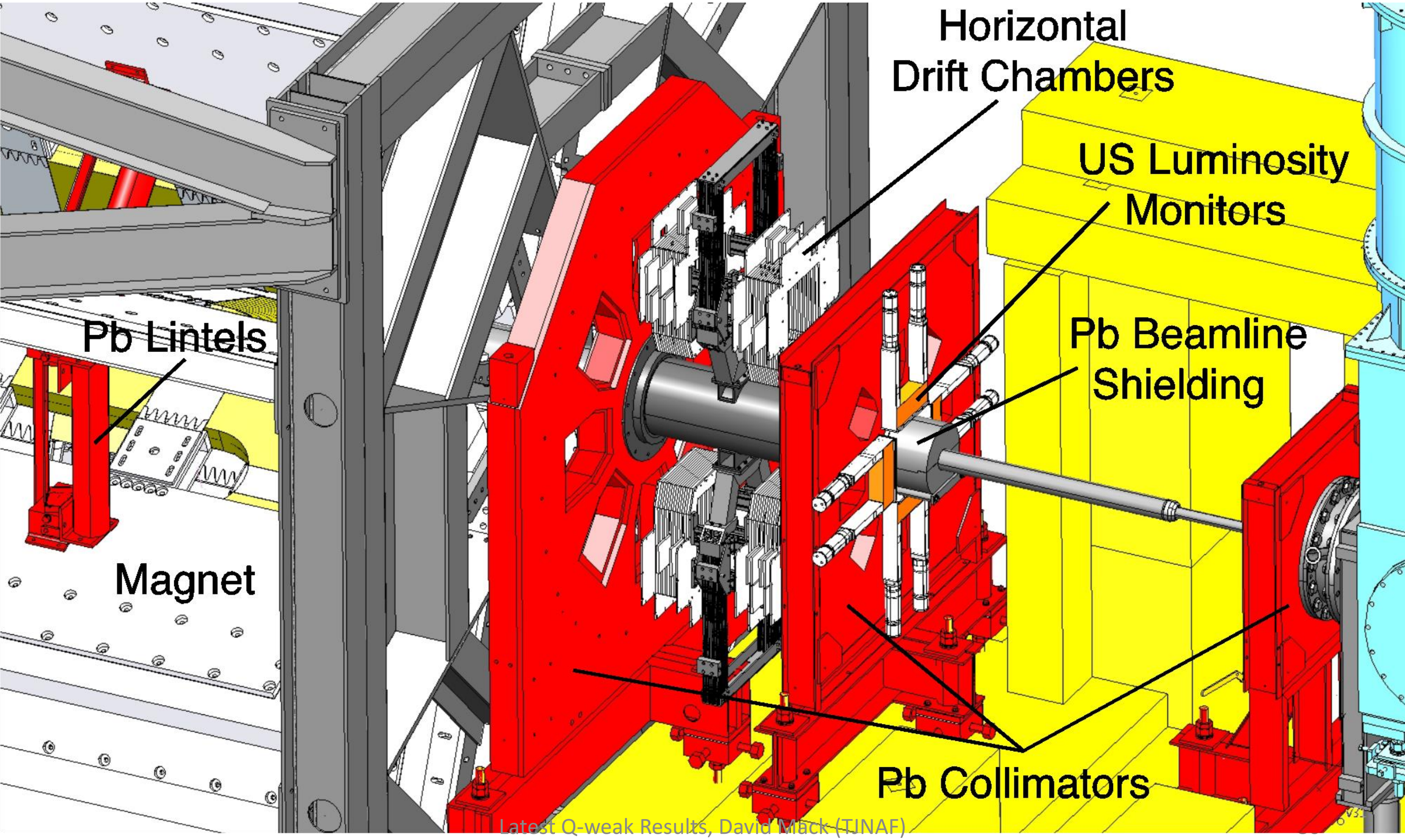

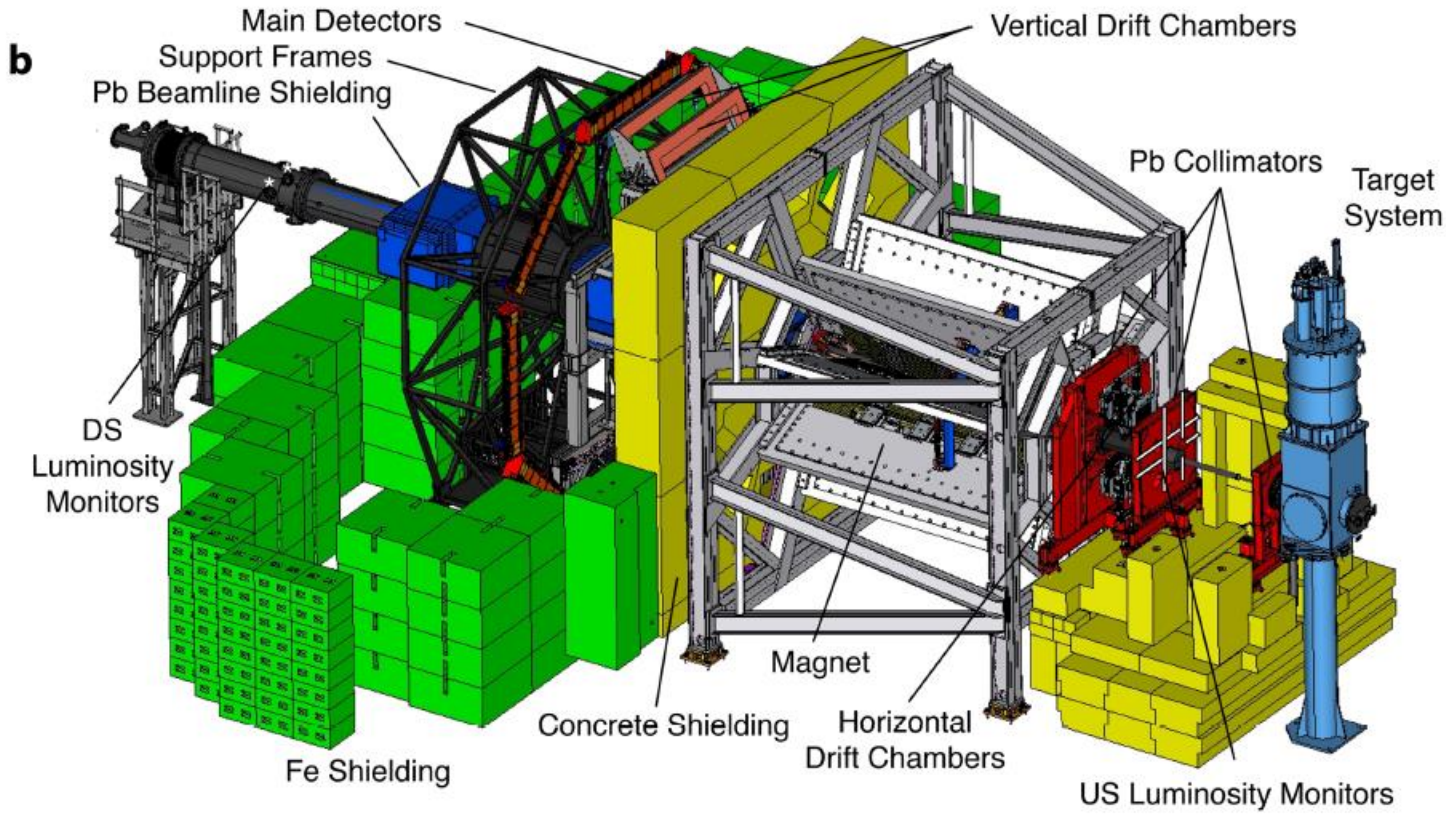
b
Main Detectors
Support Frames
Pb Beamline Shielding
Vertical Drift Chambers
Pb Collimators
Target System
DS Luminosity Monitors
Magnet
Concrete Shielding
Horizontal Drift Chambers
US Luminosity Monitors
Fe Shielding

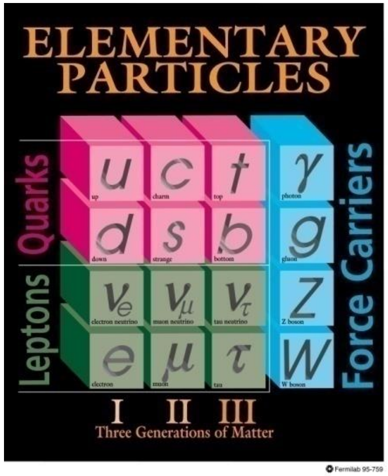

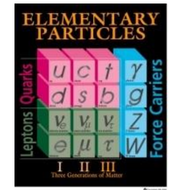

+gravity

+dark matter

+dark energy

Physics Motivation

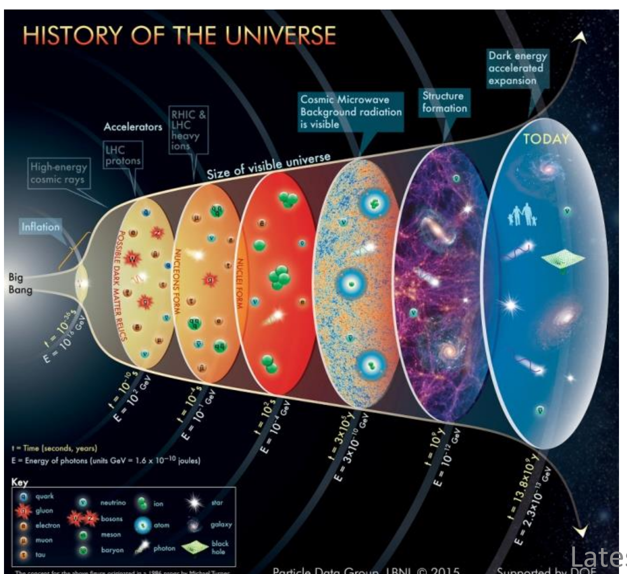

What the Data Look Like

Qweak Run 2 - Blinded Asymmetries

(statistics only - not corrected for beam polarization, Al target windows, ΔQ^2, etc.)

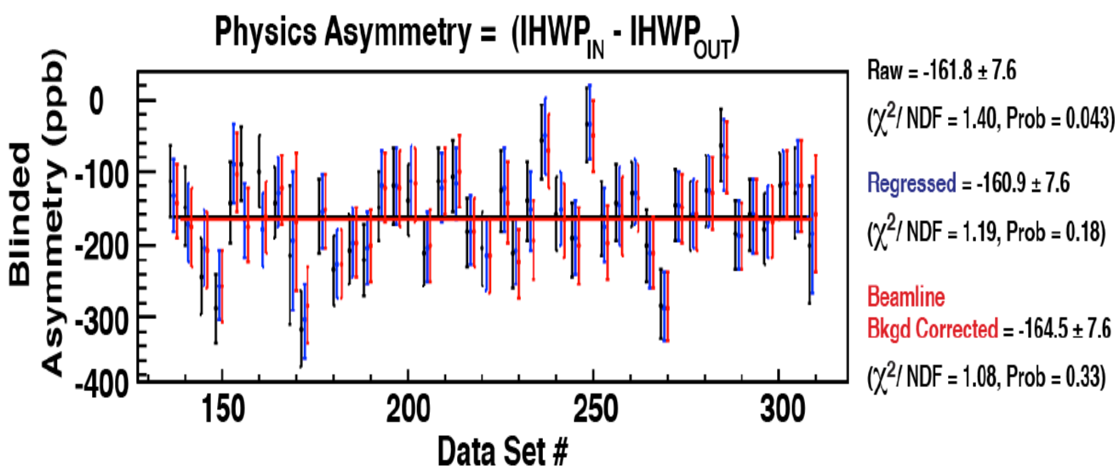

Experimental Asymmetry – Corrections barely change the average of fitted P^*A_{pv}, but the probability improves.
Noise is being removed.

P = 4.3% → 18% → 33%

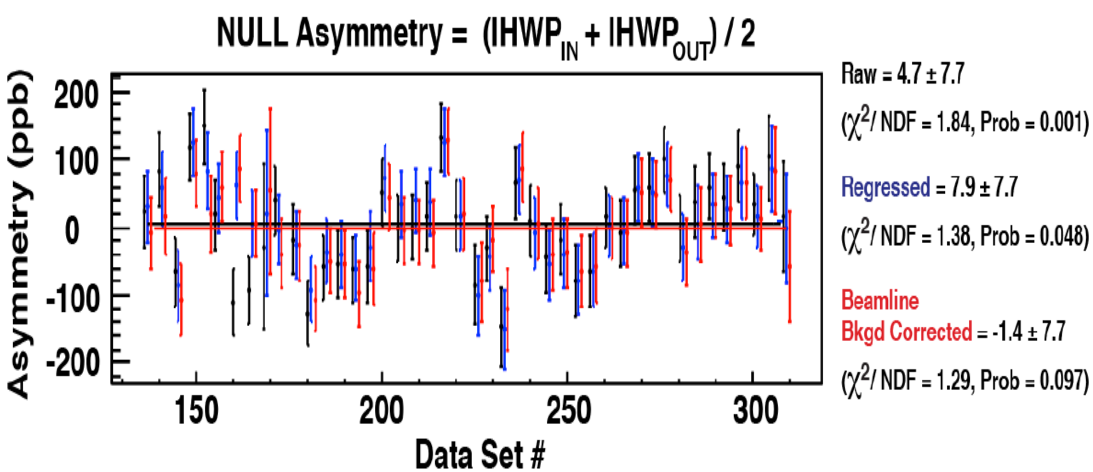

Null Asymmetry – Is consistent with zero, and the fit probability improves from a very unlikely value to a credible value after corrections.
Noise is being removed.

P = 0.1% → 4.8% → 9.7%

Target Cell

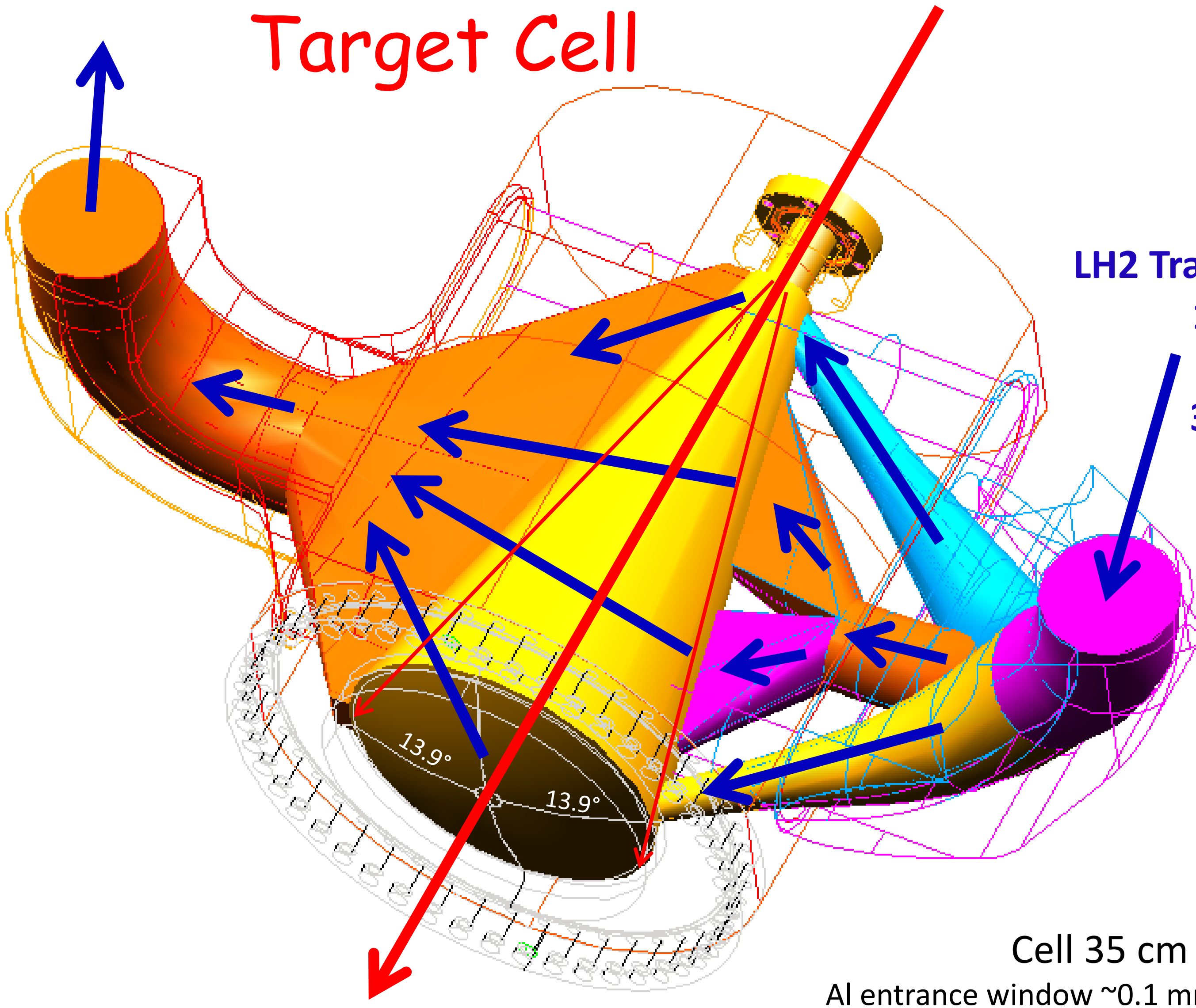

LH2 Transverse Flow:
1.1 kg/s
15 L/s
3-7 m/s

Electron Beam
180 μA, 4x4 mm²

Cell 35 cm long

Al entrance window ~0.1 mm thick, 22.2 mm Φ
Al exit window ~0.125 mm thick over 15 mm Φ,
0.635 mm thick over 173.5 mm
Scattered electron acceptance ±13.9°

Q-weak Spectrometer (detail)

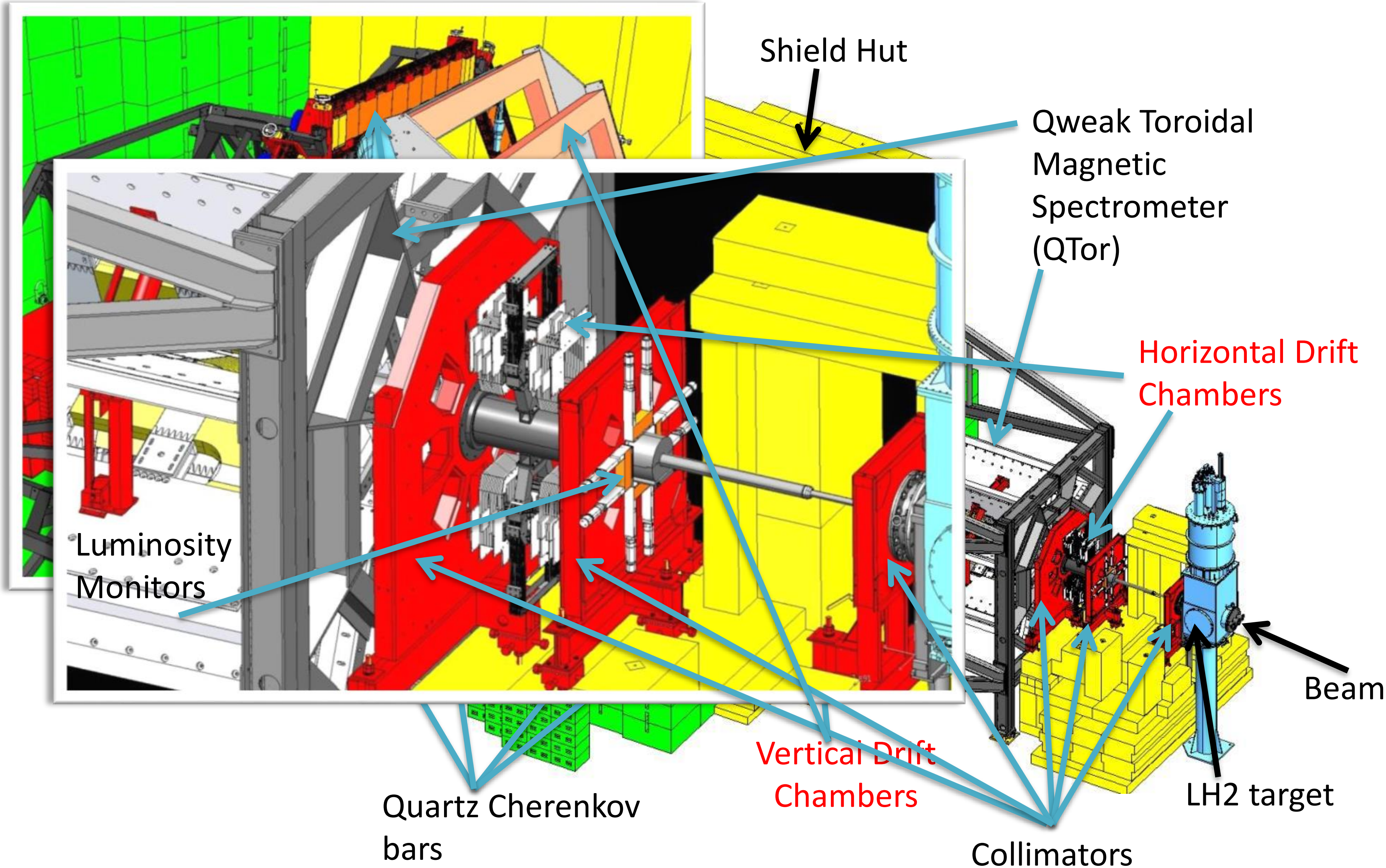

Used only during low current tracking mode operation